

Ophthalmic Biomaterials

Ophthalmic Biomaterials

Ben Muirhead

A Thesis Submitted to the School of Graduate Studies in Partial Fulfillment of the
Requirements for the Degree Doctor of Philosophy in the School of Biomedical Engineering

McMaster University © Copyright by Ben Muirhead, March 2017

DOCTOR OF PHILOSOPHY (2017)
School of Biomedical Engineering

McMaster University
Hamilton, Ontario

TITLE: Ophthalmic Biomaterials

AUTHOR: Ben Muirhead, BSc.

SUPERVISOR: Dr. Heather Sheardown

NUMBER OF PAGES: 162

Chapter 1: Introduction	1
1.1 Foreword.....	2
1.2 The Eye.....	3
1.3 Anterior segment	4
1.4 Strategies to overcome anterior barriers.....	8
1.5 Retina.....	17
1.6 Posterior segment strategies.....	17
1.7 Thermosensitive hydrogels.....	22
1.8 Natural polymers.....	23
1.9 Synthetic polymers.....	26
1.10 Architecture.....	29
1.11 References.....	32
Chapter 2: Hyaluronic acid – sulfadiazine conjugate as a treatment for dry eye diseases	52
3.1 Background.....	55
3.2 Synthesis of HASD.....	66
3.3 Preclinical DES model.....	68
3.4 Experimental approach.....	70
3.5 Creation of DED model.....	72
3.6 Rescue from disease state.....	77
3.7 Conclusions and future work.....	81
3.8 References.....	83
Chapter 3: PolyNIPAAm based cell delivery scaffold for posterior segment cell therapy	89

4.1 Background.....	91
4.2 Polymer design.....	100
4.3 Organotypic in vitro model.....	107
4.4 In vivo modelling.....	114
4.5 Conclusions and future work.....	119
4.6 References.....	121
Chapter 5: Mucoadhesive phenylboronic acid based micelles for controlled, sustained anterior segment drug delivery.....	126
5.1 Background.....	128
5.2 Micelle synthesis and characterization.....	130
5.3 In vitro testing.....	136
5.4 In vivo testing.....	140
5.5 Conclusions and future work.....	154
5.6 References.....	156
Chapter 6: Conclusions and future work.....	159

Chapter 1: Introduction

1.1 Foreword

Before this thesis turns to the expected science and engineering, I wanted to briefly qualify what is about to be read. The format of this work is somewhat unconventional and, I hope, therefore better suited to telling the story I am trying to tell. I came to Dr. Sheardown's group after an undergraduate in molecular biology followed by a brief stint in philosophy. I had absolutely no exposure to engineering, and had no idea how different the epistemological approach would be from how I had been trained. As a result, a large portion – probably the majority – of my graduate work will not be included in this thesis. It took me years to find my rhythm in a group dominated by chemical engineers and materials scientists, and while I had some successes and many dead ends, as I'm sure most graduate students do, most of what I produced was not refined enough for any sort of publication. For example, by employing my knowledge of genetics, I had hoped to create a novel, non-viral gene delivery system based on a cationic polymer (polyethylenimine was my leading contender) which could alter its charge profile after endosomal encapsulation and release its RNA cargo. I even co-authored a paper contributing to this theme.[1] While this project ultimately failed, I would never call it, or other, similarly incomplete machinations failures. Through them, I learned how to utilise my strengths, collaborate to hedge against my weaknesses, and find my place in the lab.

Eventually, with mentorship from Dr. Sheardown and other senior members of the group, I became useful as a sort of biology liaison to people who knew how to make biomaterials, but were unable to properly test them. I did tissue culture, various immunoassays, and animal testing for nearly every project created in both my lab and eventually a few others. While this sort of work can often be rote and mechanistic, I strove to form a real understanding of why things were done in certain ways, and how these processes could be modified to produce more scientific

value. It becomes difficult to create, as I had intended, a ‘sandwich’ thesis when a great deal of my contribution came as small parts of many different projects. So while this thesis is inspired by the sandwich model, it is structured more as an interconnected narrative where I move from very general explorations of cell and animal work in biomedical engineering toward increasing specificity and difficulty. Instead of simply reporting my results, I have editorialised them to try and give the reader a sense of why I made certain decisions and why other options were not pursued. The traditional paper structure was eschewed in favour of something deliberately more prosaic. While reading this thesis, I hope its structure mirrors my progress through the PhD program, and the reader can follow my journey.

1.2 The eye

The eye is an extremely fragile organ prone to an unusually large array of pathologies. The eye is generally divided into two anatomical regions: the posterior and anterior segments. The globe of the eye is surrounded by a tough coat of connective tissue called the sclera, which is colloquially referred to as the white of the eye. The sclera is continuous with the cornea, a transparent structure responsible for 70% of the refractive power of the eye, which, along the conjunctiva, aqueous humour, iris, lens, ciliary body and trabecular meshwork makes up the primary anterior structures. The cornea and conjunctiva are hydrated and lubricated with a stratified solution which makes up the tear film. This film is highly structured and precisely regulated liquid protected from evaporation by a thin lipid layer, and hydrating a mucin rich layer proximal to the ocular surface. The posterior segment is composed primarily of an aqueous matrix called the vitreous, the light sensitive retina, the capillary rich tissue supplying it with blood called the choroid, and Bruch’s membrane separating the two. Unique among the tissues of the body, the eye is made up of several cell types and tissues with particular characteristics and homeostatic

requirements. The cornea, for example, is the only purposefully transparent tissue in the body, while the retina is made up of dozens of cell types, most of which derive from a neural lineage with an extremely limited capacity for renewal. In short, the complexity, narrow metabolic requirements, and limited self-renewal and self-correction result in an organ often in need of medical intervention. Unfortunately, the eye is a very difficult organ to reach. Despite the physical accessibility of the anterior segment, rapid tear turnover quickly removes any topically applied therapeutic. Tight junctions between cells, as well as hydraulic pressure from the aqueous humour conspire to further limit penetration and bioavailability: less than 5% of topically applied drugs reach anterior structures.[2] The posterior segment is even less accessible – less than 1% of a topically applied drug will typically reach posterior structures.[2] Outflow from the posterior segment through the trabecular meshwork and Schlem’s canal ensures rapid clearance of drug. The tight junctions of the blood retinal barrier ensure anything delivered into systemic circulation will be ineffective at treating ocular tissues. Taken together, the eye is a failure prone organ resistant to conventional treatment options in desperate need of biomedical innovation.

1.3 Anterior segment

Barriers that pose a challenge to anterior segment therapeutics can be divided into two categories. Static barriers include the tight junctions of the corneal epithelium and endothelium, the thickness and density of the corneal stroma, and the blood–aqueous barrier made up of tight junction separating systemic blood supply from the eye. Dynamic barriers include stromal flow, lymphatic flow, and, most importantly, tear production and drainage.[3] Efflux pumps, such as

MDR1 [P-glycoprotein (P-gp)], the multidrug resistance protein (MRP), and the breast cancer resistance protein (BCRP) expressed on cell membranes can actively remove drug that defeats these static and dynamic barriers.[4] Along with these corneal barriers, the conjunctiva and tear film represent a significant barrier to drug delivery.

1.3.1 Conjunctiva and tear film

The conjunctiva is so named by conjoining the eyelids with the eyeball. It is composed of 2 layers: the outer epithelia made of stratified epithelial cells and the inner stroma made of substantia propria. The number of epithelial layers varies depending on anatomical location, but is generally between 2 and 10.[5] It is a thin mucous membrane that covers the posterior surface of the eyelids and is then reflected onto the eyeball, where it extends to the edge of the cornea. This junction is indirect, with the conjunctiva forming a fornix on three sides of the globe and an extendible plica on the fourth side. The fornixes and plica of the conjunctiva are loose arching folds connecting the conjunctival membrane lining the inside of the eyelid with the conjunctival membrane covering the eyeball. This arrangement allows the globe and eyelids to move independently.[6] The conjunctiva, embedded with secretory goblet cells, helps with tear film production through the production of electrolytes and mucins.[7] The outer apical epithelial cells form tight junctions (zonula adherens) with a transepithelial electrical resistance of $\sim 1.2 \text{ k}\Omega\text{cm}$ [8], greatly impeding paracellular diffusion. The stroma is replete with nerves, blood, and lymph vessels. The water content of this tissue is a barrier to hydrophobic compounds, while its active blood and lymphatic circulation can remove drug from the local microenvironment. Only hydrophilic drugs smaller than 20kDa are considered permeable across the conjunctiva. The

conjunctiva possesses esterase activity and expresses efflux proteins (P-gp)[9] further impeding drug transport.

The tear film is a multi-layered liquid that coats the exposed surface of the eye to protect and hydrate it. This tear film is the first barrier against drug delivery due to its structure, composition, and its rapid turnover and drainage into the systemic circulation. Tear film thickness over the cornea and conjunctiva ranges from 3–9 μm , but the precorneal pocket can hold a tear volume of approximately 30 μL until it overflows.[10] The tear film is composed of 3 layers: an outer lipid layer secreted by meibomian glands at the rim of the eyelids inside the tarsal plate, a middle aqueous layer, and an inner mucin layer.[11] The principal components secreted into the tear film include electrolytes, glucose, immunoglobulins, lysozymes, and lactoferrin. These components aid in lubrication, nourishment, maintenance, and repair of the corneal epithelium.[12] The mucin layer, essential for the hydration and lubricity of the ocular surface, is also a barrier to permeation. Mucins are large, negatively charged glycoproteins with high water content due to sialic acid carbohydrate residues.[13] These hydrophilic, negatively charged molecules can act to repel other negatively charged or hydrophobic molecules. An entire class of mucus-penetrating drug carriers has recently come to prominence in the literature in an effort to improve drug delivery across this barrier.[14-16] Under normal conditions, tear flow turnover occurs at approximately 1.2 $\mu\text{L}/\text{min}$; this rate can increase dramatically during transient receptor potential (TRP) channel stimulation caused by injury or irritation, resulting in ‘reflex tears’ attempting wash out or dilute harmful substances.[17] The reflex response can be particularly problematic when applying an irritating medication. Excessive tear production and subsequent drainage through the nasolacrimal duct will often lower bioavailability to <5%. [18]

1.3.2 Cornea

Continuous with the conjunctiva, the cornea is a multilayered, transparent, avascular, highly innervated tissue.[19] It is organized into three physiological layers: the epithelium, stroma, and endothelium. Separating these layers are two membranes: Bowman's layer (BL) and Descemet's membrane (DM).[20] The epithelium provides a similar function as elsewhere in the body – it acts as an active barrier to external biological and chemical agents, as well as maintaining the smooth geometry on the anterior surface of the eye. The epithelium is composed of 5–6 layers of columnar cells derived from the epidermal ectoderm.[21] Mature epithelial cells form highly lipophilic tight junction, which restrict hydrophilic drug entry into ocular tissues.[22] BL separates the epithelium from the stroma, and consists of randomly arranged collagen fibres and proteoglycan types I and III. The stroma constitutes about 90% of the thickness of the cornea and is an innervated tissue comprised of 300-500 aligned collagen lamellae superimposed one on another in orthogonal orientations. Each layer is 1-2 μm in thickness with uniform spacing between them. It is this unique highly organized placement of collagen lamellae which is responsible for optical transparency.[23] While the lipophilic epithelium may be permeable to hydrophobic drug, the stroma certainly is not. In this way, with alternating hydrophobic and hydrophilic barriers, the chemistry of a therapeutic becomes almost irrelevant – the cornea can stop nearly anything from penetrating deeper into ocular tissues. The molecular components of the stromal matrix are secreted by keratocytes which are scattered in between these layers throughout the stroma. The stroma provides structural strength, shape, stability, and transparency to the cornea.[24] Separating the corneal endothelium from the stroma is DM, a highly elastic apparently structureless membrane that covers the inner surface of the stroma and is composed of

type VIII collagen.[25] Derived from the cranial neural crest,[26] the endothelium is a monolayer of hexagonal cells organized in a tessellated mosaic on covering the posterior surface of Descemet's membrane. They uniformly cover the whole posterior corneal surface, and at its periphery reach the trabecular meshwork (TM) in the angle between the cornea and iris root.[27] Adjacent cells communicate through gap junctions and tight junctions, whereas the basal surface is adhered to Descemet's membrane by hemidesmosomes.[28] Tight junction protein ZO-1 forming supramolecular assemblies are found close to the apical domains of endothelial cells, allowing the endothelium to function as a barrier, forming resistance to the permeability of solutes and fluid through paracellular transport routes.[29] The endothelial layer also generates osmotic pressure through ion transport mechanisms that counterbalances a continuous leak of fluid into the corneal stroma. This movement is facilitated by integral proteins in the cellular membrane, the aquaporins (AQP), which function as water selective channels.[30] This continuous efflux of water across the endothelial cells into the aqueous is another mechanism by which diffusing drug might be removed.[31] Transmembrane efflux pumps are expressed throughout the cornea, but in particularly high abundance on its endothelium. Transport studies conducted across the human and rabbit cornea demonstrated active involvement of drug efflux pumps at the cell surface that restricts drug diffusion into ocular tissues.[32, 33]

1.4 Strategies to overcome anterior barriers

1.4.1 Prodrugs

Prodrugs are modified drug molecules designed to be therapeutically inactive until enzymatic or chemical bioreversion into an active form.[34] These derivatives are typically synthesized via

ester, amide, or other enzymatically cleavable linkages providing the link between a drug and promoiety.[35] Among the ocular tissues, the highest esterase activity has been found in the iris-ciliary body followed by the cornea and aqueous humor, while the highest aminopeptidase activity has been reported in lipophilic corneal epithelium and the iris-ciliary body followed by the conjunctiva and the hydrophilic corneal stroma.[36] Lipophilic ester and transporter-targeted prodrug approaches are by far the most popular. For example, timolol, a common anti-hypertensive medication used to treat glaucoma, was found to have significant cardiac and respiratory off target side effects due to systemic exposure from eye drops. By creating a lipophilic prodrug version using acetyl-, propionyl-, and butyryl- esters, timolol exhibited a 2 to 3-fold increase in corneal permeability and a 4 to 6-fold higher concentration in the aqueous humour. This increase in bioavailability warranted a reduction in dosage and concomitant reduction in side effects.[37] Recent prodrug research tends to be more focused on transporter targeted moieties which take advantage of intramembrane peptide transporter assemblies within the corneal epithelium.[38] For example, a series of dipeptide ester prodrugs modifying acyclovir (ACV) and ganciclovir (GCV) were created to improve the clinical efficacy of these antiviral drugs at fighting common eye infections such as herpes simplex. Prodrugs like valine-valine-acyclovir, glycine-valine-acyclovir, tyrosine-valine-acyclovir, valine-tyrosine-acyclovir, tyrosine-valine-ganciclovir, and valine-valine-ganciclovir all demonstrated enhanced transcorneal permeability, achieving a higher ocular bioavailability.[39] These prodrugs exhibited a higher antiviral efficacy while demonstrating less cytotoxicity.[40] Prodrugs have been, and remain, a popular and reasonably effective method of improving drug penetration through ocular barriers, improving tissue specificity, and increasing therapeutic bioavailability.

1.4.2 Poloxamers

Triblock copolymers possessing an A-B-A configuration of poly(ethylene oxide) poly(propylene oxide)-poly(ethylene oxide) (PEO-PPO-PEO), referred to as poloxamers or by their trade name Pluronics, are a family of materials which, due to their amphiphilic structures, can significantly improve drug solubility and enhance the viscosity of topical formulations.[41] Poloxamer 407, a copolymer with 101 unit PEO repeats sandwiching 56 units of PPO has been shown to enhance the delivery of the nonsteroidal anti-inflammatory drug (NSAID) indomethacin.[42] In addition to a nearly 3-fold increase in indomethacin levels in the aqueous humour, anti-inflammatory studies performed on an immunogenic uveitis model demonstrated a more rapid resolution of the symptoms. Furthermore, most poloxamers are thermosensitive, a topic which will be discussed in greater detail. Briefly, by heating properly formulated poloxamers above a lower critical solution temperature (LCST) they undergo a solution to gel transition, greatly increasing in viscosity. By applying a thermosensitive poloxamer to the surface of the eye, the gelation prevents rapid clearance and increases bioavailability. *In vivo* efficacy studies in rabbits have demonstrated the viability of this approach, showing a significant increase in the clinical efficacy and concentration of several drugs.[43, 44]

1.4.3 Cyclodextrins

Cyclodextrins are a group of toroidal naturally occurring cyclic oligosaccharides that are produced as a result of the bacterial breakdown of α -D-glucose polymers, such as cellulose. They can form water-soluble complexes with lipophilic drugs, which 'hide' in the central cavity. Cyclodextrins thus act as carriers by keeping hydrophobic drug molecules in solution and

delivering them to a membrane surface where they escape from the cyclodextrin cavity into the lipophilic membrane. Cyclodextrins have been used successfully to enhance the ocular delivery of glaucoma drugs (ie carbonic anhydrase inhibitors, prostaglandin, pilocarpine),[45-47] NSAIDs (ie indomethacin),[48] and antifungal drugs (ie voriconazole).[49]

1.4.4 Polymeric nanoparticles

This category is perhaps too varied to be described under a single subheading. Nevertheless, a brief overview of polymer based nanoparticle delivery system will be provided. In general, drug and particle can interact through adsorption, entrapment, encapsulation, or conjugation. The enormous library of potential chemistries, sizes, and properties of polymers can provide enhancement to less sophisticated alternatives, like liposomes, which can cause irritation and toxicity.[50] Drug/polymer assemblies can provide controlled release through tuneable diffusion across a membrane, dissolution, or physical erosion of the polymer carrier. By masking hydrophobic drugs, nanoparticles can improve solubility while protecting against chemical or enzymatic attack.[51] Common, FDA approved polyesters such as poly(lactic-co-glycolic acid) (PLGA) or polycaprolactone (PCL) have been used extensively to encapsulate highly hydrophobic drugs often applied topically to the eye. NSAIDs are a common class of anti-inflammatory drugs where poor solubility, hydrophobicity, and generally low bioavailability limit their usefulness in the eye. By packaging them in PLGA nanoparticles, NSAIDs can see significantly enhanced corneal transport and clinical efficacy.[52] Natural polymers can be used

as well. Cyclosporine A (CycA)-loaded chitosan nanoparticles were successful in selectively increasing CycA levels in the cornea by a factor of 2 and in the conjunctiva by a factor of 4 when compared with a simple aqueous suspension.[53] Using polymeric systems to specifically target cell binding ligands can be a highly effective approach. Hyaluronic acid (HA) is a glycosaminoglycan which binds to CD44, a cell-surface glycoprotein overexpressed in most ocular tissues, including the cornea.[54] By incorporating HA into nanoparticle systems, CD44-mediated active transport through the corneal epithelium and endothelium can greatly enhance drug transport across the cornea.[55]

1.4.5 Micelles

Micelles consist of amphiphilic compounds that generally self-assemble in aqueous media to form organized supramolecular structures. Micelles are formed in various size (10nm to 1000nm) and shapes (spherical, cylindrical and star-shaped, etc.) depending on the molecular weights of the core and corona forming blocks.[56] The self-assembly take place above certain concentration, referred to as critical micelle concentration (CMC). The driving force of the self-assembly and maintenance of supramolecular assembly is hydrophobic interactions of core forming blocks for typical micellar structures. The corona-forming block is water soluble and renders micelles soluble in the aqueous phase. Leveraging the hydrophobic core, micelles have been utilized to enhance the water solubility of hydrophobic molecules.[57] Micelles can be formed using a variety of starting materials. Polymeric micelles employ block copolymers with distinct hydrophobic and hydrophilic regions.[58] Surfactant micelles can be formed by molecules possessing a hydrophilic head and hydrophobic tail.[59] For the delivery of charged

macrostructures like nucleotides or peptides, polyion complex micelles have been widely investigated. This special class of micelles are formed by electrostatic interactions between polyion copolymers, comprised of a neutral segment and an ionic segment, and an oppositely charged ionic species which is typically the therapeutic in drug delivery applications.[60] Micelles are perhaps the most commonly employed approach to formulate drug into a clear, aqueous solution for ophthalmic application. For example, methoxy poly(ethylene glycol)-hexylsubstituted poly(lactide) diblock copolymers were employed to encapsulate and deliver CycA. Results from *in vitro* and *in vivo* studies showed that the formulation was transparent, highly stable, biocompatible, and significantly improved clinical efficacy.[61]

1.4.6 Nanoemulsions

Nanoemulsions offer several advantages in ocular drug delivery, including the ability to solubilise both hydrophilic and hydrophobic therapeutics, excellent stability, and viscous, spreadable mechanical properties.[62] Furthermore, surfactants used to stabilise emulsions can also act as penetration enhancers, thereby improving drug permeability across ocular tissues.[63] Until the recent release of Shire's Xiidra, Allergan's Restasis was the only FDA approved treatment for dry eye disease. Restasis is composed of 0.5% CycA held in an emulsion of carbomer copolymer type A, a proprietary pentaerythritol allyl, castor oil, and the surfactant polysorbate 80. The regulatory approval enjoyed by Restasis is testament to the impact of emulsion drug delivery strategies.[64]

1.4.7 Cubosomes

Some amphiphilic lipids can self-assemble to form curved bicontinuous liquid crystalline materials in aqueous media. These honeycombed structures have gained considerable attention since they impart unique properties of practical interest.[65] Like an emulsion, cubosomes, being dispersions of an inverted type bicontinuous cubic phase, separate two continuous aqueous regions with a lipid bilayer have the ability to dissolve therapeutics of varying polar characteristics. The drug release from cubosomes has shown enhancement in bioavailability by solubilisation of poorly water soluble drugs, decrease in adverse effects, enhancement of intracellular penetration, protection against degradation, and sustained drug release.[66] In the ophthalmic space, cubosomes are a small but growing area of interest. Flurbiprofen (FB) was loaded into cubosomes prepared using hot and high-pressure homogenization. In this study, FB was able to permeate the cornea at nearly 3 times the concentration, providing significantly greater clinical effect than FB in phosphate buffered saline.[67]

1.4.8 Mucoadhesives

The most pressing issue with conventional topical drug delivery to the eye is the short residence time on the ocular surface preventing penetration to target tissues. One method to alleviate this deficiency is to use materials that interact with ocular mucin. This essentially traps drug on the ocular surface to increase the bioavailability of the drug and reduce losses due to lacrimal drainage.

There are many natural and synthetic materials that have been found to be mucoadhesive in some capacity. Categorically, the groups responsible for adhesion to mucin are non-ionic, anionic,

cationic, thiol, and phenylboronic acid polymers. Non-ionic polymers such as methyl cellulose, hydroxypropyl cellulose, and hyaluronic acid typically form the weakest bonds with mucin, although hyaluronic acid in particular can also bind to CD44 which is also prevalent on the ocular surface.[68] Anionic polymers such as poly(acrylic acid), poly(methacrylic acid), carboxymethyl cellulose, and alginate use carboxyl groups to form hydrogen bonds with mucins.[69] Cationic polymers can interact electrostatically with negatively charged sialic acid residues common in mucin molecules.[70] Thiomers are able to form disulphide bonds with cysteine residues in mucin, creating a very long lasting and stable connection.[71] Phenylboronic acid (PBA) is a relatively new class of synthetic mucoadhesive polymers which can form complexes with 1,2-cis-diols.[72] Modifying or creating a drug delivery vehicle to contain mucoadhesive groups can greatly increase bioavailability of its cargo. In one example, CycA encapsulated in a PBA modified micelle resulted in a 14-fold reduction in the amount of drug applied to the ocular surface to achieve the same clinical effect.[73]

1.4.9 Mucin penetrating particles (MPPs)

MPPs take the opposite approach to mucoadhesion and view mucus as a barrier which must be crossed to improve penetration into other ocular tissues. As the bulk viscosity of human mucus is typically 10^3 to 10^4 times higher than water, it was long assumed that diffusion through mucus at rates faster than mucociliary clearance was impossible.[74] However, a series of studies have firmly established that particulates are capable of diffusing through low viscosity pores within the highly elastic mucin fiber matrix at rates similar to water.[75] The strategy, therefore, when creating MPPs is to minimize interaction with mucins through sufficient hydrophilicity and

electrostatic neutrality.[76] Coating nanoparticles with low molecular weight PEG is by far the most widely studied mucus penetrating strategy.[77] Another, more direct approach involves the inclusion of mucolytic agents. No penetration approach is perfect, and the ‘stickiness’ and steric hindrance imposed by mucin networks will always have some effect. For example, recombinant human DNase (rhDNase) can hydrolyze DNA that forms dense entanglements with mucin glycoproteins and other mucus constituents, thus destroying crosslinks and reducing viscoelasticity.[78] N-acetyl-l-cysteine (NAC) is another common mucolytic which can substitute free thiol groups for the disulfide bonds connecting mucin proteins.[79] Polystyrene nanoparticles with a high density of low molecular weight (2kDa) PEG grafted to the surface improve transit through mucosa by up to 3 orders of magnitude in the eye.[80]

1.4.10 Rings and lenses

All the strategies listed above assume a drug formation delivered via drop. Given the widespread appeal of contact lenses, there has been a concerted effort to create a more reliable drug releasing device from on-eye lenses and rings. In general, lens-based drug delivery devices can be categorised as corneal lenses – the same type of lens as conventional contact lenses, hybrid scleral/corneal lenses, or scleral rings depending on where they sit on the ocular surface. Corneal delivery devices have the potential for excellent patient compliance if they serve a dual purpose by providing vision correction. There has been a great deal of interest devoted to converting conventional contact lenses into drug releasing depots. Perhaps the most sophisticated approach involves the use of molecular imprinting to create drug-specific cavities for enhanced

delivery.[81] This technique has been employed using a variety of lens materials, including hydrogel[82] and as silicone hydrogel lenses.[83] In both cases, molecular imprinting can greatly enhance drug loading, and allow much more control over release rate. Corneal/scleral lenses and scleral rings are dedicated drug delivery devices, and have no overlap with refractive correction. As scleral rings do not cover the cornea at all, they come with no possibility of disrupting vision, and can circumvent some of the discomfort many lens users experience when contact is made with the sensitive cornea.[84] While controlled release lens-based devices are an interesting and growing field which may find a natural user base in existing contact lens wearers, they are certainly more invasive and involved than a simple drop. It is unclear if their greater pharmacokinetic properties will counteract their inconvenience.

1.5 Retina

The retina, like many other central nervous system structures, contains a huge diversity of neuronal types. Mammalian retinas contain approximately 55 distinct cell types, each with a different function.[85] The retina is organized into three layers of cell bodies referred to as the outer nuclear layer (ONL), inner nuclear layer (INL) and the ganglion cell layer (GCL) which are separated by two layers of neuropil – the outer plexiform layer (OPL) and the inner plexiform layer (IPL). Retinal neurons comprise sensory photoreceptive cells (rods and cones), interneurons (horizontal cells, bipolar cells and amacrine cells) and output neurons (retinal ganglion cells (RGCs)). There are many subtypes of each type of neuron that vary not only in terms of their function and morphology, but also in their frequencies. Each cell type is

distributed such that the entire retina has the full complement of cell types, and each subtype is evenly tiled across the retina.[86] Underpinning this extremely complex and metabolically demanding tissue is the retinal pigment epithelium (RPE), a pigmented monolayer of cells arranged into a hexagonal, cobblestone-like mosaic anchored to Bruch's membrane. The vascular choriocapillaris, located on the other side of Bruch's membrane, supplies the retinal blood supply.[87] There are a huge variety of pathologies affecting the retina and associated neural circuitry which are currently controlled with frequent intraocular injections. In an effort to improve treatment efficacy, a number of alternative drug delivery platforms have innovated on the status quo, and will be discussed below.

1.6 Posterior segment strategies

Before delving into posterior segment treatment strategies, it should be noted that all of the approaches listed above, which aim to increase ocular permeation and bioavailability, also apply to the back of the eye. Indeed, many drugs aimed at posterior conditions – glaucoma medications for example – are typically delivered via eyedrop. However, due to the poor penetration to the posterior segment, despite the most exotic innovations, some treatments require a more direct approach. Typically, this is accomplished via direct injection into the vitreous, which, while highly effective, is associated with significant risk, including retinal detachment, haemorrhage, injection, cataract formation, and patient discomfort.[88] Furthermore, due to clearance from the eye and the relatively short half-life of drug *in vivo*, scheduled injections are needed, often monthly.[89] Novel drug delivery paradigms which can minimise injection frequency or forgo an injection altogether represent a revolutionary innovation in ophthalmics.

1.6.1 Implantable controlled release devices

Perhaps the most obvious solution to intravitreal drug delivery involves the use of an implanted scaffold within the vitreal chamber. The scope of this enterprise is enormous, with many intravitreal implants already in use. Some devices, such as SurModics' iconic I-vation implantable drug delivery system, is anchored to the outer wall of the eye. The I-vation device is shaped like a helical screw, which gives it a large surface area from which to elute drug, but also allows it to self-fasten through the sclera without the use of sutures. It is made of a nonferrous metal alloy covered in a proprietary copolymeric coating, and can deliver a variety of relevant therapeutics for up to 2 years.[90] While the I-vation is firmly secured away from the visual axis, other implanted devices are left to float free. The Posurdex system (now Ozurdex), which takes its name from its role delivering dexamethasone to the posterior segment, is a bioresorbable copolymer of lactic acid and glycolic acid impregnated with the corticosteroid dexamethasone. The device is smaller than a grain of rice, and can release therapeutic quantities of dexamethasone for up to 6 months following placement.[91] A similar but non-degrading device called Iluvien is able to release a continuous, appropriate dose of the corticosteroid fluocinolone acetonide for over 36 months. However, as this device is non-degrading, they stay in the eye for as long as the patient lives, and in some cases can cause serious problems as a result.[92]

Generally speaking, all implantable devices work in the same way, with differences in geometry, method of insertion, and degradability. While there are certainly advantages and disadvantages to the various approaches, it is still too early to predict how these devices will compare. For a complete review of implanted intravitreal drug releasing devices, see the review by Barar et al.[93]

1.6.2 Particles

Encasing pharmaceuticals in polymeric particles of various design can control and prolong release as well as protect them from the degradative environment found inside living things. Micro- or nanoparticles are typically small enough not to significantly interfere with vision even when suspended in the vitreous (although cloudiness is not uncommon), and can provide sustained release for weeks or even months.[94] Microspheres have been examined for intravitreal administration by a number of groups with some success.[95] The size of these particles seems to be their most critical parameter – particularly in the eye where inflammation of any kind can be catastrophic. Microparticles larger than 10 μ m, cannot be ingested by phagocytic cells, which can lead a damaging immune response. Conversely, particles smaller than 5 μ m may undergo phagocytosis, leading to rapid degradation and a concomitant increase in drug release, resulting in a shorter than desired treatment.[96] Likewise, nanoparticles have seen some success in this space. Triamcinolone acetonide formulated in PLGA nanoparticles was able to achieve a similar clinical effect with a much more lenient dosing schedule than drug alone in a rabbit model of uveitis.[97] However, the potential immune interactions and off target effects of nanotechnology are even more contentious than with larger microparticles; there are currently no commercial formulations using these modalities.[98]

1.6.3 Iontophoresis

Iontophoresis is a non-invasive technology that increases the permeability of ocular barriers to ionized drugs using electric current. Using this approach, no injection is required to force large

amounts of drug into the posterior segment. However, as only a therapeutic is transported, the problem of clearance and frequent redosing remains. Iontophoresis devices are currently undergoing clinical trials for a variety of indications with some success.[99]

1.6.4 *In situ* gelling systems

Polymers which can form gels after injection are an extremely attractive solution to intravitreal drug delivery. Unlike the fixed-dose, rigid polymeric systems described earlier, *in situ* forming gels can be mixed with drug and injected, creating drug releasing scaffolds of at arbitrary sizes, and release rates. The use of intelligent materials that undergo a stimuli-induced phase transition from liquid to gel thus offer an extremely flexible and elegant solution to posterior segment therapeutics while staying within a minimally invasive envelope. There are numerous strategies used to form gels, including changes in light, pH, temperature, or the interaction of previously separate reactive groups. In the Sheardown lab, we are interested in the potential use of thermally gelling biomaterials based on PNIPAAm, for minimally invasive posterior segment drug delivery.[100] Thermosensitive hydrogels offer several unique advantages in this space, which will be discussed in further detail in the following section. Other forms of stimuli responsive materials have been used successfully in the back of the eye. PEG-anthracene grafted hyaluronan hydrogels can crosslink or decrosslink in response to specific frequencies of light. These hyaluronic acid photogels can be stimulated to both release drug when needed and stop drug release when symptoms are under control, all with non-invasive UV exposure.[101] Hydrophobic phase separation was used to create an injectable hydrogel system based on PEG and a vitamin E (Ve) methacrylate copolymer for posterior segment therapeutics. The hydrogel

forms immediately in an aqueous environment, driven by aqueous induced polymer chain rearrangement and phase separation, which is a spontaneous process with water uptake. The hydrogels can be customized to give the desired water content, mechanical strength, and drug release kinetics simply by formulating the PEG-coVe polymer with an appropriate solvent mixture or by varying the molecular weight of the polymer.[102] Poly(ethylene glycol) methacrylate (PEGMA) materials are an intriguing category of *in situ* gelling system which rely on a specialized injection device which keeps two reactive components separate until mixing them just before injection. In one example, PEGMA precursor materials modified with either alkyne or azide were designed to be injected through a double barrel syringe with a mixing head. After injection, the ‘click chemistry’ reaction between the reactive groups would crosslink the gel in situ, trapping therapeutic inside.[103]

1.6.5 Micro-Electromechanical Devices

While still considered futuristic by clinicians, micro-electromechanical (MEMS) drug delivering systems may soon be incorporated into mainstream ocular drug delivery. If shrunk to an appropriately small form factor, MEMS can rest on the surface of the eye and deliver drugs through a canula or microneedle array.[104] Drug release profiles from MEMS devices are actively managed and thus are not governed by diffusion like all previous examples. Moreover, externally accessible, refillable reservoirs allow administration of subsequent doses without the need for surgical intervention. One such device designed for intravitreal drug delivery uses inexpensive glass capillary microneedles embedded in a flexible Polydimethylsiloxane matrix and a remotely controllable electroosmotic pump.[105]

1.7 Thermosensitive hydrogels

The biological application of hydrogels began with the use of poly(2-hydroxyethyl methacrylate) (pHEMA) as a soft contact lens material in the early 1960s. Recently, hydrogels have gained enormous traction as useful and versatile biomaterials. In general, hydrogels are considered to be cross-linked 3-D networks containing covalent bonds, physical cross-links, hydrogen bonds, strong van der Waals interactions, and crystallite associations. These various interactions can ultimately lead to a very interesting effect: hydrogels can often self-structure with changes in temperature. This temperature sensitivity can be divided into two broad categories: those that phase separate from solution upon heating and those that phase separate upon cooling. The first display a lower critical solution temperature (LCST) in their phase diagram, the latter an upper critical solution temperature (UCST). Both types of systems possess an interesting potential for use in biomedical applications due to their ability to respond to their environment. The motivation behind research in this field is the development of appropriately named ‘smart’ materials that exploit this kind of responsivity.

While many common biomaterials leverage their UCST – gelatin or agarose for example – these types of materials have not found a biomedical niche the way LCST materials have.[106] LCST materials are homogeneous at low temperatures, but when heated, aggregation of hydrophobic groups induces phase separation and hydrogel formation.[107]

1.8 Natural polymers

1.8.1 Chitosan materials

Chitosan is a polysaccharide made from chitin, the monomeric element found in the exoskeletons of arthropods. When discussing naturally derived polymers, the aggregate biomass of chitin on earth is second only to cellulose.[108] Chitosan alone is not thermosensitive, but can be made so through the addition of glycerophosphate (GP)[109] At elevated temperatures, GP forms strong hydrogen bonds with chitosan, which leads to gel formation through a variety of interactions, including (1) electrostatic attractions between chitosan ammonium groups and the GP phosphate group, (2) hydrogen bonds between chitosan chains, due to the decreased electrostatic repulsion after neutralization of the ammonium groups by GP, and (3) chitosan-chitosan hydrophobic interactions.[110] This chitosan-GP hydrogel system has an unusually long gelation time (approximately 10 minutes), and is not ideal for applications requiring instantaneous gelation or where a faster gelation is needed. To expedite this process, a derivative of chitosan, chitosan chloride, can be used. Its improved solubility facilitates a gelation time of less than one minute.[111] Gels of this type have been used to encapsulate mesenchymal stem cells (MSCs) for delivery into acute injured kidney. Results show that these hydrogels improve the retention and survival of grafted MSCs, as well as enhance the proliferation activity and reduce apoptosis of host renal cells. Significant improvement of the renal function, microvessel density and tubular cell proliferation were observed after treatment, indicating enormous potential as a cell carrier for treatment of acute kidney injuries[112] Thermosensitive chitosan derivatives have seen particular utility as a cell delivery scaffold for cartilage tissue engineering. Chondrocytes, the cells responsible for producing and maintaining cartilaginous matrices, benefit an enormous amount from the anchorage provided by chitosan delivery vehicles.[113, 114] Release kinetics from chitosan scaffolds indicate a relatively rapid ejection of both protein and low molecular weight drugs – complete release occurs within a few hours. [115] This significantly impedes

adoption of chitosan based drug delivery scaffolds when sustained therapeutic release is desired. Exotic solutions, such as the encapsulation of a drug-loaded liposome within a chitosan-GP matrix can greatly enhance retention time.[116] Potential toxicity is another concern of chitosan based drug delivery systems. *In vivo* experimentation shows significant adverse inflammation in response to these materials, which may limit their utility.[117]

1.8.2 Cellulose materials

The structural unit in plant cell walls, cellulose is the most abundant naturally derived polymer in the world. It is a linear polymer with β -(1,4)-D-glucose as the repeating monomeric unit.[118] While not in itself thermosensitive, several cellulose derivatives such as methylcellulose (MC) and hydroxypropylmethylcellulose (HPMC) have an established biomedical precedent and FDA approval. [118] . At low temperatures, these polymers exist in a fully hydrated state with minimal intramolecular interaction. When heated, interactions between the methoxy groups result in gradual dehydration and ultimately gel formation.[119] While the LCST values of MC and HPMC are physiologically irrelevant (45°C and 80°C respectively), gelation temperature can be lowered both chemically and physically.[110] The addition of NaCl or a reduction of hydroxypropyl content has been shown to result in physiologically useful LCSTs. Physically blending cellulose based hydrogels with other materials can also improve their properties. Blending hyaluronan and MC (HAMC), for example, has demonstrated rapid thermoreversible *in situ* gelation, degradability and good *in vivo* tolerance. This combination has been used to encapsulate and locally deliver both drugs and cells to fragile tissues requiring a minimally invasive approach, such as the spine[120] and retina.[121]

1.8.3 Xyloglocan materials

Xyloglucan, a hemicelluloses, has also been used as a thermosensitive gel. In its native form, the xyloglucan polysaccharides do not form a gel. However, when some of the galactose residues have been removed, xyloglucan exhibits temperature responsive behavior.[122] Upon heating, xyloglucan aqueous solutions gel in two distinct stages. In the first, thin membranes form within the hydrogel extremely rapidly. In the second, a three-dimensional network of thin membranes form, resulting in a dramatic increase in the modulus, which is tunable based on concentration.[123] Xyloglucan has been studied in a variety of biomedical contexts – particularly as a drug delivery scaffold.[124] Xyloglucan materials have been used to aid in axonal regrowth, which is an essential part of recovery from brain injury. To encourage axonal sprouting, scaffolds can be used to support axon extension and provide an artificial cellular microenvironment for neurones.[125] Thermally gelling xyloglucan, particularly when grafted with poly-D-lysine (PDL), maintains and supports the differentiation of cortical neurones and neural stem cells, and enhances the regenerative capacity of the brain.[126]

1.8.4 Elastin-like polypeptides

Elastin-like polypeptides (ELPs) are synthetic elastin-inspired polymers with a pentapeptide amino acid repeat structure, Val-Pro-Gly-Xaa-Gly, where the Xaa residue can be any natural

amino acid except proline.[127] Above an LCST, ELPs form a gel through coacervative aggregation, the properties of which can be manipulated through concentration, temperature, molecular weight, and salt content.[128] ELPs are interesting biomaterial candidates as they degrade into simple amino acid residues. Further, the Xaa residue gives the system enormous tunability, allowing not only variable amino acid sequences, but functionalization with other elements.[129] Using transgenic producers such as E.coli, the dispersity and composition of ELPs can be precisely tailored to a variety of tasks.[130] Furthermore, ELPs can be easily purified as a result of their thermogelling behavior.[131] ELPs have been used in several different capacities as drug delivery vehicles for tumors. In one strategy, tumor tissues were passively targeted by employing drug-conjugated ELPs which accumulate within permeable tumor tissues following systemic delivery.[132] In another approach, ELP-drug conjugates were engineered to gel between 37 and 42°C were immobilized in target tissues with externally locally applied heat.[133] Direct injection has also proven successful; gelation within tumorous tissues driven by physiological heat was able to produce a sustained release depot directly within the tumor.[134]

1.9 Synthetic polymers

1.9.1 Poly(ethylene oxide)(PEO) materials

Triblock polyethers with a PEO-PPO-PEO configuration, known as Pluronics or Poloxamers are a well studied group of thermosensitive biomaterials. Using a range of monomeric molecular weights and block lengths, these copolymers can be engineered to phase transition from a liquid to gel across a range of temperature and pH conditions.[135] The combination of hydrophilic

ethylene oxide and hydrophobic propylene oxide units creates an amphiphilic molecule that can self-associate into micelles above an LCST. As the temperature of the system increases, the PPO chains become less soluble, and intramolecular hydrophobic interaction governs gel formation.[136] Pluronic micelles typically possess a diameter ranging from 10 to 100 nm and consist of a hydrophobic PPO-rich core and a hydrated, hydrophilic PEO-rich shell.[88] Pluronic hydrogels have a fast dissolution rate, which makes long term delivery of therapeutic agents a challenge. However, they are easily modified due to terminating hydroxyl groups, allowing facile functionalization for a variety of applications. For example incorporating crosslinkable groups can greatly improve stability.[137] Polyethers cannot be degraded easily in vitro or in vivo, rendering Pluronic hydrogels non-degradable. This limits their applicability where degradable materials are required.

PEO based polyester hydrogels are a different class of materials with comparatively improved mechanical properties and which readily biodegrade. Polyesters such as polylactide (PLA),[138] poly(lactide-co-glycolide)(PLGA),[139] polyglycolide(PGA)[140] and polycaprolactone (PCL)[141] have been copolymerized to PEO to impart thermoresponsiveness. PEO containing copolymers have attracted significant interest, and have been used in a variety of tissues for many different reasons.[142] While generally well tolerated immunologically, degradation products of these polyesters, such as PLA, PLGA, and PCL are invariably acidic, which can significantly alter the pH of a tissue microenvironment, as well as having the potential to provoke a severe inflammatory response.[143]

1.9.2 Polyacrylamide derivatives

Many n-substituted polyacrylamides are thermosensitive. Polymers such as poly(N,N-dimethylacrylamide),^[144] poly(N-vinyl caprolactam)^[145] and poly(N-(2-hydroxypropyl)methacrylamide lactate)^[146], for example, all undergo a reversible phase transitions in response to elevating temperature. Poly(N -isopropylacrylamide)(PNIPAAm) is by far the most studied temperature sensitive polyacrylamide. Due to increasing hydrophobic interaction between the n-substituted groups, it undergoes a rapid gelation when heated above its physiologically relevant LCST of approximately 32°C. Unmodified, PNIPAAm lacks relevant properties for most conceivable biomedical applications. A variety of chemical modifications have therefore been attempted to satisfy its many potential uses. One of the major limitations of PNIPAAm is that it is nondegradable. Degradable materials facilitate their elimination following the completion of their task without the potential of secondary surgical removal or infinite residence times. Ultimately, it is desirable to preserve the thermal phase transition properties of PNIPAAm, while promoting eventual degradation and clearance from the body following a therapeutic effect. Direct degradation of the PNIPAAm molecule is typically undesirable, as NIPAAm in its monomeric form is highly toxic, acting as a neurotoxin and having the potential to cause birth defects.^[147] A common strategy to accomplish this goal involves the introduction of a hydrophobic group which participates in the gelation of the polymer, but which are themselves hydrolytically labile. For example, NIPAAm-based polymers were synthesized with 2-hydroxyethyl methacrylate-monolactate (HEMA-monolactate) groups. As the hydrolytically labile lactate ester side groups were cleaved, the hydrophilicity of the copolymer increased, raising the LCST. If the LCST is raised above body temperature, the thermoreversible NIPAAm-based copolymers revert back into liquid state, allowing clearance from the body with no low molecular weight by-products.^[148] Similar clearance mechanisms were imparted

through crosslinking of degradable poly(amino acids) or copolymerization with dimethyl- γ -butyrolactone acrylate (DBA).[149]

1.9.3 Polyphosphazenes

Polyphosphazenes are emerging candidates as thermosensitive biomaterials. They are hybrid organic-inorganic polymers with alternating nitrogen and phosphorus atoms joined by alternating single and double bonds.[150] Polyphosphazenes are extremely versatile; attached to every phosphorous group are two organic groups which can be modified to impart various functionalities - including thermosensitivity. Polyphosphazene-based hydrogels have good biocompatibility and their degradation products - ammonia, phosphate and ethanol - are non-toxic.[151] Their fast *in situ* gelation, coupled with highly tunable degradation kinetics and *in vivo* biocompatibility make polyphosphazenes intriguing materials.

1.10 Architecture

A critical factor when designing *in situ* forming hydrogel scaffolds is the type of polymeric architecture that will be most suitable for the intended application. Besides simple bulk gels, polymeric interactions can result in interpenetrating networks (IPNs), micelles, polymersomes, and films. Hydrogel architecture can be divided into two general categories: physical and chemical. Physical gels result from the entanglement of polymer chains or the spontaneous ordering of micelles, whereas crosslinked gels are covalently bound.[152] The thermoresponsive characteristics of these categories are different as well; crosslinked networks will swell or

deswell in response to temperature, while physically linked gels undergo a sol-gel phase transition. Covalently linked networks are often formed prior to implantation, but can also be formed *in situ* via a two-part system where ingredients mix during implantation.

IPNs consist of two or more polymer networks that are bound through physical entanglement in such a way that the networks can only be separated through bond breakage. IPNs are intriguing materials due to the ability of each component of these networks to offer an independent set of properties. Synergistic or otherwise complementary functionality across these different members can produce effects greater than the sum of their parts. a powerful tool for drug delivery as each polymer in the network can introduce specific properties, such as temperature-sensitivity, and new properties can arise from the interaction of the various polymers within the network.

Furthermore, aggregate properties can often be tuned by simply altering the polymer ratio, without the need for complex chemistry. IPNs have extensive precedent in drug and cell delivery. As another example, a chitosan–PNIPAM interpenetrating network was able to significantly increase loading capacity of the NSAID diclofenac compared to a pure PNIPAM hydrogel while maintaining thermosensitivity necessary to regulate the release kinetics.[153] Furthermore, a tissue engineering study found collagen–hyaluronic acid IPNs were able to more acutely mimic extracellular matrix than either component alone.[154]

As discussed earlier, amphiphilic block copolymers can spontaneously assemble into micelles with a hydrophilic corona and a hydrophobic core. Therefore, they are particularly useful at masking and solubilising hydrophobic drugs. Micelles have found particular use as component of chemotherapy, where they provide hydrophobic cancer drugs with the solubility needed to access the blood stream.[155] As tumour vasculature is typically malformed and leaky, micelles loaded with drug tend to accumulate there. Building thermoresponsivity into micelles has the potential

to improve clinical efficacy in tissue microenvironments with different temperature profiles. For example, PNIPAAm based thermoresponsive micelles have been created which alter their drug release kinetics as a result of temperature-driven deformation.[156]

Similar to micelles, polymersomes are another class of self-assembling particles made up of amphiphilic components. Polymersomes have both a hydrophilic corona and core, with a hydrophobic sphere sandwiched between them. Unlike a micelle, polymersomes allow the encapsulation of both hydrophilic and hydrophobic therapeutics within its multi-layered interior. Further, polymersome geometry provides rate controlling surfaces for both hydrophilic and hydrophobic cargo, facilitating controlled release; hydrophilic drugs stored in the core will need to diffuse through a hydrophobic layer, and drugs in the hydrophobic layer will need to penetrate the hydrophilic corona.[157] PNIPAAm containing polymersomes have been used in exotic temperature sensitive drug delivery. For example, the chemotherapeutic drug doxorubicin was packaged into PEG-PNIPAAm polymersomes that could trap it when heated above their LCST, but would disassemble upon cooling. These particles, after being deposited within the tumour, could be cooled with a cryoprobe to release their cargo.[158]

Thermoresponsive films have enormous utility in tissue culture. Tissue culture plates coated with a thermosensitive film can facilitate the delamination of intact cell sheets with intact extracellular matrix by undergoing a gel-sol transition. Thus, while indirect, thermosensitive films are essential for modern tissue engineering.[159]

1.11 References

1. Thakur, A., et al., *Strategies for ocular siRNA delivery: Potential and limitations of non-viral nanocarriers*. J Biol Eng, 2012. **6**(1): p. 7.
2. Cholkar, K., et al., *Novel strategies for anterior segment ocular drug delivery*. J Ocul Pharmacol Ther, 2013. **29**(2): p. 106-23.
3. Duvvuri, S., S. Majumdar, and A.K. Mitra, *Role of metabolism in ocular drug delivery*. Curr Drug Metab, 2004. **5**(6): p. 507-15.
4. Yang, J.J., K.J. Kim, and V.H. Lee, *Role of P-glycoprotein in restricting propranolol transport in cultured rabbit conjunctival epithelial cell layers*. Pharm Res, 2000. **17**(5): p. 533-8.
5. Hosoya, K., V.H. Lee, and K.J. Kim, *Roles of the conjunctiva in ocular drug delivery: a review of conjunctival transport mechanisms and their regulation*. Eur J Pharm Biopharm, 2005. **60**(2): p. 227-40.
6. Liu, S., et al., *Expression and function of muscarinic receptor subtypes on human cornea and conjunctiva*. Invest Ophthalmol Vis Sci, 2007. **48**(7): p. 2987-96.
7. Dartt, D.A., *Regulation of mucin and fluid secretion by conjunctival epithelial cells*. Prog Retin Eye Res, 2002. **21**(6): p. 555-76.
8. Takahashi, Y., et al., *Anatomy of secretory glands in the eyelid and conjunctiva: a photographic review*. Ophthal Plast Reconstr Surg, 2013. **29**(3): p. 215-9.
9. Gukasyan, H.J., et al., *Metabolism and transport of purinergic receptor agonists in rabbit conjunctival epithelial cells*. Adv Exp Med Biol, 2002. **506**(Pt A): p. 255-9.

10. Hodges, R.R. and D.A. Dartt, *Tear film mucins: front line defenders of the ocular surface; comparison with airway and gastrointestinal tract mucins*. *Exp Eye Res*, 2013. **117**: p. 62-78.
11. Holly, F.J. and M.A. Lemp, *Tear physiology and dry eyes*. *Surv Ophthalmol*, 1977. **22**(2): p. 69-87.
12. Sapkota, K., et al., *Goblet cell density association with tear function and ocular surface physiology*. *Cont Lens Anterior Eye*, 2015. **38**(4): p. 240-4.
13. Floyd, A.M., et al., *Mucin deficiency causes functional and structural changes of the ocular surface*. *PLoS One*, 2012. **7**(12): p. e50704.
14. Yu, T., et al., *Mucus-Penetrating Nanosuspensions for Enhanced Delivery of Poorly Soluble Drugs to Mucosal Surfaces*. *Adv Healthc Mater*, 2016. **5**(21): p. 2745-2750.
15. Popov, A., et al., *Mucus-penetrating nanoparticles made with "mucoadhesive" poly(vinyl alcohol)*. *Nanomedicine*, 2016. **12**(7): p. 1863-1871.
16. Craparo, E.F., et al., *Pegylated Polyaspartamide-Polylactide-Based Nanoparticles Penetrating Cystic Fibrosis Artificial Mucus*. *Biomacromolecules*, 2016. **17**(3): p. 767-77.
17. Davidson, H.J. and V.J. Kuonen, *The tear film and ocular mucins*. *Vet Ophthalmol*, 2004. **7**(2): p. 71-7.
18. Ustundag-Okur, N., et al., *Novel nanostructured lipid carrier-based inserts for controlled ocular drug delivery: evaluation of corneal bioavailability and treatment efficacy in bacterial keratitis*. *Expert Opin Drug Deliv*, 2015. **12**(11): p. 1791-807.

19. Stachs, O., et al., *In vivo three-dimensional confocal laser scanning microscopy of the epithelial nerve structure in the human cornea*. Graefes Arch Clin Exp Ophthalmol, 2007. **245**(4): p. 569-75.
20. Oh, J.Y., et al., *Corneal cell viability and structure after transcorneal freezing-thawing in the human cornea*. Clin Ophthalmol, 2010. **4**: p. 477-80.
21. Mathew, J.H., J.P. Bergmanson, and M.J. Doughty, *Fine structure of the interface between the anterior limiting lamina and the anterior stromal fibrils of the human cornea*. Invest Ophthalmol Vis Sci, 2008. **49**(9): p. 3914-8.
22. Hornof, M., E. Toropainen, and A. Urtti, *Cell culture models of the ocular barriers*. Eur J Pharm Biopharm, 2005. **60**(2): p. 207-25.
23. Eghrari, A.O., S.A. Riazuddin, and J.D. Gottsch, *Overview of the Cornea: Structure, Function, and Development*. Prog Mol Biol Transl Sci, 2015. **134**: p. 7-23.
24. Hu, W., et al., *The structure and development of Xenopus laevis cornea*. Exp Eye Res, 2013. **116**: p. 109-28.
25. Palchesko, R.N., J.L. Funderburgh, and A.W. Feinberg, *Engineered Basement Membranes for Regenerating the Corneal Endothelium*. Adv Healthc Mater, 2016. **5**(22): p. 2942-2950.
26. Hayashi, K., et al., *Immunohistochemical evidence of the origin of human corneal endothelial cells and keratocytes*. Graefes Arch Clin Exp Ophthalmol, 1986. **224**(5): p. 452-6.
27. He, Z., et al., *Revisited microanatomy of the corneal endothelial periphery: new evidence for continuous centripetal migration of endothelial cells in humans*. Stem Cells, 2012. **30**(11): p. 2523-34.

28. Fischbarg, J. and D.M. Maurice, *An update on corneal hydration control*. Exp Eye Res, 2004. **78**(3): p. 537-41.
29. Srinivas, S.P., *Dynamic regulation of barrier integrity of the corneal endothelium*. Optom Vis Sci, 2010. **87**(4): p. E239-54.
30. Verkman, A.S., *Role of aquaporin water channels in eye function*. Exp Eye Res, 2003. **76**(2): p. 137-43.
31. Miller, D.W., M. Hinton, and F. Chen, *Evaluation of drug efflux transporter liabilities of darifenacin in cell culture models of the blood-brain and blood-ocular barriers*. Neurorol Urodyn, 2011. **30**(8): p. 1633-8.
32. Karla, P.K., et al., *Molecular expression and functional evidence of a drug efflux pump (BCRP) in human corneal epithelial cells*. Curr Eye Res, 2009. **34**(1): p. 1-9.
33. Dey, S., et al., *Molecular evidence and functional expression of P-glycoprotein (MDR1) in human and rabbit cornea and corneal epithelial cell lines*. Invest Ophthalmol Vis Sci, 2003. **44**(7): p. 2909-18.
34. Anand, B.S., S. Dey, and A.K. Mitra, *Current prodrug strategies via membrane transporters/receptors*. Expert Opin Biol Ther, 2002. **2**(6): p. 607-20.
35. Rodriguez-Aller, M., et al., *In vivo characterisation of a novel water-soluble Cyclosporine A prodrug for the treatment of dry eye disease*. Eur J Pharm Biopharm, 2012. **80**(3): p. 544-52.
36. Babizhayev, M.A. and A. Kasus-Jacobi, *State of the art clinical efficacy and safety evaluation of N-acetylcarnosine dipeptide ophthalmic prodrug. Principles for the delivery, self-bioactivation, molecular targets and interaction with a highly evolved*

- histidyl-hydrazide structure in the treatment and therapeutic management of a group of sight-threatening eye diseases. Curr Clin Pharmacol, 2009. 4(1): p. 4-37.*
37. Chang, S.C., et al., *Relative effectiveness of prodrug and viscous solution approaches in maximizing the ratio of ocular to systemic absorption of topically applied timolol. Exp Eye Res, 1988. 46(1): p. 59-69.*
38. Anand, B.S. and A.K. Mitra, *Mechanism of corneal permeation of L-valyl ester of acyclovir: targeting the oligopeptide transporter on the rabbit cornea. Pharm Res, 2002. 19(8): p. 1194-202.*
39. Gunda, S., S. Hariharan, and A.K. Mitra, *Corneal absorption and anterior chamber pharmacokinetics of dipeptide monoester prodrugs of ganciclovir (GCV): in vivo comparative evaluation of these prodrugs with Val-GCV and GCV in rabbits. J Ocul Pharmacol Ther, 2006. 22(6): p. 465-76.*
40. Vadlapudi, A.D., R.K. Vadlapatla, and A.K. Mitra, *Current and emerging antivirals for the treatment of cytomegalovirus (CMV) retinitis: an update on recent patents. Recent Pat Antiinfect Drug Discov, 2012. 7(1): p. 8-18.*
41. Chen, Y., et al., *Ocular delivery of cyclosporine A based on glyceryl monooleate/poloxamer 407 liquid crystalline nanoparticles: preparation, characterization, in vitro corneal penetration and ocular irritation. J Drug Target, 2012. 20(10): p. 856-63.*
42. Hippalgaonkar, K., et al., *Indomethacin-loaded solid lipid nanoparticles for ocular delivery: development, characterization, and in vitro evaluation. J Ocul Pharmacol Ther, 2013. 29(2): p. 216-28.*

43. Quinteros, D., et al., *Hybrid formulations of liposomes and bioadhesive polymers improve the hypotensive effect of the melatonin analogue 5-MCA-NAT in rabbit eyes.* PLoS One, 2014. **9**(10): p. e110344.
44. Gao, Y., et al., *PLGA-PEG-PLGA hydrogel for ocular drug delivery of dexamethasone acetate.* Drug Dev Ind Pharm, 2010. **36**(10): p. 1131-8.
45. Gupta, V., et al., *PLGA microparticles encapsulating prostaglandin E1-hydroxypropyl-beta-cyclodextrin (PGE1-HPbetaCD) complex for the treatment of pulmonary arterial hypertension (PAH).* Pharm Res, 2011. **28**(7): p. 1733-49.
46. Bragagni, M., et al., *Cyclodextrin complexation highly enhances efficacy of arylsulfonyleido benzenesulfonamide carbonic anhydrase inhibitors as a topical antiglaucoma agents.* Bioorg Med Chem, 2015. **23**(18): p. 6223-7.
47. Aktas, Y., et al., *Influence of hydroxypropyl beta-cyclodextrin on the corneal permeation of pilocarpine.* Drug Dev Ind Pharm, 2003. **29**(2): p. 223-30.
48. Rudrangi, S.R., et al., *Influence of the preparation method on the physicochemical properties of indomethacin and methyl-beta-cyclodextrin complexes.* Int J Pharm, 2015. **479**(2): p. 381-90.
49. Sun, X., et al., *Voriconazole Compositated Polyvinyl Alcohol/Hydroxypropyl-beta-Cyclodextrin Nanofibers for Ophthalmic Delivery.* PLoS One, 2016. **11**(12): p. e0167961.
50. Cholkar, K., et al., *Novel Nanomicellar Formulation Approaches for Anterior and Posterior Segment Ocular Drug Delivery.* Recent Pat Nanomed, 2012. **2**(2): p. 82-95.
51. Kumar, R. and V.R. Sinha, *Lipid Nanocarrier: an Efficient Approach Towards Ocular Delivery of Hydrophilic Drug (Valacyclovir).* AAPS PharmSciTech, 2016.

52. Valls, R., et al., *Transcorneal permeation in a corneal device of non-steroidal anti-inflammatory drugs in drug delivery systems*. Open Med Chem J, 2008. **2**: p. 66-71.
53. Zhang, L., et al., *Preparation and in vitro and in vivo characterization of cyclosporin A-loaded, PEGylated chitosan-modified, lipid-based nanoparticles*. Int J Nanomedicine, 2013. **8**: p. 601-10.
54. Liu, Y., L. Ren, and Y. Wang, *Crosslinked collagen-gelatin-hyaluronic acid biomimetic film for cornea tissue engineering applications*. Mater Sci Eng C Mater Biol Appl, 2013. **33**(1): p. 196-201.
55. Contreras-Ruiz, L., et al., *Intracellular trafficking of hyaluronic acid-chitosan oligomer-based nanoparticles in cultured human ocular surface cells*. Mol Vis, 2011. **17**: p. 279-90.
56. Wang, G., et al., *Self-Assembled Thermoresponsive Nanogels Prepared by Reverse Micelle --> Positive Micelle Method for Ophthalmic Delivery of Muscone, a Poorly Water-Soluble Drug*. J Pharm Sci, 2016. **105**(9): p. 2752-9.
57. Pepic, I., et al., *A nonionic surfactant/chitosan micelle system in an innovative eye drop formulation*. J Pharm Sci, 2010. **99**(10): p. 4317-25.
58. Mandal, A., et al., *Polymeric micelles for ocular drug delivery: From structural frameworks to recent preclinical studies*. J Control Release, 2017. **248**: p. 96-116.
59. Kalmar, E., et al., *Novel sample preparation method for surfactant containing suppositories: effect of micelle formation on drug recovery*. J Pharm Biomed Anal, 2013. **83**: p. 149-56.

60. Wang, J., et al., *Selective intracellular drug delivery from pH-responsive polyion complex micelle for enhanced malignancy suppression in vivo*. *Colloids Surf B Biointerfaces*, 2015. **135**: p. 283-90.
61. Di Tommaso, C., et al., *Novel micelle carriers for cyclosporin A topical ocular delivery: in vivo cornea penetration, ocular distribution and efficacy studies*. *Eur J Pharm Biopharm*, 2012. **81**(2): p. 257-64.
62. Li, X., et al., *Mucoadhesive dexamethasone acetate-polymyxin B sulfate cationic ocular nanoemulsion--novel combinatorial formulation concept*. *Pharmazie*, 2016. **71**(6): p. 327-33.
63. Tayel, S.A., et al., *Promising ion-sensitive in situ ocular nanoemulsion gels of terbinafine hydrochloride: design, in vitro characterization and in vivo estimation of the ocular irritation and drug pharmacokinetics in the aqueous humor of rabbits*. *Int J Pharm*, 2013. **443**(1-2): p. 293-305.
64. Bataoel, A., *Restasis use in the chronic dry eye patient*. *Insight*, 2007. **32**(3): p. 21.
65. Karami, Z. and M. Hamidi, *Cubosomes: remarkable drug delivery potential*. *Drug Discov Today*, 2016. **21**(5): p. 789-801.
66. Hartnett, T.E., A.J. O'Connor, and K. Ladewig, *Cubosomes and other potential ocular drug delivery vehicles for macromolecular therapeutics*. *Expert Opin Drug Deliv*, 2015. **12**(9): p. 1513-26.
67. Han, S., et al., *Novel vehicle based on cubosomes for ophthalmic delivery of flurbiprofen with low irritancy and high bioavailability*. *Acta Pharmacol Sin*, 2010. **31**(8): p. 990-8.
68. Khutoryanskiy, V.V., *Advances in mucoadhesion and mucoadhesive polymers*. *Macromol Biosci*, 2011. **11**(6): p. 748-64.

69. Rillosi, M. and G. Buckton, *Modelling mucoadhesion by use of surface energy terms obtained from the Lewis acid-Lewis base approach. II. Studies on anionic, cationic, and unionisable polymers*. Pharm Res, 1995. **12**(5): p. 669-75.
70. de Oliveira Fulgencio, G., et al., *Mucoadhesive chitosan films as a potential ocular delivery system for ofloxacin: preliminary in vitro studies*. Vet Ophthalmol, 2014. **17**(2): p. 150-5.
71. Bhatia, M., M. Ahuja, and H. Mehta, *Thiol derivatization of Xanthan gum and its evaluation as a mucoadhesive polymer*. Carbohydr Polym, 2015. **131**: p. 119-24.
72. Liu, Y., L. Ren, and Z. Liu, *A unique boronic acid functionalized monolithic capillary for specific capture, separation and immobilization of cis-diol biomolecules*. Chem Commun (Camb), 2011. **47**(17): p. 5067-9.
73. Liu, S., et al., *Prolonged Ocular Retention of Mucoadhesive Nanoparticle Eye Drop Formulation Enables Treatment of Eye Diseases Using Significantly Reduced Dosage*. Mol Pharm, 2016. **13**(9): p. 2897-905.
74. Lamont, J.T., *Mucus: the front line of intestinal mucosal defense*. Ann N Y Acad Sci, 1992. **664**: p. 190-201.
75. Olmsted, S.S., et al., *Diffusion of macromolecules and virus-like particles in human cervical mucus*. Biophys J, 2001. **81**(4): p. 1930-7.
76. Ensign, L.M., et al., *Mucus penetrating nanoparticles: biophysical tool and method of drug and gene delivery*. Adv Mater, 2012. **24**(28): p. 3887-94.
77. Nance, E., et al., *Brain-penetrating nanoparticles improve paclitaxel efficacy in malignant glioma following local administration*. ACS Nano, 2014. **8**(10): p. 10655-64.

78. Osman, R., et al., *Inhalable DNase I microparticles engineered with biologically active excipients*. *Pulm Pharmacol Ther*, 2013. **26**(6): p. 700-9.
79. Henke, M.O. and F. Ratjen, *Mucolytics in cystic fibrosis*. *Paediatr Respir Rev*, 2007. **8**(1): p. 24-9.
80. Lai, S.K., Y.Y. Wang, and J. Hanes, *Mucus-penetrating nanoparticles for drug and gene delivery to mucosal tissues*. *Adv Drug Deliv Rev*, 2009. **61**(2): p. 158-71.
81. White, C.J. and M.E. Byrne, *Molecularly imprinted therapeutic contact lenses*. *Expert Opin Drug Deliv*, 2010. **7**(6): p. 765-80.
82. Tieppo, A., et al., *Sustained in vivo release from imprinted therapeutic contact lenses*. *J Control Release*, 2012. **157**(3): p. 391-7.
83. White, C.J., S.A. DiPasquale, and M.E. Byrne, *Controlled Release of Multiple Therapeutics from Silicone Hydrogel Contact Lenses*. *Optom Vis Sci*, 2016. **93**(4): p. 377-86.
84. Shikamura, Y., et al., *Hydrogel Ring for Topical Drug Delivery to the Ocular Posterior Segment*. *Curr Eye Res*, 2016. **41**(5): p. 653-61.
85. Masland, R.H., *The fundamental plan of the retina*. *Nat Neurosci*, 2001. **4**(9): p. 877-86.
86. Kirkwood, B.J., *Anatomy of the retina*. *Insight*, 2012. **37**(4): p. 5-8.
87. Karnowski, T.P., et al., *Automatic detection of retina disease: robustness to image quality and localization of anatomy structure*. *Conf Proc IEEE Eng Med Biol Soc*, 2011. **2011**: p. 5959-64.
88. Batrakova, E.V. and A.V. Kabanov, *Pluronic block copolymers: evolution of drug delivery concept from inert nanocarriers to biological response modifiers*. *J Control Release*, 2008. **130**(2): p. 98-106.

89. Choonara, Y.E., et al., *A review of implantable intravitreal drug delivery technologies for the treatment of posterior segment eye diseases*. J Pharm Sci, 2010. **99**(5): p. 2219-39.
90. Barnett, P.J., *Mathematical modeling of triamcinolone acetonide drug release from the I- vation intravitreal implant (a controlled release platform)*. Conf Proc IEEE Eng Med Biol Soc, 2009. **2009**: p. 3087-90.
91. Rishi, P., et al., *Short-term results of intravitreal dexamethasone implant (OZURDEX((R))) in treatment of recalcitrant diabetic macular edema: A case series*. Oman J Ophthalmol, 2012. **5**(2): p. 79-82.
92. El-Ghrably, I.A., A. Saad, and C. Dinah, *A Novel Technique for Repositioning of a Migrated ILUVIEN((R)) (Fluocinolone Acetonide) Implant into the Anterior Chamber*. Ophthalmol Ther, 2015. **4**(2): p. 129-33.
93. Barar, J., et al., *Advanced drug delivery and targeting technologies for the ocular diseases*. Bioimpacts, 2016. **6**(1): p. 49-67.
94. Moshfeghi, A.A. and G.A. Peyman, *Micro- and nanoparticulates*. Adv Drug Deliv Rev, 2005. **57**(14): p. 2047-52.
95. Liu, W., M. Griffith, and F. Li, *Alginate microsphere-collagen composite hydrogel for ocular drug delivery and implantation*. J Mater Sci Mater Med, 2008. **19**(11): p. 3365-71.
96. Kunzmann, A., et al., *Toxicology of engineered nanomaterials: focus on biocompatibility, biodistribution and biodegradation*. Biochim Biophys Acta, 2011. **1810**(3): p. 361-73.
97. Sabzevari, A., et al., *Polymeric triamcinolone acetonide nanoparticles as a new alternative in the treatment of uveitis: in vitro and in vivo studies*. Eur J Pharm Biopharm, 2013. **84**(1): p. 63-71.

98. De Jong, W.H. and P.J. Borm, *Drug delivery and nanoparticles: applications and hazards*. Int J Nanomedicine, 2008. **3**(2): p. 133-49.
99. Patane, M.A., et al., *Ocular iontophoresis of EGP-437 (dexamethasone phosphate) in dry eye patients: results of a randomized clinical trial*. Clin Ophthalmol, 2011. **5**: p. 633-43.
100. Fitzpatrick, S.D., et al., *Development of injectable, resorbable drug-releasing copolymer scaffolds for minimally invasive sustained ophthalmic therapeutics*. Acta Biomater, 2012. **8**(7): p. 2517-28.
101. Wells, L.A., S. Furukawa, and H. Sheardown, *Photoresponsive PEG-anthracene grafted hyaluronan as a controlled-delivery biomaterial*. Biomacromolecules, 2011. **12**(4): p. 923-32.
102. Zhang, J., et al., *An Injectable Hydrogel Prepared Using a PEG/Vitamin E Copolymer Facilitating Aqueous-Driven Gelation*. Biomacromolecules, 2016. **17**(11): p. 3648-3658.
103. Smeets, N.M., et al., *Injectable poly(oligoethylene glycol methacrylate)-based hydrogels with tunable phase transition behaviours: physicochemical and biological responses*. Acta Biomater, 2014. **10**(10): p. 4143-55.
104. Lo, R., et al., *A passive MEMS drug delivery pump for treatment of ocular diseases*. Biomed Microdevices, 2009. **11**(5): p. 959-70.
105. Mahadevan, G., H. Sheardown, and P. Selvaganapathy, *PDMS embedded microneedles as a controlled release system for the eye*. J Biomater Appl, 2013. **28**(1): p. 20-7.
106. Seuring, J. and S. Agarwal, *Polymers with upper critical solution temperature in aqueous solution*. Macromol Rapid Commun, 2012. **33**(22): p. 1898-920.

107. Schacht, E., et al., *Polyacetal and poly(ortho ester)-poly(ethylene glycol) graft copolymer thermogels: preparation, hydrolysis and FITC-BSA release studies*. *J Control Release*, 2006. **116**(2): p. 219-25.
108. Kumar, M.N., et al., *Chitosan chemistry and pharmaceutical perspectives*. *Chem Rev*, 2004. **104**(12): p. 6017-84.
109. Li, Z. and J. Guan, *Thermosensitive hydrogels for drug delivery*. *Expert Opin Drug Deliv*, 2011. **8**(8): p. 991-1007.
110. Van Vlierberghe, S., P. Dubruel, and E. Schacht, *Biopolymer-based hydrogels as scaffolds for tissue engineering applications: a review*. *Biomacromolecules*, 2011. **12**(5): p. 1387-408.
111. Shi, W., et al., *Characterization of pH- and thermosensitive hydrogel as a vehicle for controlled protein delivery*. *J Pharm Sci*, 2011. **100**(3): p. 886-95.
112. Gao, J., et al., *The use of chitosan based hydrogel for enhancing the therapeutic benefits of adipose-derived MSCs for acute kidney injury*. *Biomaterials*, 2012. **33**(14): p. 3673-81.
113. Mirahmadi, F., et al., *Enhanced mechanical properties of thermosensitive chitosan hydrogel by silk fibers for cartilage tissue engineering*. *Mater Sci Eng C Mater Biol Appl*, 2013. **33**(8): p. 4786-94.
114. Park, K.M., et al., *Thermosensitive chitosan-Pluronic hydrogel as an injectable cell delivery carrier for cartilage regeneration*. *Acta Biomater*, 2009. **5**(6): p. 1956-65.
115. Sun, J., et al., *Injectable chitosan-based hydrogel for implantable drug delivery: body response and induced variations of structure and composition*. *J Biomed Mater Res A*, 2010. **95**(4): p. 1019-27.

116. Wang, W., et al., *A novel chitosan-based thermosensitive hydrogel containing doxorubicin liposomes for topical cancer therapy*. *J Biomater Sci Polym Ed*, 2013. **24**(14): p. 1649-59.
117. Molinaro, G., et al., *Biocompatibility of thermosensitive chitosan-based hydrogels: an in vivo experimental approach to injectable biomaterials*. *Biomaterials*, 2002. **23**(13): p. 2717-22.
118. Teeri, T.T., et al., *Biomimetic engineering of cellulose-based materials*. *Trends Biotechnol*, 2007. **25**(7): p. 299-306.
119. Mihardja, S.S., et al., *The effect of a peptide-modified thermo-reversible methylcellulose on wound healing and LV function in a chronic myocardial infarction rodent model*. *Biomaterials*, 2013. **34**(35): p. 8869-77.
120. Kang, C.E., et al., *A new paradigm for local and sustained release of therapeutic molecules to the injured spinal cord for neuroprotection and tissue repair*. *Tissue Eng Part A*, 2009. **15**(3): p. 595-604.
121. Ballios, B.G., et al., *A hydrogel-based stem cell delivery system to treat retinal degenerative diseases*. *Biomaterials*, 2010. **31**(9): p. 2555-64.
122. Itoh, K., et al., *In situ gelling xyloglucan/alginate liquid formulation for oral sustained drug delivery to dysphagic patients*. *Drug Dev Ind Pharm*, 2010. **36**(4): p. 449-55.
123. Nisbet, D.R., et al., *Morphology and gelation of thermosensitive xyloglucan hydrogels*. *Biophys Chem*, 2006. **121**(1): p. 14-20.
124. Wells, L.A., et al., *Responding to change: thermo- and photo-responsive polymers as unique biomaterials*. *Crit Rev Biomed Eng*, 2010. **38**(6): p. 487-509.

125. Nisbet, D.R., et al., *Review paper: a review of the cellular response on electrospun nanofibers for tissue engineering*. J Biomater Appl, 2009. **24**(1): p. 7-29.
126. Nisbet, D.R., et al., *Implantation of functionalized thermally gelling xyloglucan hydrogel within the brain: associated neurite infiltration and inflammatory response*. Tissue Eng Part A, 2010. **16**(9): p. 2833-42.
127. Al-Abd, A.M., et al., *Pharmacokinetics of doxorubicin after intratumoral injection using a thermosensitive hydrogel in tumor-bearing mice*. J Control Release, 2010. **142**(1): p. 101-7.
128. Ge, X., T. Hoare, and C.D. Filipe, *Protein-based aqueous-multiphasic systems*. Langmuir, 2010. **26**(6): p. 4087-94.
129. Bessa, P.C., et al., *Thermoresponsive self-assembled elastin-based nanoparticles for delivery of BMPs*. J Control Release, 2010. **142**(3): p. 312-8.
130. Meyer, D.E. and A. Chilkoti, *Genetically encoded synthesis of protein-based polymers with precisely specified molecular weight and sequence by recursive directional ligation: examples from the elastin-like polypeptide system*. Biomacromolecules, 2002. **3**(2): p. 357-67.
131. McDaniel, J.R., D.J. Callahan, and A. Chilkoti, *Drug delivery to solid tumors by elastin-like polypeptides*. Adv Drug Deliv Rev, 2010. **62**(15): p. 1456-67.
132. MacKay, J.A., et al., *Self-assembling chimeric polypeptide-doxorubicin conjugate nanoparticles that abolish tumours after a single injection*. Nat Mater, 2009. **8**(12): p. 993-9.
133. Meyer, D.E., et al., *Drug targeting using thermally responsive polymers and local hyperthermia*. J Control Release, 2001. **74**(1-3): p. 213-24.

134. Liu, W., et al., *Injectable intratumoral depot of thermally responsive polypeptide-radionuclide conjugates delays tumor progression in a mouse model*. J Control Release, 2010. **144**(1): p. 2-9.
135. Klouda, L. and A.G. Mikos, *Thermoresponsive hydrogels in biomedical applications*. Eur J Pharm Biopharm, 2008. **68**(1): p. 34-45.
136. Yang, Y., et al., *A novel mixed micelle gel with thermo-sensitive property for the local delivery of docetaxel*. J Control Release, 2009. **135**(2): p. 175-82.
137. Choi, W.I., et al., *Remarkably enhanced stability and function of core/shell nanoparticles composed of a lecithin core and a pluronic shell layer by photo-crosslinking the shell layer: in vitro and in vivo study*. Acta Biomater, 2010. **6**(7): p. 2666-73.
138. Buwalda, S.J., et al., *Influence of amide versus ester linkages on the properties of eight-armed PEG-PLA star block copolymer hydrogels*. Biomacromolecules, 2010. **11**(1): p. 224-32.
139. Yu, D., et al., *Bone regeneration of critical calvarial defect in goat model by PLGA/TCP/rhBMP-2 scaffolds prepared by low-temperature rapid-prototyping technology*. Int J Oral Maxillofac Surg, 2008. **37**(10): p. 929-34.
140. Jiang, X., et al., *Fabrication of two types of shell-cross-linked micelles with "inverted" structures in aqueous solution from schizophrenic water-soluble ABC triblock copolymer via click chemistry*. Langmuir, 2009. **25**(4): p. 2046-54.
141. He, C., S.W. Kim, and D.S. Lee, *In situ gelling stimuli-sensitive block copolymer hydrogels for drug delivery*. J Control Release, 2008. **127**(3): p. 189-207.

142. Yu, L., et al., *Biodegradability and biocompatibility of thermoreversible hydrogels formed from mixing a sol and a precipitate of block copolymers in water*. *Biomacromolecules*, 2010. **11**(8): p. 2169-78.
143. Jiang, W.W., et al., *Phagocyte responses to degradable polymers*. *J Biomed Mater Res A*, 2007. **82**(2): p. 492-7.
144. Akimoto, J., et al., *Temperature-induced intracellular uptake of thermoresponsive polymeric micelles*. *Biomacromolecules*, 2009. **10**(6): p. 1331-6.
145. Alzari, V., et al., *Stimuli responsive hydrogels prepared by frontal polymerization*. *Biomacromolecules*, 2009. **10**(9): p. 2672-7.
146. Censi, R., et al., *Photopolymerized thermosensitive poly(HPMA lactate)-PEG-based hydrogels: effect of network design on mechanical properties, degradation, and release behavior*. *Biomacromolecules*, 2010. **11**(8): p. 2143-51.
147. Ankareddi, I., et al., *Developmental toxicity assessment of thermoresponsive poly(N-isopropylacrylamide-co-acrylamide) oligomers in CD-1 mice*. *Birth Defects Res B Dev Reprod Toxicol*, 2008. **83**(2): p. 112-6.
148. Neradovic, D., et al., *The effect of the processing and formulation parameters on the size of nanoparticles based on block copolymers of poly(ethylene glycol) and poly(N-isopropylacrylamide) with and without hydrolytically sensitive groups*. *Biomaterials*, 2004. **25**(12): p. 2409-18.
149. Cui, Z., B.H. Lee, and B.L. Vernon, *New hydrolysis-dependent thermosensitive polymer for an injectable degradable system*. *Biomacromolecules*, 2007. **8**(4): p. 1280-6.

150. Ahn, S., E.C. Monge, and S.C. Song, *Ion and pH effect on the lower critical solution temperature phase behavior in neutral and acidic poly(organophosphazene) counterparts*. Langmuir, 2009. **25**(4): p. 2407-18.
151. Potta, T., C. Chun, and S.C. Song, *Chemically crosslinkable thermosensitive polyphosphazene gels as injectable materials for biomedical applications*. Biomaterials, 2009. **30**(31): p. 6178-92.
152. Matanovic, M.R., J. Kristl, and P.A. Grabnar, *Thermoresponsive polymers: insights into decisive hydrogel characteristics, mechanisms of gelation, and promising biomedical applications*. Int J Pharm, 2014. **472**(1-2): p. 262-75.
153. Alvarez-Lorenzo, C., et al., *Temperature-sensitive chitosan-poly(N-isopropylacrylamide) interpenetrated networks with enhanced loading capacity and controlled release properties*. J Control Release, 2005. **102**(3): p. 629-41.
154. Suri, S. and C.E. Schmidt, *Photopatterned collagen-hyaluronic acid interpenetrating polymer network hydrogels*. Acta Biomater, 2009. **5**(7): p. 2385-97.
155. Quan, C.Y., et al., *Core-shell nanosized assemblies mediated by the alpha-beta cyclodextrin dimer with a tumor-triggered targeting property*. ACS Nano, 2010. **4**(7): p. 4211-9.
156. Wei, H., et al., *Synthesis and applications of shell cross-linked thermoresponsive hybrid micelles based on poly(N-isopropylacrylamide-co-3-(trimethoxysilyl)propyl methacrylate)-b-poly(methyl methacrylate)*. Langmuir, 2008. **24**(9): p. 4564-70.
157. De Hoog, H.P., et al., *A hydrogel-based enzyme-loaded polymersome reactor*. Nanoscale, 2010. **2**(5): p. 709-16.

158. S. Qin, et al., *Temperature-Controlled Assembly and Release from Polymer Vesicles of Poly(ethylene oxide)-block- poly(N-isopropylacrylamide)*. *advanced materials*, 2006. **18**(21): p. 2905-2909.
159. Ozaydin-Ince, G., A.M. Coclite, and K.K. Gleason, *CVD of polymeric thin films: applications in sensors, biotechnology, microelectronics/organic electronics, microfluidics, MEMS, composites and membranes*. *Rep Prog Phys*, 2012. **75**(1): p. 016501.

Chapter 2: Hyaluronic acid – sulfadiazine conjugate as a treatment for dry eye disease

Scientific Contributions

- Develop and characterize a mucoadhesive polymer composed of the disaccharide hyaluronan and sulfadiazine
- Explore the dry eye market to understand the potential impact of disruptive technologies in this space
- Demonstrate biocompatibility *in vitro* and *in vivo*
- Create and validate a dry eye model induced by benzalkonium chloride with which to measure the effectiveness of this treatment

Publications from this work

- Hyaluronic acid – sulfadiazine conjugate as a treatment for dry eye disease (manuscript in preparation)

Abstract

Dry eye disease (DED) is a multifactorial disease affecting the ocular surface for which there is no putative cure. Topical lubricants or drops are by far the most widely used therapy for DED, but typically have a very low residence time on the ocular surface, and therefore provide transient relief. Hyaluronic acid (HA) is the most common naturally occurring glycosaminoglycan in the eye with an extensive pedigree in existing anterior segment therapeutics. HA is shear thinning, highly lubricious, and can bind enormous amounts of water, relieving DED symptoms. HA also binds CD44, a multifunctional cell surface receptor which can increase goblet and epithelial cell survival while lowering inflammation. Sulfadiazine (SD) is a broad spectrum antimicrobial which has been in use since the Second World War. It has recently been identified as a potent matrix metalloprotease inhibitor (MMPi). Overactivity of MMPs, particularly MMP-9, is so congruent with DED that it has become a de facto marker in the clinic. By conjugating HA to SD, a novel formulation has been developed which synergistically combines the mucoadhesiveness of HA with an active ingredient. HA-SDZ materials are prepared by dissolving , 1-ethyl-3-(3-dimethylaminopropyl) carbodiimide hydrochloride (EDC), Hydroxybenzotriazole (HOBT), and an excess of SD in 70% DMSO:30% water. The solution is heated to 70°C for 24 hours, and excess SDZ is precipitated by increasing the water content. This formulation was tested in New Zealand White (NZW) rabbits which were chemically induced to display DED symptoms by topically administering a 0.1% Benzalkonium Chloride (BAC) solution twice daily for 14 days. These DED rabbits were rescued with HA-SD, and their performance was compared to commercially available eye drop Systane Ultra. This rescue is assessed using fluorescein staining with a slit lamp ophthalmoscopy, Schirmer's testing, conjunctival impression cytology (CIC), and conventional histology. HA-SD performed at least

as well as Systane Ultra at relieving DED symptoms after scoring on a modified Draize test. HA-SD returned all relevant metrics (tear film, CIC, staining) to normal levels much faster than untreated controls. While HA is a common ingredient in many ophthalmic formulations, this is the first time HA has been used to tether an MMPi to the ocular surface for the treatment of DED.

2.1 Background

Dry eye syndrome (DES) is a multifactorial disease affecting the ocular surface and tear film for which there is no putative cure. Dry eye symptoms typically reflect a series of distinct pathological processes that interfere with tear film homeostasis and place the corneal epithelium under hyperosmolar and inflammatory stress.[1] In mild or moderate forms of the disorder, DED can be a persistent discomfort, and can affect functional visual acuity to such a degree that it impairs normal daily activities;[2] In its more severe forms, DED can lead to corneal opacity and blindness.[3]

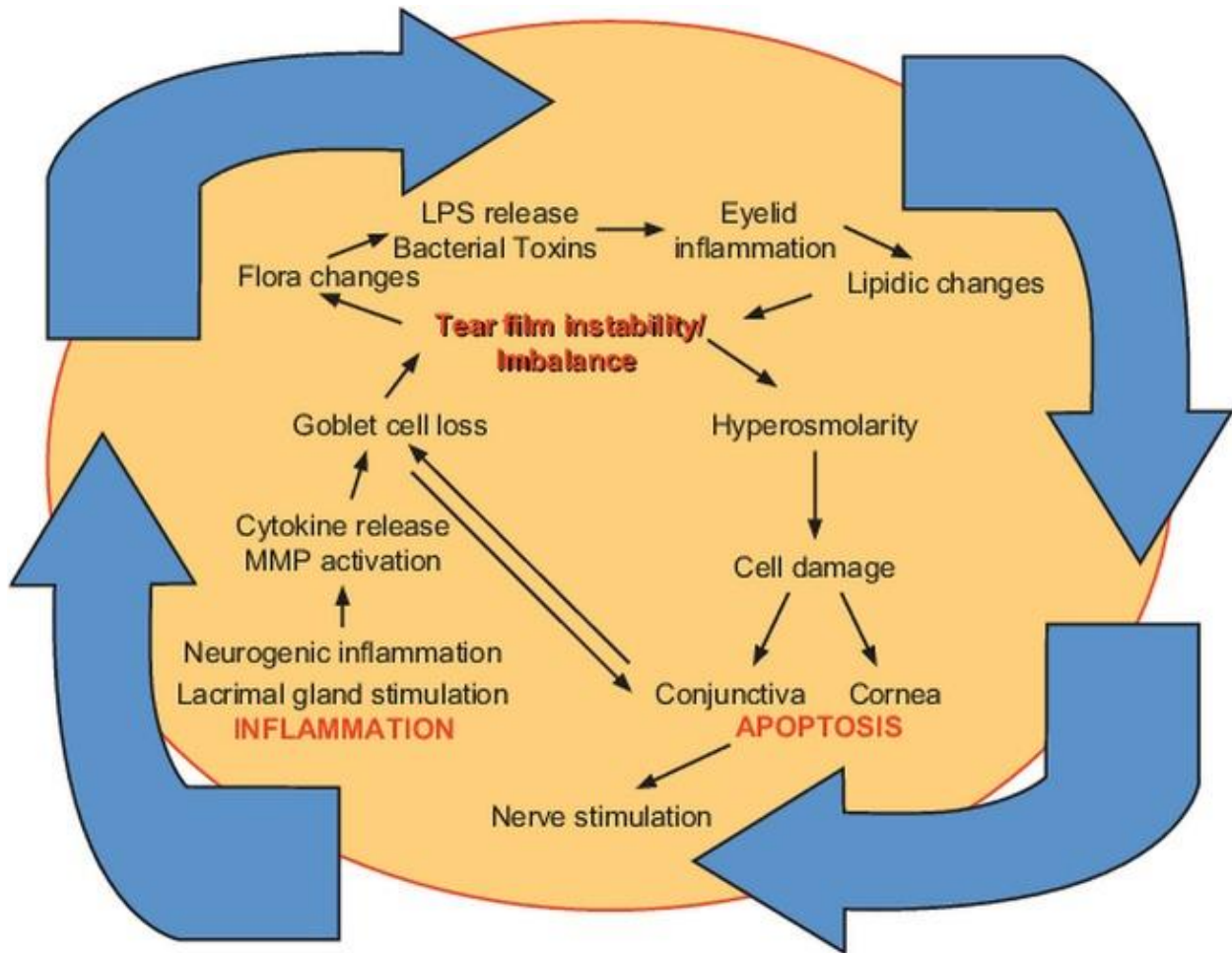


Figure 1 – The vicious cycle of inflammatory DED[4]

Under normal conditions, the tear film forms a protective layer that hydrates and lubricates the ocular surface. This heterogeneous coating is made up of an outer lipid layer shielding the underlying aqueous layer and mucin.[5] The aqueous secretion is derived primarily from the lacrimal gland and comprises the majority of the tear. The lipid layer on the outer surface of the tear film is produced by holocrine meibomian gland secretions and acts primarily as a barrier limiting evaporation of the underlying aqueous layer.[6] As a system, these elements establish a protective and nourishing barrier for the eye. The meibomian and lacrimal glands contribute many additional proteins which are involved in immunity, fatty acid metabolism, and the physicochemical integrity of the tear film. Alterations in the protein composition of these secretions can often reflect changes indicative of disease; dysregulation of these paracrine secretions form a great deal of the esoterica associated with DES.[7]

Because of the dynamic interplay between these constituents of the tear film, a breakdown in the production of any one, or all, of these components can result in instability of the tear film, reducing both the quantity and the quality of tears as seen in Figure 1.[8] The mechanisms causing dry eye are traditionally attributed to either impaired lacrimal production causing aqueous-deficient dry eye (ADDE) or excessive evaporation, often as a result of meibomian gland dysfunction (MGD), causing evaporative dry eye (EDE). In early stages of the pathogenesis of dry eye, only one system is typically dysfunctional; in more severe cases, both the lacrimal and the meibomian glands may be compromised, resulting in a hybridized etiology with signs of both ADDE and EDE. In some rare cases, neither the lacrimal nor meibomian glands show signs of dysfunction despite apparent DES symptoms. These cases represent an active field of research in corneal ophthalmology.

A number of risk factors have been associated with the development of DES, including gender, age, hormonal dysfunction, contact lens wear, off target drug effects, autoimmune disease (particularly Sjogren's syndrome), and refractive surgery.[9-11]The estimates for the prevalence of DES vary from 14.4% to 48% depending on how it is measured (Table 1). As Allergan is a pharmaceutical company operating in this space, their 48% claim may not be entirely reliable. Regardless, it is clear DES is extremely prevalent. DES is approximately twice as common in women as men, and, like many other diseases, it increases in prevalence with age.[12, 13] Because elderly populations are so female dominated, DES is positioned to become an unprecedented unmet need as populations age. DES is also an extremely under-diagnosed medical condition; while there is an estimated 60 million North Americans with DES, an estimated 45 million have not been diagnosed.[14]

Table 1 – Reported prevalence of DED

Study	Prevalence
Salisbury Eye Study	14.6%
Beaver Dam	14.4%
Blue Mountains	16.6%
Shihpai (East Asian cohort)	33.7%
Sumatra (South East Asian cohort)	27.5%
Allergan Survey	48.0%

Despite poor performance, topical lubricants are by far the most widely used therapy for DES. In a survey of DES sufferers, the average patient has tried at least 3 different brands of artificial tears, and 97% remain dissatisfied and frustrated.[15] Besides topical lubricants, Allergan’s Restasis, a cyclosporine-based corticosteroid ophthalmic emulsion, and Shire’s Xiidra, an T-cell antagonist, are the only compounds approved for the treatment of DES. Despite an explosion of interest and clinical trials, there are still no other viable pharmaceutical options available (Table 2).

Compound	Function	Company	Status
Diquafosol tetrasodium 2%	P2Y2 purinogenic agonist	Santen	Failed
RGN-259	Thymosin-β4 mimetic	RegeneRx	Failed
Bromfenac	NSAID	Bausch + Lomb	Failed
EGP-437	Corticosteroid	EyeGate Pharma	Failed
RX-10045	Synthetic resolvin analogue	Resolvix Pharmaceuticals	Failed
Lifitegrast	LFA-1 antagonist	SARcode	Phase III
CF ₁₀₁	A3AR mediated	Can-Fite BioPharma	Phase III
Cyclokot	Immunosuppressive	Novgali	Phase II
Rebamipide	Mucin secretagogue	Otsuka-Acucela	Phase II

MIM-D3	Nerve growth factor peptidomimetic	Mimetogen	Phase II
Restasis X	Immunosuppressive	Allergan	Phase II
ISV-101	NSAID	InSite	Phase II
Difluprednate 0.05%	Corticosteroid	Alcon	Phase II
Mapracorat	Glococorticoid receptor agonist	Bausch + Lomb	Phase II
DE-101	Anti-inflammatory	Santen	Phase II
LX214	Calcineurin inhibitor	LuxBioscience	Phase I
Sodium Hyaluronate	CD44 ligand	Alcon	Phase III

To address this clear unmet need, an array of complicated and expensive treatments has emerged. To address the symptoms of ADDE, a biomaterial device can be surgically implanted into the lacrimal punctum to prevent proper tear drainage and increase the residence time of tear film on the cornea. These devices come in all sorts of shapes and material compositions, and can be temporary (resorbable) or permanent. These devices come with the chance of infection, displacement, dacryocystitis, and only address the symptoms of ADDE DES, which is a minority (14%) of cases (figure 1).[16]

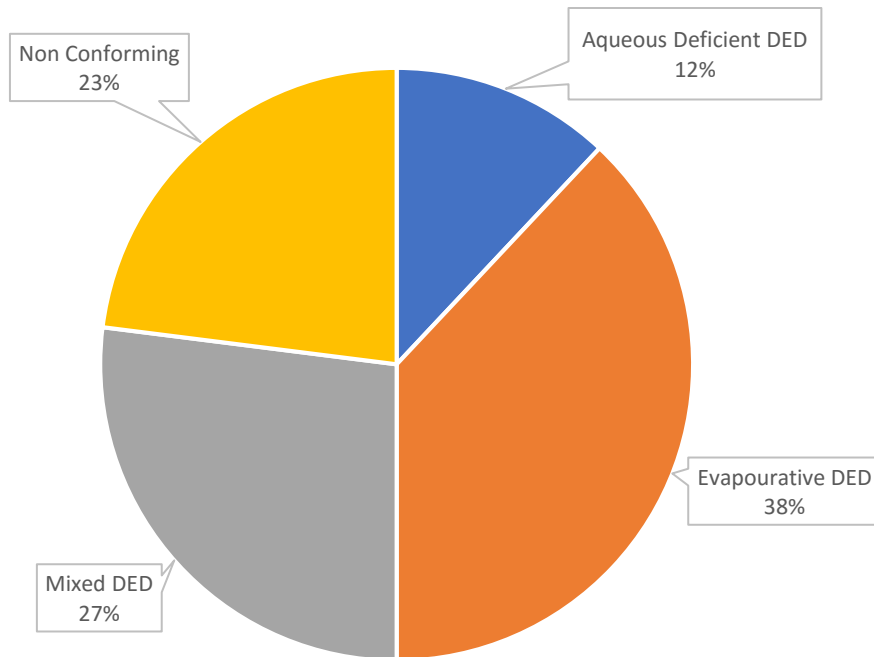


Figure 2 – Subtype of DED found through clinical evaluation in the United States. Note that 23% of cases are not aqueous deficient or evaporative in nature, and remain mysterious.

Recently, device based rather than drug based solutions have made an appearance in this space. Lipiflow has become a popular option to address MGD. Lipiflow is an in-clinic device marketed by TearScience designed to administer therapeutic levels of heat, pressure, and mechanical manipulation with the goal of relieving meibomian gland obstruction. The device applies heat to the palpebral surfaces of the upper and lower eyelids directly over the meibomian glands, while simultaneously applying graded pulsatile pressure to the outer eyelid surfaces to express the meibomian glands (figure 2). While studies have shown some efficacy,[17] Lipiflow is only effective in cases where MGD is the cause of DES symptoms. Further, it does nothing to help with meibomian gland infection, inflammation of the posterior eyelid margin, or metabolic dysregulation causing MGD. In short, this complicated and expensive device may help with

meibomian gland obstruction, but is certainly not appropriate for most cases of DES.

Nevertheless, it is selling extremely well and breaking analyst expectations consistently.

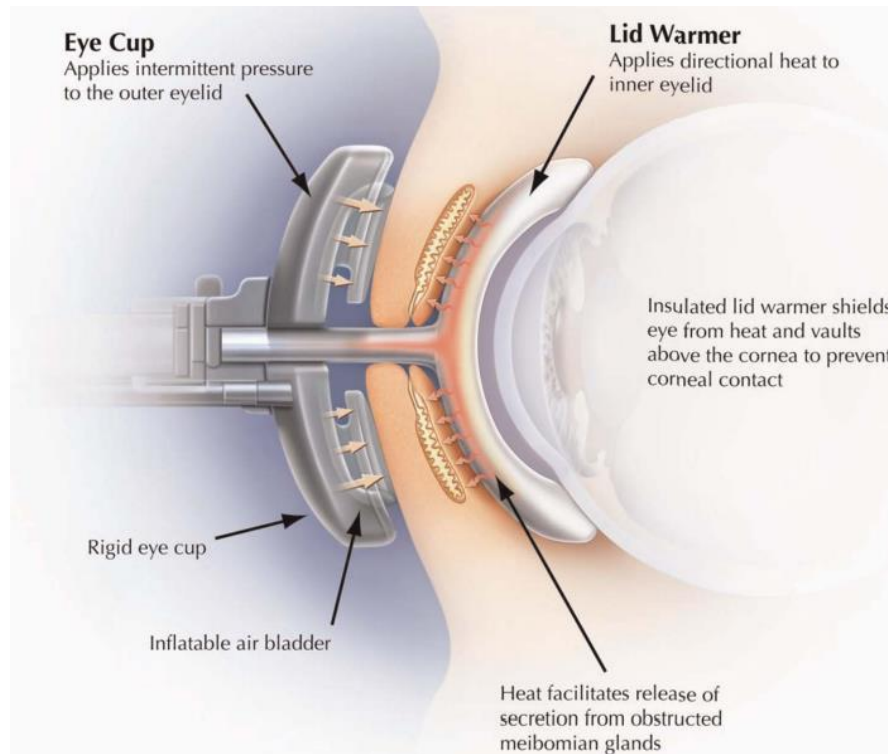


Figure 3 – Schematic of the Lipiflow device by TearScience. The device works by massaging and expressing meibomian glands to increase the production of protective tear film lipids

Oculeve is another device breaking new ground in the dry eye space. This implanted device stimulates natural tear production by delivering neurostimulating micro-electrical pulses to directly to the lacrimal gland. Tear delivery rates can be adjusted *in situ* with a wireless controller. Oculeve has recently been acquired for US\$125 million by Allergan, which has made it clear they expect this device to be extremely successful. Like the Lipiflow, however, this device is only capable of addressing a subpopulation of DED sufferers – in this case the aqueous

deficient which are a minority of cases. Further, recent clinical data has shown some ambiguity in outcome, particularly with corneal staining.[18]

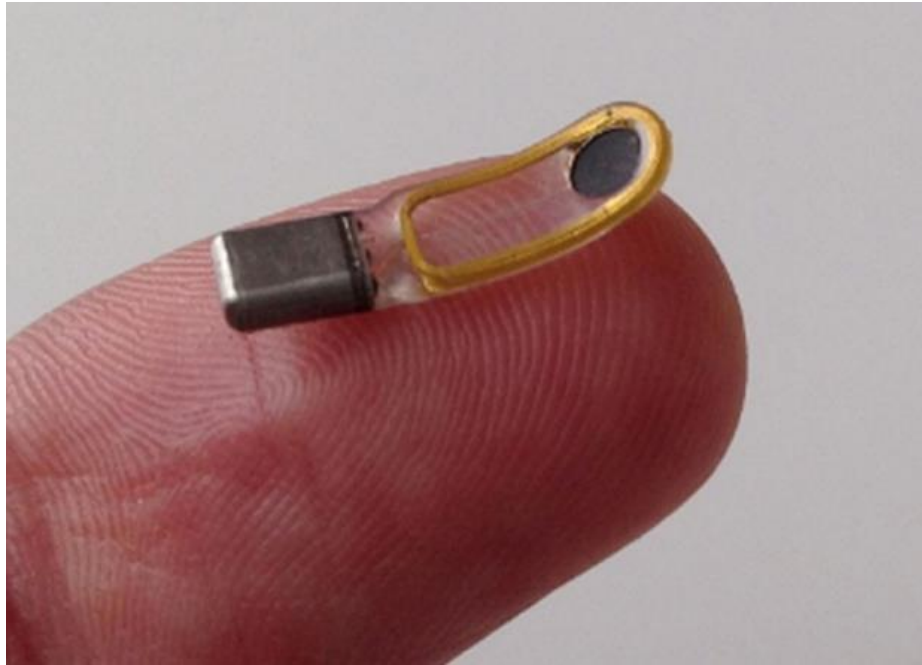


Figure 4 – The Oculeve neurstimulation device for increasing tear production.

Autologous serum is the final category of DED treatment currently under consideration. Blood serum and tear film are very similar in composition. Serum also contains several components which are very expensive to produce in a pharmacological setting but which are nevertheless necessary for proper tear film function. Key factors such as epidermal growth factor (EGF), fibronectin and vitamin A, which support the proliferation, maturation, migration and differentiation of corneal and conjunctival epithelia, as well as immunoglobulins, lysozymes and complement, which have bacteriostatic properties are all found in abundance in serum.[19] By harvesting and processing patient blood, a drop can be created which has been shown to be much more effective than simple over-the-counter lubricating alternatives.[20] However, the cost for

this sort of personalised medicine approach can often be prohibitive, and the underlying etiology of their disease may result in deficiencies in blood serum in the same factors potentially missing from tear film. These examples, including the Lipiflow, Oculieve, and autologous tear film, coupled with the extensive list of drugs currently in development, hint at a market which is lucrative and underserved, receptive to increasingly elaborate and expensive solutions.

Currently, medical treatment for DES averages \$1300 per patient per year in direct costs, and up to \$18,000 per year in productivity losses. The economic consequences of this disease are devastating, representing hundreds of billions of dollars per year globally.[21] However, the market opportunity is enormous. If top primary diagnosis codes are examined, DES tops all other categories of eye disease by far (figure 3). The market for DES treatments is expected to grow from \$1.6 billion in 2013 to \$5.5 billion in 2022 – a compound annual growth rate of 12%.[22] To address the unmet need effective treatment of DES represents, and to capture some of the enormous market potential therein, a novel hyaluronic acid based treatment has been developed.

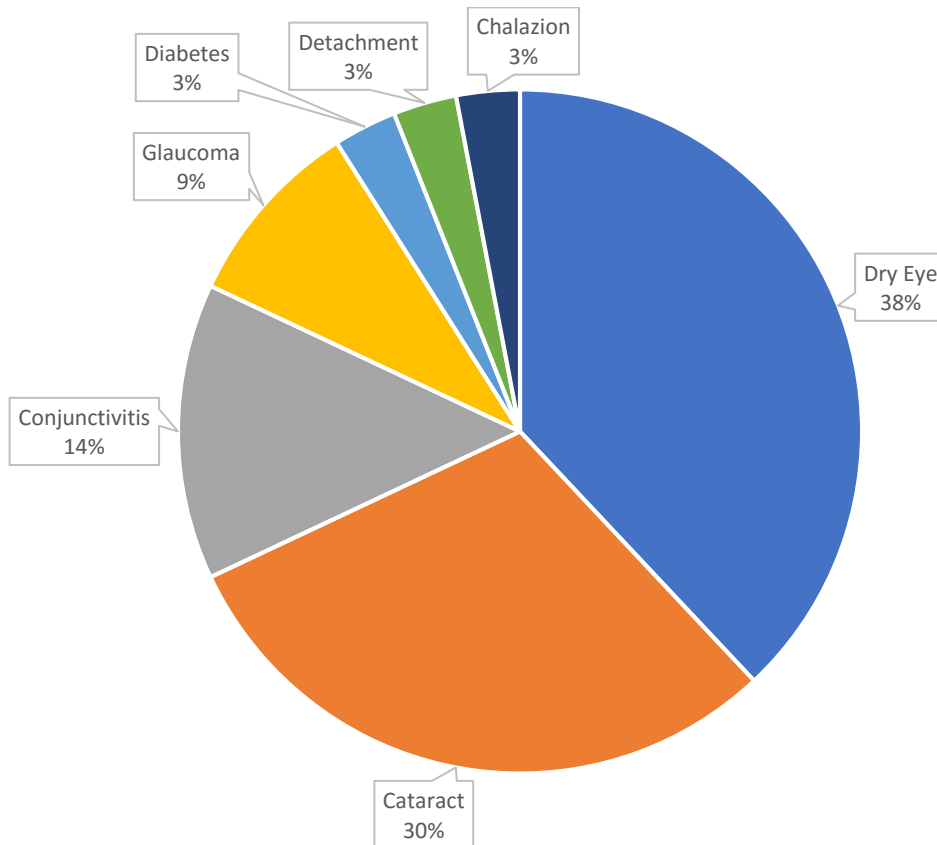


Figure 5 – Primary Dx codes for ophthalmology from CMS.gov

Hyaluronic acid (HA) is the most common glycosaminoglycan in the eye. HA is already widely used in a variety of ophthalmic applications, including as an over the counter treatment for DES.[23] HA has an immense arsenal of potentially beneficial applications for anterior segment therapeutics. Most obviously, HA can stabilize tear film and increase lubricity by binding water. HA has been shown to be mucoadhesive, which greatly increases its residence time in the eye after administration.[24] In this project, this property is exploited to anchor another active ingredient to the ocular surface, preventing its clearance, reducing the need for reapplication, and increasing its efficacy. HA binds CD44, a multistructural, multifunctional cell surface receptor

found on most cell types in the body – including epithelial cells which make up the corneal surface and immune cells which surveil the eye. In aggregate, the effect exerted through this receptor interaction improves corneal wound healing and downregulates inflammation.[25]

Sulfonamides (SAm) are a class of molecule which form the basis of several groups of drugs.

The SAm group is an extremely flexible moiety, and can interact with a variety of agonists. Most well known for the antimicrobial properties of sulfa drugs, which prefaced the antibiotic revolution in the 1930s, SAmS are used as diuretics, diabetes treatments, and can manage inflammation as a COX-2 inhibitor. In short, SAmS have a long and successful precedent in medicine. More recently, our lab has shown SAmS can specifically inhibit the activity of matrix metalloproteinases (MMPs).[26] Other groups experimenting with SAm based compounds have since reported similar findings; MMP-inhibiting SAmS are now an active field of research with the goal of creating novel drugs to treat the spectrum of disorders in which MMPs are implicated.[27, 28]

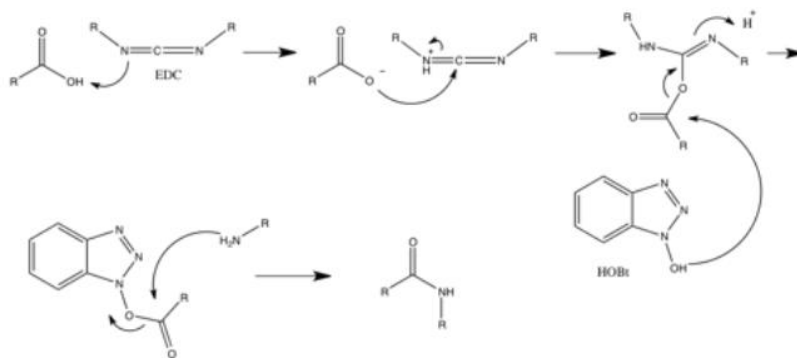
MMPs are a family of zinc containing hydrolases with broad proteolytic activity and highly homogeneous structures. These enzymes are involved in the degradation of several extracellular proteins including extracellular matrix (ECM) components, and also play a crucial role in tissue remodelling and in regulating various biological and pathological processes. Dysregulation of MMPs is highly relevant in many disease states, including DES. Recent findings have shown DES correlates with significant upregulation and increased activity of MMPs in the tear film.[29] In particular, DES has been associated with over-expression and increased activity of corneal MMP-9, which is so strongly implicated in the disease it has become a clinically relevant de facto marker for diagnosis. [30]

We propose the combination of HA and a candidate SAm (sulphadiazine, [SD]) will result in novel and highly effective treatments for DES. Greater than the clinical benefits of the constituent parts, the mucoadhesive properties of HA will give the SAm sufficient time and proximal concentration to function, solving a fundamental problem with drug delivered via eye drop. To test this hypothesis, a preclinical animal model was developed using New Zealand White rabbits (NZW), and a battery of optometric tests were devised to assess rescue from a disease state.

2.2 Synthesis of HASD

HA of various molecular weights between ~5000 to ~1,000,000 was modified with sulphadiazine (SD). If the molecular weight of HA affects function, this range of molecular weights, spanning two orders of magnitude, will ensure any trends are obvious.

HASD materials were prepared by dissolving HA with an excess of SD molecules in 70% DMSO:30% water. The coupling reaction was initiated by activating the carboxylic acids on each HA monomer with a combination of 1-ethyl-3-(3-dimethylaminopropyl) carbodiimide hydrochloride (EDC) and Hydroxybenzotriazole (HOBt). The solution was buffered to pH 4.5, heated to 70°C for 24 hours, and any excess of sulfadiazine (SDZ) was precipitated by increasing the water content. A primary amine on the SD molecule reacts covalently with the activated carboxylic acid, forming HASD. Materials were dialysed extensively, freeze-dried, and gamma irradiated to sterilize for preclinical use. These materials were characterized by NMR.



Activation with 1-ethyl-3-(3-dimethylaminopropyl)carbodiimide (EDC) and Hydroxybenzotriazole (HOBT).

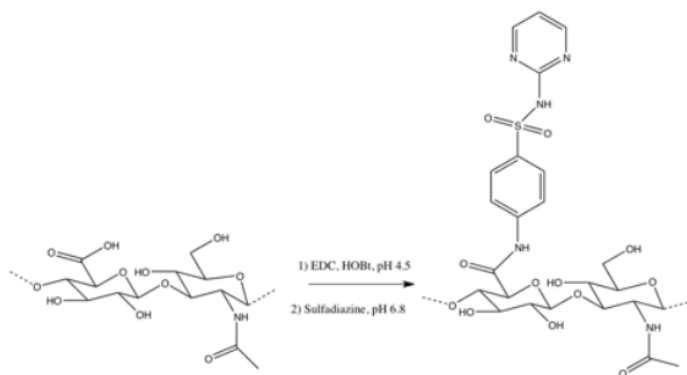


Figure 6 – Reaction schema for the synthesis of HASD

$^1\text{H-NMR}$ data (600MHz) indicates both SDZ and HA are present in the correct ratios. The peak assignment and integration of the spectrum obtained can be seen in as seen in Figure 7.

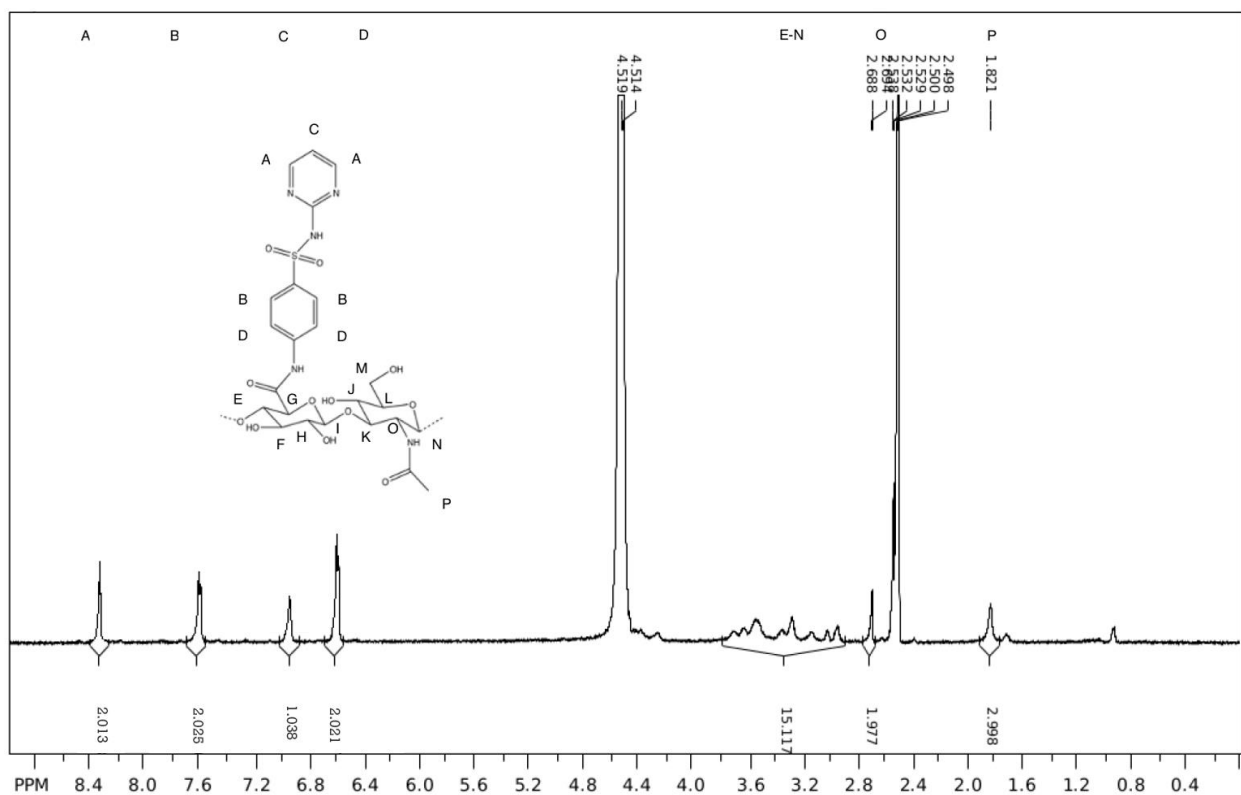


Figure 7 - ¹H-NMR of HASD

2.3 Preclinical DES Model

Considering the complicated etiology, a huge variety of animal models have been created to mimic the different pathophysiologic mechanisms of DED.[31] In brief, some of these models include transgenic mice resembling Sjogren's syndrome[32]; mouse models induced by botulinum toxin B[33] or a desiccating controlled environment[34]; rat models induced by evoked dacryoadenitis[35] or anticholinergic drugs[36]; rabbit models induced by closure of the meibomian gland orifices[37], controlled environment [38], evoked dacryoadenitis [39], preganglionic parasympathetic denervation[40], or removing of the lacrimal gland [41]; canine models formed by canine distemper virus [42]; and monkey models by removal of the lacrimal

gland [43]. However, while all of these attempts produced eye dryness to some extent, none of them mirrored the underlying etiologies of the human disease.

Benzalkonium chloride (BAC) is a common preservative used in ophthalmic formulations since the 1940s. Only recently has there been any real interest in its safety.[44] It has ironically been shown to destabilise tear film, induce drying of the eye, and worsen preexisting dry eye.[45] BAC affects and inflames both the cornea and the conjunctiva, resulting in the closure and dysfunction of lacrimal glands, inducing ADDE. However, it also possesses surfactant properties, allowing it to solubilise the lipid phase of the tear film. When used in ophthalmic formulations, this effectively increases drug penetration, making it a useful excipient. However, it also destroys the evaporative protection of the tear film, inducing EDE.[46] BAC is therefore a multipronged antagonist, both reducing tearfilm production and increasing evaporation while causing the irritation and inflammation typical of severe DES. BAC also does not suffer from the variability of surgical procedures, where the skill of the surgeon can greatly affect results. BAC can therefore produce a very successful model of DES more in accordance with normative etiology and pathophysiology than competing models.

To create this model, the left eye of a NZW was used for twice-daily topical administration of 0.1% BAC drops (used at a concentration range of 0.004%– 0.02% in topical multidose solutions) for 14 days. The albino rabbit was chosen because its large eyes make it easy to observe damage using conventional ophthalmic tools and techniques. In addition, it has a large conjunctival sac accentuated by loose lids which is able to easily accept test material and hold it against the eye.

2.4 Experimental Approach

A suite of qualitative and quantitative tests were used to track disease progression and rescue. While not exhaustive, these tests were selected to provide enough information to accurately describe the health of the cornea, conjunctiva, tear film, and other relevant anterior structures. In all cases, the left eye was be the experimental eye, with the contralateral eye serving as a control.

Slit lamp ophthalmoscopy was used to perform thorough optometric exams at predetermined time points throughout the treatment process. A modified Draize and Hackett-McDonald ocular scoring was used to grade the health of the eye. This test uses a variety of metrics which convert observations into a standardized numerical result. To enhance any potential damage or disruption to the corneal surface, fluorescein and Rose Bengal stains were applied as an ocular dye strip. Intact corneal epithelium with a normal layer of associated tear film will not stain: only a damaged ocular surface binds these dyes.

Schirmer's tear flow test was used to measurement aqueous tear production. A Schirmer's filter paper strip was inserted into the conjunctival sac location around the junction of the middle and outer thirds of the lower lid and the eyelid were lightly held shut. Capillary action draws tear film up the paper strip, and gives a numerical assessment, measured in millimetres, of how much tear film is present. Tear film is perhaps the most significant abnormal feature of DES.



Figure 8 – demonstration of Shirmer’s test.

Tonometry is a process by which intraocular pressure (IOP), measured in mmHg, can be determined. Inflammation is a common feature of DES, which can lead to elevated IOP. A Tonolab tonometer specially designed for rodent preclinical applications was used to assess changes in IOP throughout treatment with gentle, painless, tangential contact with the corneal surface.

Conjunctival impression cytology (CIC) is a technique used to remove a small section of the superficial layers of the ocular surface epithelium. The cells thus removed can be subjected to histological, immunohistological, or molecular analysis. While assessing the corneal epithelium, CIC is also the best method available to assess the prevalence of conjunctival goblet cells, which are the main source of ocular surface mucoproteins that lubricate and protect the ocular surface. Polytetrafluoroethylene (PEFT) cell culture inserts were gently pressed against the temporal bulbar and palpebral conjunctivas. The nature of the PEFT membrane forces cells to stick to it. Once removed, this membrane with attached cellular material was fixed in 4% formalin, stained with haematoxylin and eosin (H&E), and observed under a microscope to assess tissue health.

2.5 Creation of DED model

Before beginning a preclinical trial of HASD, extensive *in vitro* cell viability assays and preliminary *in vivo* acute toxicology assays were performed to verify HASD was biocompatible. Those tests will not be shown here, but were all satisfactory. While dosing animals with BAC to induce DED like symptoms, measurements were taken to validate the model.

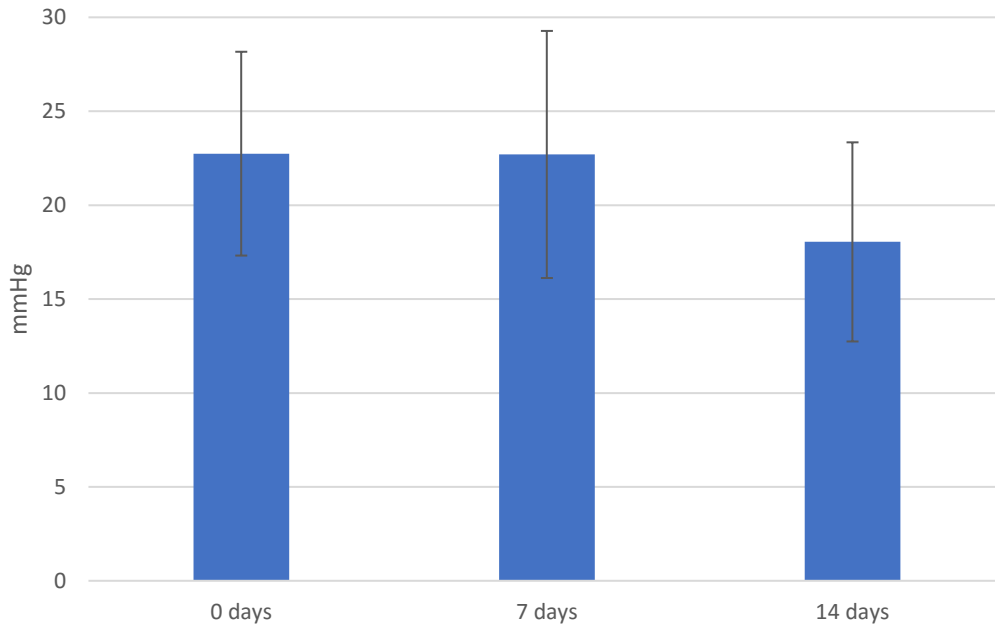


Figure 9 – Twice daily administration of 0.1% BAC resulted in no significant alterations in intraocular pressure of NZW rabbits. Error = 1 standard deviation, $n = 12$, $p = 0.089$, F ratio = 0.79 .

While not a common clinical measurement for DED, ocular hypertension is often caused by the inflammation present in dry eyes. Inflamed ocular tissues can reduce or even block outflow of aqueous humour through the trabecular meshwork and Schlemm’s canal, raising IOP.[47]

Further, as HASD is hypothesized to reduce MMP-9 expression and therefore inflammation, IOP is a simple way to potentially assess a significant reduction in MMP-9 activity. As seen in figure 9, throughout the 14 days animals were dosed with 0.1% BAC, there was no significant change in IOP. Further, the variance in measurement, even with each animal, was prohibitively large.

IOP was therefore discarded for future testing as a useful DED metric.

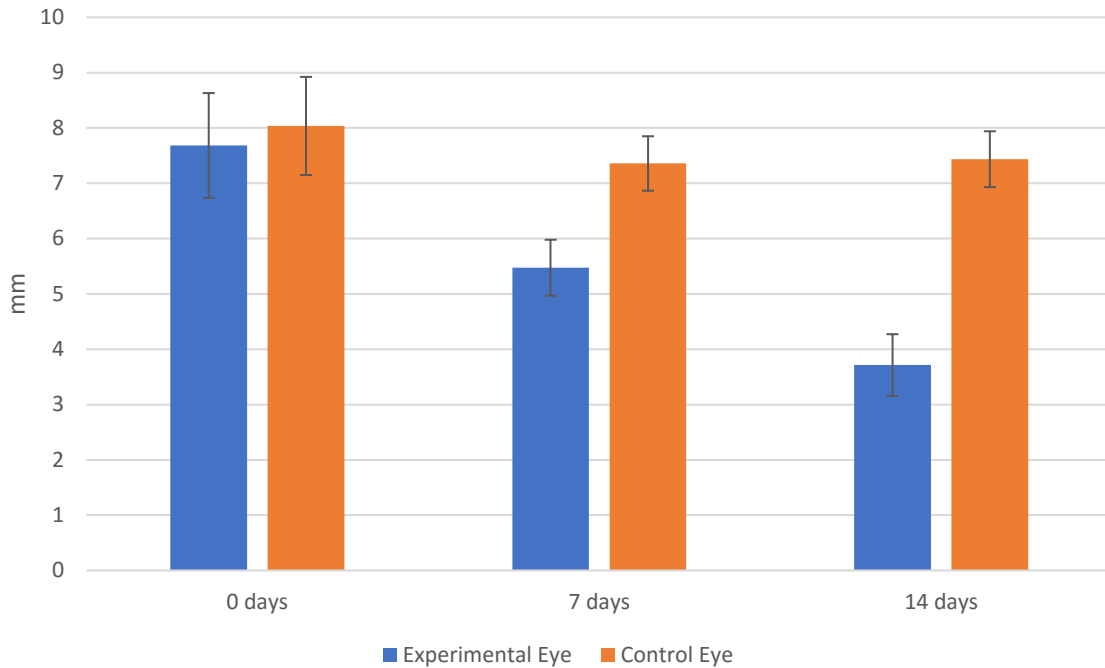


Figure 10 – Effect of twice daily administration of 0.1% BAC on tear volume. Error = 1 standard deviation, n = 12. 7 days and 14 days are both significantly different with $p < 0.05$

Schirmer's test, which measures tear volume by observing capillary migration along a standardised strip of paper, is probably the most direct and most used assessment of DED. There was a significant drop in tear volume as a result of BAC dosing, almost cutting normal values in half.

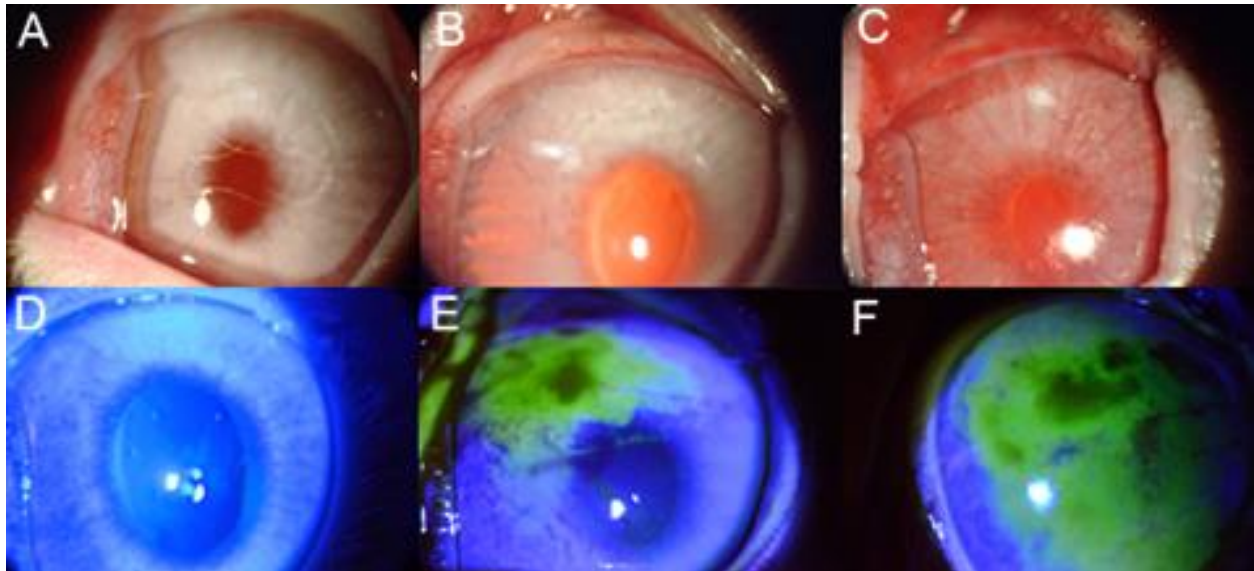


Figure 11 – Effect of twice daily administration of 0.1% BAC on ocular surface as examined through a slit lamp.

A visual slit lamp ophthalmoscopic examination was performed to corroborate the creation of DED like symptoms in this model. Described in figure 11, healthy eyes (A, D) showed significant increase in redness (limbal hyperemia), irritation, epithelial roughness, tear film breakup, and neovascularisation at both the 7 day timepoint (B, E) and especially after the full 2 weeks (C, F). Fluorescein staining also increased to cover nearly the entire bulbar surface by 14 days (F), indicating a compromised corneal epithelium. Taken together, by the end of the 14-day induction period, model symptoms were indistinguishable from genuine severe dry eye.






PANEL	Grade	Criteria
A 	0	Equal to or less than panel A
B 	I	Equal to or less than panel B, greater than A
C 	II	Equal to or less than panel C, greater than B
D 	III	Equal to or less than panel D, greater than C
E 	IV	Equal to or less than panel E, greater than D
>E	V	Greater than panel E

Figure 12 – Oxford grading scheme for dry eye

There are numerous semi-quantitative grading schema for the assessment of DED, which can use a variety of variables. For these experiments, data collected was converted onto the Oxford Scheme. While this particular grading tool is perhaps less nuanced or specific than competitors, it is by far the simplest and most reproducible between clinicians. The phenotype of the DED being created in this model, the complexity of other assessment practices which might let clinicians more accurately diagnose a sub-type of DED, is unnecessary. Figure 13 illustrates the extent of corneal staining and redness numerically.

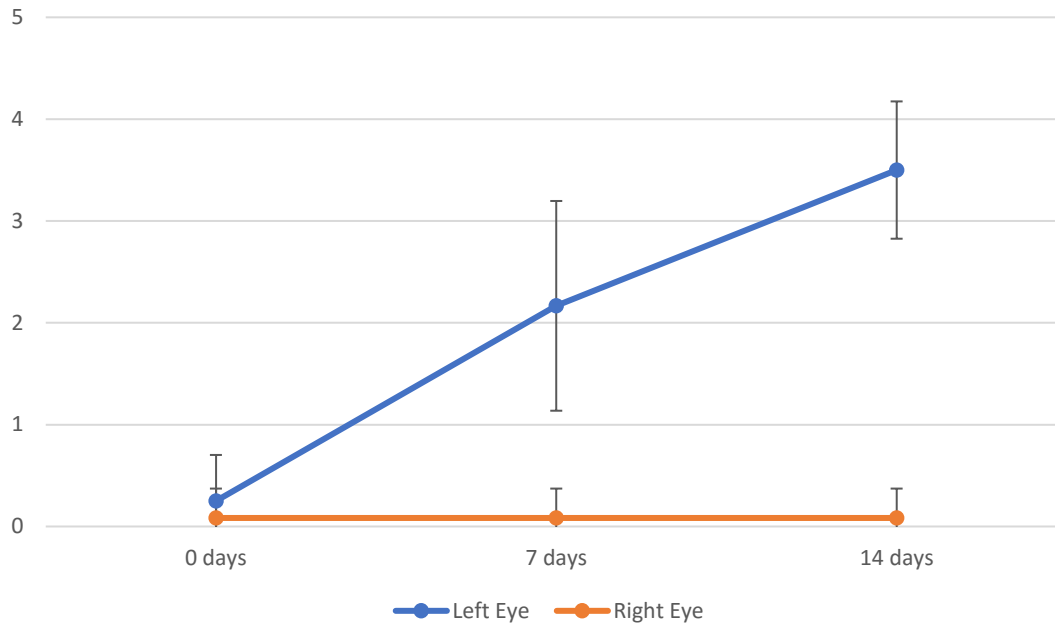


Figure 13 – Oxford scheme grading for BAC dosed eye (left eye) and control eye (right eye) after staining with Rose Bengal. Error = standard deviation, n = 12. Both 7 days and 14 days are significantly different with $p < 0.05$

CIC examination of the corneal surface can give a histological level of detail to the cornea without sacrificing the animal. Figure 14 is an example of CIC staining across DED induction. Samples are stained with Periodic acid–Schiff stain (PAS), which colours mucins and other glycoproteins. This resolves mucin producing goblet cells in particular relief. As can be seen starting at day 0 and progressing to day 14, the corneal epithelium becomes progressively disrupted and decellular. By day 14, the epithelium is clearly fragmented, and very few goblet cells remain. This destruction of the corneal epithelium forms part of the feedback system (Figure 1) which can result in a progressive DED; without mucins to reduce friction and bind water, symptoms worsen.

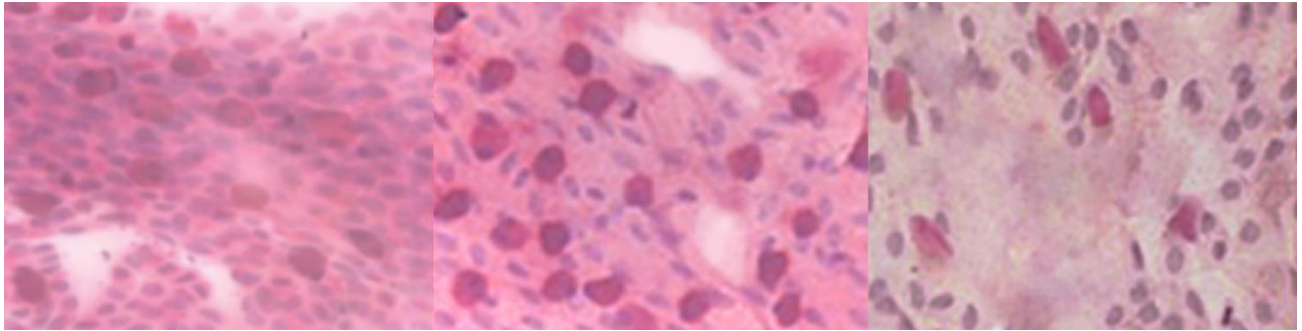


Figure 14 – CIC staining throughout 0.1% BAC dosing. Day 0 (left) shows a normal cornea, while day 7 (middle) and day 14 (right) show progressive decellularization and dysplasia of the corneal epithelium.400x magnification.

By combining all of the data presented above, a very convincing model of DED was created and characterised. Procedural order was extremely important throughout. The drop of alcaine anaesthetic given to the animals before examination can mask corneal staining and dryness. It can further be wicked up in Schirmer's test giving falsely high readings. The preservatives used in fluorescein swabs can cause irritation and themselves initiate higher than appropriate Oxford scores. After optimising the order and timing of these various interventions, we have created a very reliable and repeatable preclinical DED model.

2.6 Rescue from disease state

A variety of HASD variants were created by varying the molecular weight of the HA component. After initial testing (data not shown) did not substantiate any performative differences between

them, the HASD with 125kDa HA molecule was selected as the candidate to examine in the disease model. Animals were given a 100µL drop of either HASD, phosphate buffered saline (PBS), the leading over-the-counter dry eye drop Systane Ultra by Alcon, or nothing at all for 4 days. After the 4-day test period had elapsed, animals were reassessed to measure any improvement.

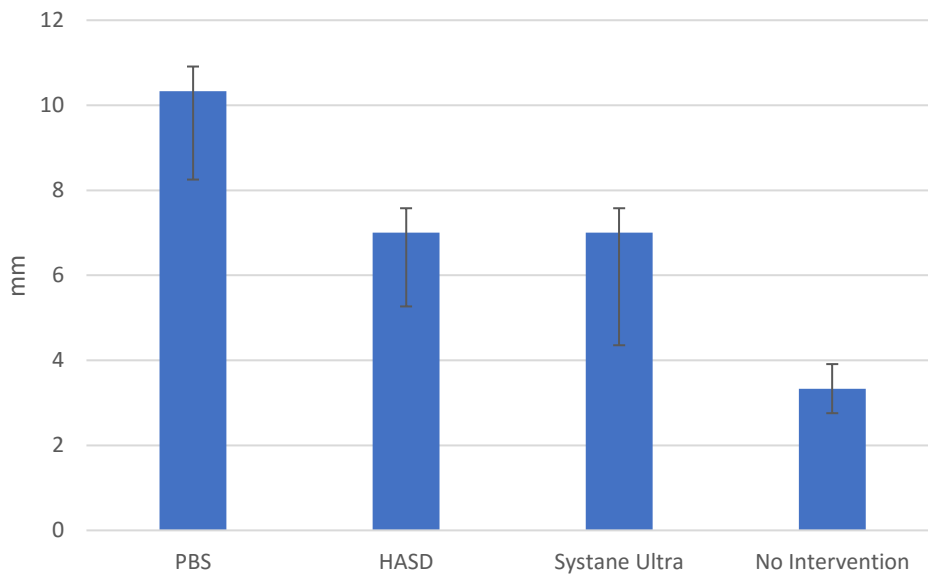


Figure 15 – Schirmer’s test showing DED rescue after 96 hours of treatment. Error = standard deviation, n=3, ANOVA shows significant difference $p = 0.014$, F ratio = 1.63.

As seen in Figure 15, Schirmer’s test shows significant improvement from the 3.7 mm average reading seen in Figure 10. At first glance, it seems as if a simple PBS drop was the best performer; animals dosed with PBS had significantly more tear volume than HASD or the most effective artificial tears on the market: Systane Ultra. However, this result is somewhat counterintuitive. Excessive tears are produced in response to irritation when neural impulses in the cornea result in

cholinergic parasympathetic response.[48] The abnormally high tear volume seen after PBS instillation (2.9mm higher than controls) suggests the eye remains in distress and not that it has recovered. Due to the cessation of BAC dosing, the eye has begun to recover, and is now able to tear in response to its injury, but it has not healed These ‘distress’ tears are furthermore mostly water and contain none of the rich metabolic or lubricating factors present in normal tears.[49] Both HASD and Systane Ultra have returned tear volume very near to control levels, with no significant difference between the two. Without any intervention, tear volume remains low.

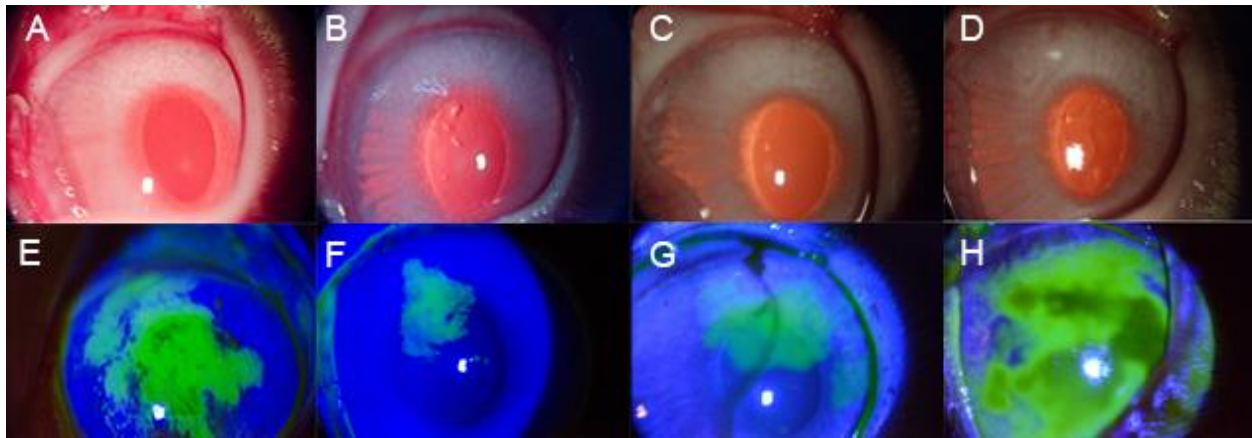


Figure 16 – Slit lamp ophthalmoscopy using brightfield (A-D) and fluorescein (E-H) imaging modes. Representative samples after treatment from PBS (A, E), HASD (B, F) Systane Ultra (C, G) and no treatment (D, H).

As seen in Figure 16, slit lamp ophthalmoscopy corroborates Schirmer’s test. Eyes treated with PBS continue to show neovascularisation and a great deal of corneal staining, although much of the redness has abated. Eyes treated with HASD and Systane Ultra both appear almost totally recovered - even healthy eyes will often have some small amount of staining. Untreated eyes remain hyperemic and vascularised, and continue to stain throughout the cornea and conjunctiva.

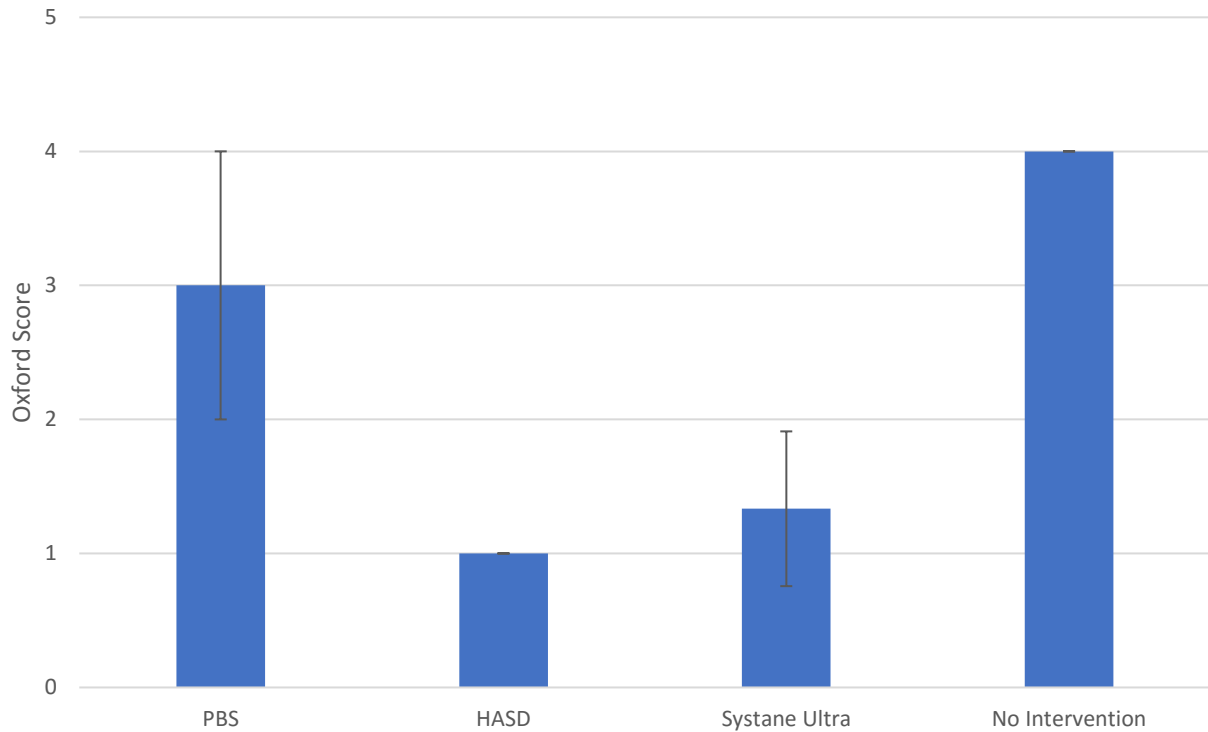


Figure 17 – Oxford scores after DED rescue. Error = standard deviation, n=3, ANOVA shows significant difference $p=0.01$, F ratio = 1.61.

Oxford Scheme scoring further validates these results. No intervention produced the worst score, followed by PBS, leaving HASD and Systane Ultra approximately equivalent again.

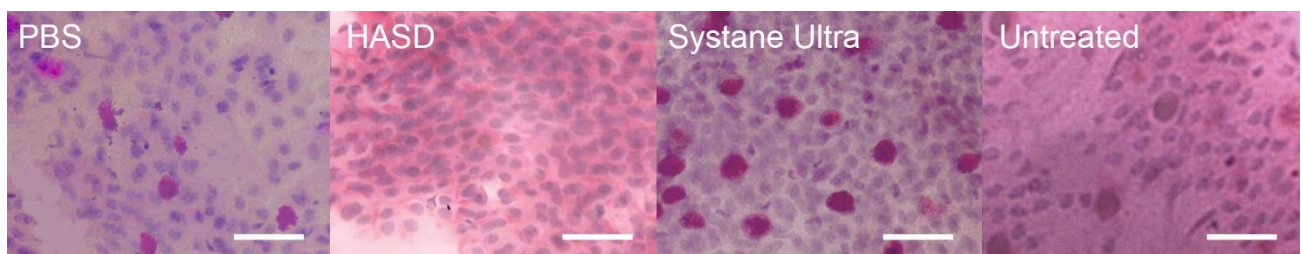


Figure 18, CIC after DED rescue. 400x zoom, scale bar = 100 μ m.

CIC completes this story. Both PBS and untreated eyes have few goblet cells and inconsistent epithelium. HASD and Systane Ultra treated eyes clearly have a much healthier cornea.

2.7 Conclusion and future work

A preclinical rabbit model of DED was created and animals were treated with the conceptually novel compound HASD to measure the clinical potential of this novel compound. While it performed well – at least as well as the best artificial tear solution Systane Ultra – this comparison is perhaps unfair to HASD. This model produced DED-like symptoms through the use of a caustic chemical; none of the endocrine, morphological, or physiochemical causes found in real world DED exist in this model. As HASD is designed to inhibit inflammation and tissue remodelling by deactivating MMP-9, it is possible HASD could cure DED in people where MMP-9 dysregulation is a causative factor. The best Systane Ultra can do is relieve discomfort by increasing lubricity and providing moisture. While this may have done well within the context of this model, HASD has enormous potential to improve on the status quo in human trials.

By far the biggest limitation of HASD is the inclusion of SDZ. While SDZ has an extensive precedent in the eye, primarily as an antimicrobial agent on the World Health Organisation's list of essential medicines, approximately 3% of the population is allergic.[50] Furthermore, its low solubility make it extremely cumbersome to work with – particularly in an industrial setting where production efficiency becomes a central concern. MMPs catalyze the hydrolysis of peptide bonds through stabilization of the cleaving water molecule and the transition state of the substrate. This stabilization depends on a zinc ion chelated by three histidine residues in the active site of the enzyme. Therefore, many groups capable of binding to this zinc can interfere with MMP function, effectively inhibiting them. Swapping out this SDZ for a more appropriate

compound, while keeping the lubricity enhancing, CD44 binding HA ought to be relatively simple. Hydroxamate structures, for example, have been shown to bind zinc and act as an MMP inhibitor (MMPI). Drugs based on these hydroxamate derivatives, such as Ilomastat, have already been used effectively as a cancer chemotherapy.[51] Further, the sulfonamide group in SDZ is found in a library of other materials. A key component to the allergic response initiated by SDZ is the arylamine group at N4. Other sulfonamide containing compounds do not necessarily have this issue, and evidence suggests those allergic to SDZ have no cross-reactivity with sulfonamides that lack this arylamine group.[52] The list of suitable alternatives, many of which are approved by the FDA in some capacity, is enormous. MMPIs based on thiols, pyrimidines, pyrones, phosphorus and tetracycline have all been designed and validated in the literature, often with specificity to MMP subtypes.[53] Finally, endogenous MMPIs, known as tissue inhibitors of metalloproteinases (TIMPs) represent a relatively new area of exploration. While perhaps more synthetically complex than other options, TIMPs obviously come with no biocompatibility issues, and are extremely specific.[54] In short, HASD might have broader appeal without SDZ, and there is certainly no shortage of potential replacements.

2.8 References

1. *The epidemiology of dry eye disease: report of the Epidemiology Subcommittee of the International Dry Eye WorkShop (2007)*. Ocul Surf, 2007. **5**(2): p. 93-107.
2. Goto, E., et al., *Optical aberrations and visual disturbances associated with dry eye*. Ocul Surf, 2006. **4**(4): p. 207-13.
3. Miljanovic, B., et al., *Impact of dry eye syndrome on vision-related quality of life*. Am J Ophthalmol, 2007. **143**(3): p. 409-15.
4. Baudouin, C., et al., *Revisiting the vicious circle of dry eye disease: a focus on the pathophysiology of meibomian gland dysfunction*. Br J Ophthalmol, 2016. **100**(3): p. 300-6.
5. King-Smith, P.E., et al., *The thickness of the tear film*. Curr Eye Res, 2004. **29**(4-5): p. 357-68.
6. Bron, A.J., et al., *Functional aspects of the tear film lipid layer*. Exp Eye Res, 2004. **78**(3): p. 347-60.
7. Tong, L., et al., *Association of tear proteins with Meibomian gland disease and dry eye symptoms*. Br J Ophthalmol, 2011. **95**(6): p. 848-52.
8. Tong, L., et al., *[The dry eye]*. Praxis (Bern 1994), 2013. **102**(13): p. 803-5.
9. Viso, E., M.T. Rodriguez-Ares, and F. Gude, *Prevalence of and associated factors for dry eye in a Spanish adult population (the Salnes Eye Study)*. Ophthalmic Epidemiol, 2009. **16**(1): p. 15-21.
10. Schaumberg, D.A., et al., *Prevalence of dry eye syndrome among US women*. Am J Ophthalmol, 2003. **136**(2): p. 318-26.

11. Glasson, M.J., et al., *The effect of short term contact lens wear on the tear film and ocular surface characteristics of tolerant and intolerant wearers*. Cont Lens Anterior Eye, 2006. **29**(1): p. 41-7; quiz 49.
12. Schaumberg, D.A., et al., *Patient reported differences in dry eye disease between men and women: impact, management, and patient satisfaction*. PLoS One, 2013. **8**(9): p. e76121.
13. Schaumberg, D.A., et al., *Prevalence of dry eye disease among US men: estimates from the Physicians' Health Studies*. Arch Ophthalmol, 2009. **127**(6): p. 763-8.
14. *Mattson jack epidemeology analysis 2005*.
15. Schiffman, R.M., et al., *Utility assessment among patients with dry eye disease*. Ophthalmology, 2003. **110**(7): p. 1412-9.
16. Lemp, M.A., et al., *Distribution of aqueous-deficient and evaporative dry eye in a clinic-based patient cohort: a retrospective study*. Cornea, 2012. **31**(5): p. 472-8.
17. Lane, S.S., et al., *A new system, the LipiFlow, for the treatment of meibomian gland dysfunction*. Cornea, 2012. **31**(4): p. 396-404.
18. Friedman, N.J., et al., *A nonrandomized, open-label study to evaluate the effect of nasal stimulation on tear production in subjects with dry eye disease*. Clin Ophthalmol, 2016. **10**: p. 795-804.
19. Hussain, M., et al., *Long-term use of autologous serum 50% eye drops for the treatment of dry eye disease*. Cornea, 2014. **33**(12): p. 1245-51.
20. Semeraro, F., et al., *Effect of Autologous Serum Eye Drops in Patients with Sjogren Syndrome-related Dry Eye: Clinical and In Vivo Confocal Microscopy Evaluation of the Ocular Surface*. In Vivo, 2016. **30**(6): p. 931-938.

21. Yu, J., C.V. Asche, and C.J. Fairchild, *The economic burden of dry eye disease in the United States: a decision tree analysis*. *Cornea*, 2011. **30**(4): p. 379-87.
22. *PharmaPoint: Dry Eye Syndrome - Global Drug Forecast and Market Analysis to 2022*.
23. Maulvi, F.A., T.G. Soni, and D.O. Shah, *Extended release of hyaluronic acid from hydrogel contact lenses for dry eye syndrome*. *J Biomater Sci Polym Ed*, 2015: p. 1-26.
24. Ibrahim, H.K., I.S. El-Leithy, and A.A. Makky, *Mucoadhesive nanoparticles as carrier systems for prolonged ocular delivery of gatifloxacin/prednisolone bitherapy*. *Mol Pharm*, 2010. **7**(2): p. 576-85.
25. Oh, H.J., et al., *Effect of hypotonic 0.18% sodium hyaluronate eyedrops on inflammation of the ocular surface in experimental dry eye*. *J Ocul Pharmacol Ther*, 2014. **30**(7): p. 533-42.
26. Amoozgar, B., D. Morarescu, and H. Sheardown, *Sulfadiazine modified PDMS as a model material with the potential for the mitigation of posterior capsule opacification (PCO)*. *Colloids Surf B Biointerfaces*, 2013. **111**: p. 15-23.
27. Mori, M., et al., *Discovery of a New Class of Potent MMP Inhibitors by Structure-Based Optimization of the Arylsulfonamide Scaffold*. *ACS Med Chem Lett*, 2013. **4**(6): p. 565-9.
28. De Paiva, C.S., et al., *Corticosteroid and doxycycline suppress MMP-9 and inflammatory cytokine expression, MAPK activation in the corneal epithelium in experimental dry eye*. *Exp Eye Res*, 2006. **83**(3): p. 526-35.
29. Aragona, P., et al., *Matrix metalloproteinase 9 and transglutaminase 2 expression at the ocular surface in patients with different forms of dry eye disease*. *Ophthalmology*, 2015. **122**(1): p. 62-71.

30. Schargus, M., et al., *Correlation of Tear Film Osmolarity and 2 Different MMP-9 Tests With Common Dry Eye Tests in a Cohort of Non-Dry Eye Patients*. *Cornea*, 2015. **34**(7): p. 739-44.
31. Schrader, S., A.K. Mircheff, and G. Geerling, *Animal models of dry eye*. *Dev Ophthalmol*, 2008. **41**: p. 298-312.
32. Lavoie, T.N., B.H. Lee, and C.Q. Nguyen, *Current concepts: mouse models of Sjogren's syndrome*. *J Biomed Biotechnol*, 2011. **2011**: p. 549107.
33. Suwan-apichon, O., et al., *Botulinum toxin B-induced mouse model of keratoconjunctivitis sicca*. *Invest Ophthalmol Vis Sci*, 2006. **47**(1): p. 133-9.
34. Chen, W., et al., *A murine model of dry eye induced by an intelligently controlled environmental system*. *Invest Ophthalmol Vis Sci*, 2008. **49**(4): p. 1386-91.
35. Jiang, G., et al., *A new model of experimental autoimmune keratoconjunctivitis sicca (KCS) induced in Lewis rat by the autoantigen Klk1b22*. *Invest Ophthalmol Vis Sci*, 2009. **50**(5): p. 2245-54.
36. Jain, P., et al., *An NGF mimetic, MIM-D3, stimulates conjunctival cell glycoconjugate secretion and demonstrates therapeutic efficacy in a rat model of dry eye*. *Exp Eye Res*, 2011. **93**(4): p. 503-12.
37. Gilbard, J.P., S.R. Rossi, and K.G. Heyda, *Tear film and ocular surface changes after closure of the meibomian gland orifices in the rabbit*. *Ophthalmology*, 1989. **96**(8): p. 1180-6.
38. Fujihara, T., et al., *Establishment of a rabbit short-term dry eye model*. *J Ocul Pharmacol Ther*, 1995. **11**(4): p. 503-8.

39. Guo, Z., et al., *Autologous lacrimal-lymphoid mixed-cell reactions induce dacryoadenitis in rabbits*. *Exp Eye Res*, 2000. **71**(1): p. 23-31.
40. Toshida, H., et al., *Evaluation of novel dry eye model: preganglionic parasympathetic denervation in rabbit*. *Invest Ophthalmol Vis Sci*, 2007. **48**(10): p. 4468-75.
41. Chen, Z.Y., Q.F. Liang, and G.Y. Yu, *Establishment of a rabbit model for keratoconjunctivitis sicca*. *Cornea*, 2011. **30**(9): p. 1024-9.
42. de Almeida, D.E., et al., *Conjunctival effects of canine distemper virus-induced keratoconjunctivitis sicca*. *Vet Ophthalmol*, 2009. **12**(4): p. 211-5.
43. Maitchouk, D.Y., et al., *Tear production after unilateral removal of the main lacrimal gland in squirrel monkeys*. *Arch Ophthalmol*, 2000. **118**(2): p. 246-52.
44. Gerald, L.B., et al., *Redesigning a large school-based clinical trial in response to changes in community practice*. *Clin Trials*, 2011. **8**(3): p. 311-9.
45. Pisella, P.J., P. Pouliquen, and C. Baudouin, *Prevalence of ocular symptoms and signs with preserved and preservative free glaucoma medication*. *Br J Ophthalmol*, 2002. **86**(4): p. 418-23.
46. Xiong, C., et al., *A rabbit dry eye model induced by topical medication of a preservative benzalkonium chloride*. *Invest Ophthalmol Vis Sci*, 2008. **49**(5): p. 1850-6.
47. Barabino, S., et al., *Ocular surface immunity: homeostatic mechanisms and their disruption in dry eye disease*. *Prog Retin Eye Res*, 2012. **31**(3): p. 271-85.
48. Parra, A., et al., *Tear fluid hyperosmolality increases nerve impulse activity of cold thermoreceptor endings of the cornea*. *Pain*, 2014. **155**(8): p. 1481-91.
49. Acosta, M.C., et al., *Changes in sensory activity of ocular surface sensory nerves during allergic keratoconjunctivitis*. *Pain*, 2013. **154**(11): p. 2353-62.

50. Li, X.M. and H.Y. Wang, [*Provide against possible trouble--on knowledge, prevention and treatment of adverse drug reactions*]. Zhongguo Zhong Xi Yi Jie He Za Zhi, 2003. **23**(5): p. 327-8.
51. Khan, O.F., J. Jean-Francois, and M.V. Sefton, *MMP levels in the response to degradable implants in the presence of a hydroxamate-based matrix metalloproteinase sequestering biomaterial in vivo*. J Biomed Mater Res A, 2010. **93**(4): p. 1368-79.
52. Wiholm, B.E., *Should celecoxib be contraindicated in patients who are allergic to sulfonamides?* Drug Saf, 2002. **25**(4): p. 297-9; author reply 299-300.
53. Piette, M., et al., *Pharmacokinetic study of a new synthetic MMP inhibitor (Ro 28-2653) after IV and oral administration of cyclodextrin solutions*. Eur J Pharm Sci, 2006. **28**(3): p. 189-95.
54. Nagase, H., R. Visse, and G. Murphy, *Structure and function of matrix metalloproteinases and TIMPs*. Cardiovasc Res, 2006. **69**(3): p. 562-73.

Chapter 3: PolyNIPAAm based cell delivery scaffold for posterior segment cell therapy

Scientific Contributions

- Develop and characterize a scaffold specifically engineered for cell delivery to the subretinal space
- Test this scaffold in a novel organotypic retinal model
- Experiment with cell lines and stem cells as potential therapeutic agents
- Develop the surgical capacity to implant scaffolds in the subretinal space of rodents

Publications from this work

- Scott D. Fitzpatrick, Mohammad Abu Jafar Mazumder, David S. Baek, Xu Zhao, Hai Wang, Lindsay Fitzpatrick, Ben Muirhead, Shelley R. Boyd, Heather Sheardown (2017) Optically Transparent Thermally Gelling Drug Delivery Scaffold for Minimally Invasive Delivery to the Posterior Segment of the Eye. Manuscript awaiting publication
- PolyNIPAAm based cell delivery scaffold to rescue sodium iodate induced AMD model (manuscript in preparation)

Abstract

Diseases of the retina are a leading cause of vision loss, affecting more than 10 million people worldwide. They are Incurable, progressive, increasing in prevalence and affect the entire age spectrum. Current treatments can slow progression, but they are not curative. Stem cells offer novel treatment possibilities by not just halting, but potentially reversing the progression of these degenerative diseases and restoring vision. While many groups have made enormous progress in generating pure cultures of useful stem cell lines for therapeutic use, much less emphasis has been placed on companion bioengineered scaffolds to improve cell survival and functional integration. Despite many studies showing regeneration of damaged retinal tissues using stem cells, it is clear that cell based retinal therapies have not satisfied their immense potential. Engineered biomaterial scaffolds are thus central to the realization of cell based regenerative therapies in the eye.

To that end, a patented material for cell delivery to the retina has been created. This invention is based around Poly(N-isopropylacrylamide) (PNIPAAm), a thermoresponsive material which undergoes a reversible transition from liquid to gel when heated above a lower critical solution temperature (LCST). Harnessing this property allows the introduction of cell-loaded scaffolds into the subretinal space through minimally invasive injections, forming a gel *in situ* and providing cells with anchorage and protection. This approach diverges significantly from the status quo where cells are either injected as a simple bolus or implanted on a rigid sheet requiring extensive surgery. Ultimately, this approach could be used to facilitate a true realization of stem cell therapies for retinal tissues and significantly improve cell survival and functional integration.

3.1 Background

The retina, shown in Figure 1, is a highly specialized and interdependent tissue susceptible to a host of progressive, degenerative conditions. While the mechanisms underlying these degenerations are varied, ultimately, death of neuronal tissues within the retina characterizes the major irreversible causes of vision loss.

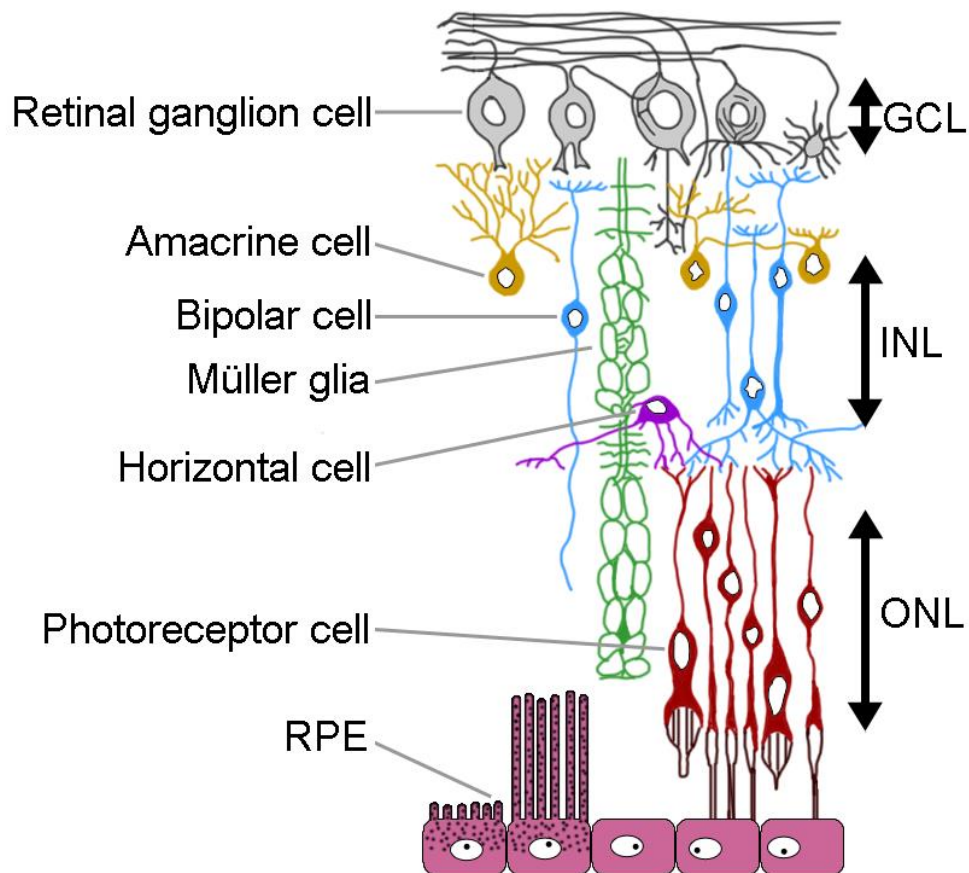


Figure 1 – The retina is a very complex peculiar tissue which has ten different layers, namely retinal pigment epithelium (RPE), photoreceptor outer segments, outer limiting membrane, outer nuclear layer, outer plexiform layer, inner nuclear layer, inner plexiform layer, ganglion cell

layer, nerve fiber layer and inner limiting membrane. The cells and membranes of these layers are interconnected and in constant physiochemical communication. Damage to any of these layers can impair function of the retina, which can lead into visual impairment or blindness.

Retinitis pigmentosa (RP) is an umbrella term representing a spectrum of hundreds of potential inherited genetic defects which cause developmental irregularities in the retina – particularly in photoreceptors. RP is a leading cause of vision loss in children, but depending on specific etiology can manifest at any age. Of particular note in the category of inherited retinal disorders, while considered distinct from RP, is Stargardt’s macular dystrophy (SMD), which alone accounts for 7% of all retinal degenerative diseases.[1] In RP, retinal degeneration typically begins with the rods; it is peripheral and low-light vision which is lost first. Central vision is often maintained for years or decades after first diagnosis. In SMD, it is typically the most metabolically active photoreceptors – the cones responsible for central vision in the macula – which are lost. By far the most prevalent form of SMD is caused by mutations in the 4th member of the ATP-binding cassette, family A (ABCA4) gene. The ATP-binding cassette (ABC) superfamily of genes codes for an enormous array of proteins specialized in the active transport of various substrates across cell membranes. ABCA4, which localizes specifically in the retina, participates in the retinoid cycle, through which the retina is able to recycle 11-*cis*-retinal, thereby allowing phototransduction. In SMD, this recycling is attenuated, and a toxic chemical (Di-retinoid-pyridinium-ethanolamine [A2E]) becomes trapped in the retinal pigment epithelium (RPE) layer, eventually destroying it. ABCA4 mutations have been found in several forms of RP, linking it with SMD in a continuum of retinal disease manifestations that present as distinct clinical phenotypes based on the type of mutation present and the level of allelic heterogeneity.

Accordingly, SMD results from partial but not complete inactivation of both alleles, allowing for residual low level ABCA4 expression, whereas the variant of RP (RP19) in which this gene is defective, the most severe of ABCA4-related conditions, would derive from the presence of two null ABCA4 alleles, fully inhibiting its expression. Photoreceptors damaged in this way will die early in life, and even if it was possible, gene therapy at this stage would be useless, and only the replacement of atrophied photoreceptor cells with healthy equivalents could offer a cure.

Diabetic retinopathy (DR) and diabetic macular edema (DME) are common microvascular complications in patients with diabetes.[2] DR/DME are the leading causes of blindness in working aged adults in the developed world.[3] The worsening diabetes epidemic suggests these diseases will continue to be primary contributors to vision loss and associated functional impairment for the foreseeable future.[4] Advanced stages of DR (proliferative retinopathies) are characterized by a loss of pericyte cells, excessive growth of abnormal retinal blood vessels, inflammation, and fluid accumulation. At any time during the progression of DR, patients with diabetes can also develop DME, which involves retinal thickening in the macula, interstitial separation, and often retinal detachment. DME represents a breakdown of the blood-retinal barrier system due to leakage of dilated, hyperpermeable capillaries and microaneurysms.[5] Early detection is by far the most successful form of control. However, this strategy is hampered by the fact that the condition is generally asymptomatic at early stages. While laser photocoagulation, a technique used to attenuate new vessel growth, as well as a slate of new anti-vascular endothelial growth factor (VEGF) drugs are available to effectively manage DR/DME, they come with severe drawbacks. Laser photocoagulation therapy destroys the retina around the sites of ablation, thereby sacrificing some parts of the peripheral retina to save central vision[6].

Anti-VEGF drugs require frequent intravitreal injections, which are associated with an increased risk of complication and suffer from patient discomfort and compliance issues. Most importantly, however, are cases of DR which go undiagnosed until significant vision loss has already developed. In these cases, there is no treatment available.

Age-related macular degeneration (AMD) is the leading causes of irreversible blindness in the elderly. The incidence of AMD is rapidly increasing as populations age. According to the presence or absence of choroidal neovascularization (CNV), AMD can be generally divided into two types: dry AMD and wet AMD. Dry AMD is primarily attributed to the accumulation of subretinal lipophilic deposits called drusen which evoke local activation of chronic inflammation and lead to atrophy of the retinal pigment epithelium (RPE). Eventually, the loss of the RPE, which is necessary for metabolic homeostasis in the outer nuclear layer, results in the permanent loss of overlying photoreceptors. Wet AMD is a neovascularization of the choriocapillaris – the capillary network which supports the retina behind its basement membrane (Bruch's membrane). As with DR, these new vessels are fragile and poorly formed, resulting in leakage and protein deposition underneath the macula. Wet AMD is a rare (>10% of cases) progression of the disease which very rapidly destroys the macula through inflammation, scarring, and physical disruption of this highly structured space.[7] The pathophysiology of AMD is very similar to SMD described above, and the two conditions can be confused for each other in a clinical setting.[8] Indeed, A2E, the same lipofuscin fluorophore which causes RPE death in SMD is a primary component of drusen. Further, mutations in the ABCA4 gene are highly correlative with development of AMD, and specific variants are often used clinically as a potential marker of disease.[9]

Collectively, the above retinopathic conditions affect hundreds of millions of people worldwide across the entire age spectrum. It is estimated that 1 in 9 Canadians suffer irrevocable visual loss by the age of 65 years, and 1 in 4 by the age of 75 years.[10] Visual loss places an enormous burden of care on the affected individuals, their care-givers, and the health care system.[11] Preventative strategies, such as dietary and lifestyle changes, can in some cases slow progression of these diseases, but are not a solution. New anti-angiogenic drugs (eg Avastin, Lucentis, Eylea, Macugen) have improved patient care but require regimented and frequent intraocular injection – often for decades.[12]

While it may be tempting to address these diseases, all of which have strong genetic concomitants, at the level of genes, it is important to note the extraordinary heterogeneity of these conditions. There are over 500 disease associated genetic variants described so far, with no upper limit yet hinted at.[13] Even the most common disease mutations (ie G1961E, G863A/delG863 and A1038V, etc) account for tiny fractions of retinal dystrophies, making gene intervention an unusually difficult therapeutic target.[14] In a modern context of CRISPR and its associated technologies, gene therapy seems to have taken some of the momentum that used to characterize stem cells. Modern gene therapy undoubtedly has an enormous role to play in combating disease – even retinal disease. In fact, recent advances in gene therapy herald new hope for slowing or reversing vision loss in patients with RP, and are presently in clinical trial for a small number out of the hundreds of potential genetic defects.⁵ Unfortunately, due to the heterogeneity of RP, such gene therapies have very limited reach, and obviously gene therapies are not useful in non-heritable conditions like DR/DME or AMD. In fact, the case can be made,

that retinopathy in particular is too personalized, and too nested in developmental and microenvironmental context for gene therapies to really function well in this space.

Given the importance of obvious importance of vision, and the complete lack of adequate treatment to rescue damaged retinal tissues, there is a tremendous unmet need to replace cells and repair and regulate their microenvironment.

Cell therapies in general, and stem cell therapies in particular, offer novel treatment possibilities, not just halting, but potentially reversing the progression of degenerative diseases. The idea of stem cell therapy was born out of one of the 20th century's most prominent tragedies. The nuclear bombings of Hiroshima and Nagasaki stimulated a surge of biomedical research aimed at understanding and treating the effects of radiation exposure. It was discovered that bone marrow, transplanted into lethally irradiated animals, could restore hematopoiesis and save their lives. In the early 1960s, Till and McCulloch began analyzing bone marrow to find out which components were responsible this unprecedented regeneration. They defined what remain the two hallmarks of stem cells: self-renewal and an ability to differentiate into other cell types.[15] Since this discovery, and particularly since the discovery of induced pluripotent stem cells (iPSCs) by Takahashi and Yamanaka in 2006, stem cell transplantation as a means of replacing or regenerating tissue has evolved rapidly, becoming foundational to modern regenerative medicine.

The retina has unique advantages as a target for cell-based therapies. While advancements in retinal surgery, imaging, and functional analysis have led to the development of once futuristic treatment modalities such as bionic microelectronic implants, these devices are fundamentally

limited by the biophysics they use.[16] The retina has become a reproducibly accessible tissue with modern vitreoretinal surgical approaches refined for the transplantation of cells to specific locations in the retina. The eye is highly compartmentalized which allows graft material to be targeted to a specific microenvironment with no chance of ‘off-target’ effects. Similar to the rest of the central nervous system (CNS), the eye is considered ‘immune privileged’ which may reduce or eliminate any inflammatory or allogeneic response usually mounted towards transplanted cells and any accompanying scaffolds. Perhaps most importantly, there are numerous tools to measure ocular structure and function including optical coherence tomography (OCT), various forms of angiography, confocal scanning laser ophthalmoscopy (cSLO) and electroretinography (ERG) which allow for extremely precise, non-invasive, and real-time examination of function and structure. These advantages have led retinal disorders to the forefront of clinical trials into cell-based paracrine and regenerative therapies.[17]

While new applications are being devised at an ever-increasing pace, in general, cell therapies to the retina target either the RPE or the photoreceptor layer. The RPE is a hexagonal, monolayer of polarized pigmented cells which serve many functions within the retina. Despite no direct involvement in phototransduction, these cells are nevertheless essential for vision. The RPE contact in tight junctions which form part of the blood-retina barrier (BRB), facilitating the selective transport of metabolites to the photoreceptor layer, thereby controlling ionic homeostasis essential for the electrically active tissues of the retina. The BRB also helps establish the immune privileged nature of the eye, which is essential for its normal functioning. Vision starts with the absorption of a photon by the chromophore 11-cis retinal. This absorption causes a trans-isomerisation, which the photoreceptors cannot re-isomerise back into 11-cis

retinal. Performing this re-isomerisation and transport of 11-cis retinal back into the photoreceptive layer is performed by the RPE. The light-sensitive photoreceptor outer segments (POS) are continually being destroyed due to photo-oxidative damage. To maintain vision, the POS are constantly renewed through phagocytosis of these oxidized fragments by the RPE.[18] Dysfunction of the RPE can therefore be disastrous; as mentioned above, several retinal diseases, including AMD and SMD, are in essence diseases of the RPE. Ultimately, degeneration of the retina implies a decrease in photoreception. As seen in Figure 1, the neural retina contains several cell types which group and process signals from photoreceptors to the optic nerve and then the primary visual cortex. Unlike the RPE, which is a relatively simple epithelial monolayer, a primary challenge when restoring the neural retina with new cells is functionally integrating them into existing circuitry of enormous complexity. In addition to being directly responsible for vision, of the neuronal retina cell types, photoreceptors are the most feasible therapeutic target as they are connected in only one direction to the brain. In retinal diseases that spare the inner retina, transplanted photoreceptors could reconnect to the inner retina and then stimulate connections all the way to the visual cortex.[19] Despite a series of high profile publications, including some clinical trials, which claim successful integration of PRs into the outer retina,[20] it has become clear that this is not actually happening. What was previously thought to be stem cell integration and differentiation has since been shown to be cell-cell fusion between the donor stem cell and the host cell in these studies.[21] This process of material transfer seems to account for the majority of ostensibly delivered cells within the host retina, and raises the need to re-evaluate the cellular mechanisms underlying photoreceptor transplantation and its relative contribution to rescue of retinal degeneration.[22]

The rest of this chapter will therefore focus on the replacement of the RPE, which is a much less complex system than the photoreceptive layer of the retina and its associated circuitry, and whose feasibility is much less contentious in the scientific community. Using endogenous progenitor populations, embryonic stem cells (ESCs) or induced pluripotent stem cells (iPSCs), several research groups have been able to guide differentiation into a cell that displays many characteristics and morphological requisites of functional RPE tissue.[23-25] There are currently several phase I/II clinical trials in progress using stem cell-based therapies to restore the RPE.[26, 27] While an enormous amount of research has been invested in stem cells – their creation, characterization, application – a commensurate investment in engineered biomaterial scaffolds to house these cells has lagged behind significantly. It is becoming increasingly obvious that for most clinical applications of stem cell technology, scaffolding is required to improve cell survival and functional integration.[28] Typically, with the exception of haemocytes, cells are delivered to target tissues one of two ways. In the first approach, cells can be delivered naked via syringe as a bolus injection. While minimally invasive, this approach results in poor integration into target tissues, no control over cell fate, migration away from the target area, massive cell death and clinical inefficacy. Alternatively, cells can be seeded and expanded *ex vivo* on or within an implantable biomaterial scaffold. While delivering cells from a scaffold addresses many of the shortcomings of injection, tissues need to be surgically dissected for insertion – a particularly undesirable requirement within the delicate tissues of the retina. Thus, a minimally invasive delivery technique which, while injectable, offers the advantages of a biomaterial scaffold could fundamentally transform cell delivery to the retina. To that effect, a series of cell scaffolds have been developed to improve cell survival and functional integration of graft tissue for retinal therapeutics.

3.2 Polymer Design

The challenge presented here was the creation of a cell scaffold perfectly tailored to the delivery of cells to the subretinal space. Aside from an obvious requirement of biocompatibility, if such a scaffold were to be invented purely as a fiction, without any need to conform to the realities of chemistry, what would it look like? Such a scaffold would certainly need to be degradable. The subretinal space is actually a misnomer – there is not normally a gap between the RPE and the outer nuclear layer of the neural retina. The ease with which these layers separate and reintegrate is one of the conveniences which make cell therapy to the retina so promising. However, separating the retina from the RPE can carry the risk of a real detachment, and also quickly results in ischemia as nutrients and waste are no longer able to diffuse quickly enough.[29] Furthermore, the mechanism through which degradation occurs should not produce undesirable byproducts. PLGA, a common scaffold material for cell delivery, degrades into its acidic monomers, and can decrease local pH.[30] This is particularly problematic in a closed tissue compartment with very limited diffusion. An ideal scaffold ought to be isovolumetric. It should not collapse in volume, thereby expelling its cargo, nor should it swell, disrupting the delicate subretinal space. One of the biggest advantages to cell scaffolding is the ability to control cell fate and improve survival and functional integration through the addition of bound factors, ligands, and other biologically relevant cues. However, to be useful in as wide a range of delivery scenarios as possible, a perfect scaffold would need to be flexible and modifiable.

Given these disparate requirements, Poly(NIPAAm-NAS- PEG-DBA) (PNNPD) was created. The core of this technology is PNIPAAm, an unusual material which exists as a liquid at room temperature, but which forms a gel when heated above a lower critical solution temperature (LCST) - 32°C for unmodified NIPAAm. By harnessing this property, a cell scaffold can form *in situ*, and a cell/scaffold construct can be injected into the subretinal space instead of surgically implanted. However, PNIPAAm on its own is non-degrading, totally unoptimized to house cells, and tends to expel its cellular cargo upon gelation (see chapter 2). PNIPAAm was therefore copolymerized with several other monomers to optimize its performance. N-acryloxysuccinimide (NAS) was added to allow the bioconjugation of differentiation cues, survival enhancers, growth factors, and binding ligands. Whatever is needed to improve cell survival and functional integration can be easily added post synthesis, which was demonstrated by the addition of an amine-modified fluorescein (Figure 2). The addition of polyethelene glycol (PEG) greatly increased the water binding capacity of an otherwise hydrophobic polymer. Through the incorporation of these hydrophilic domains, the resultant copolymer phase separates upon gelation, producing alternating microregions of differing hydrophilicity (Figure 5). If self-assembled into the correct geometry, these materials become transparent to light – an extremely useful property when working in the eye. More importantly, however, PNNPD does not shrink upon gelation, and therefore its cellular cargo remains encapsulated, overcoming one of the most significant limitations of NIPAAm based polymers in general (see chapter 2). Finally, the incorporation of Dimethyl- γ -butyrolactone acrylate (DBA) facilitates a biocompatible degradability. Intact, the lactone ring structure on DBA is relatively hydrophobic. However, it is susceptible to hydrolytic attack resulting in a ring opening and a concomitant shift towards

hydrophilicity. Because the gelation mechanism of PNIPAAm is dependent on intramolecular hydrophobic interactions, as the copolymer becomes more hydrophilic, it begins to reliquify and become soluble. Once in solution, PNNPD can easily be cleared from the body through the renal system, assuming that the molecular weight of the degraded fragments is such that it can be cleared from the body. Taken together, PNNPD is a degradable, isovolumetric, transparent, *in situ* gelling copolymer scaffold with the potential for facile customization.

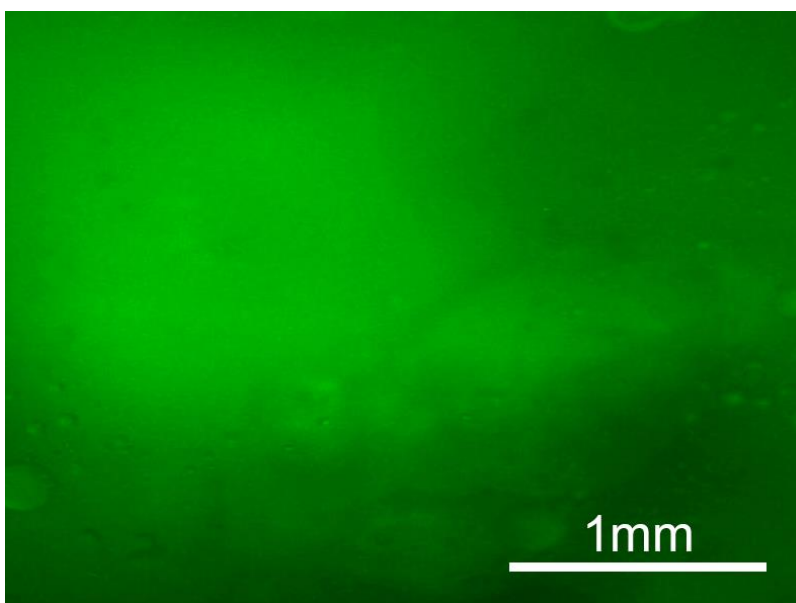


Figure 2 – PNNPD after modification with 5-Aminofluorescein (Sigma-Aldrich, SKU 210626) and viewed under a fluorescent microscope 20x.

PNNPD copolymers were synthesized via free radical polymerization. NIPAAm (80%) NAS (4%), PEO (4%), DBA (12) and BPO (1%) were dissolved in a 10% (m/v) 1,4-dioxane monomer solution. Dry nitrogen was bubbled through the solution for 15 min to displace oxygen, and the flask was then sealed and subsequently heated to 70°C for 24 h in a temperature-controlled oil bath with constant stirring to provide uniform mixing. Following the reaction, the polymer

solution was cooled to room temperature and precipitated dropwise in an excess of anhydrous ethyl ether. The copolymer was further purified by repeated precipitation from THF into anhydrous ethyl ether. The resulting polymer was dried for 24 h in a vacuum oven at 50°C and further purified by extensive dialysis in deionized water before being freeze-dried, and stored at -20°C.

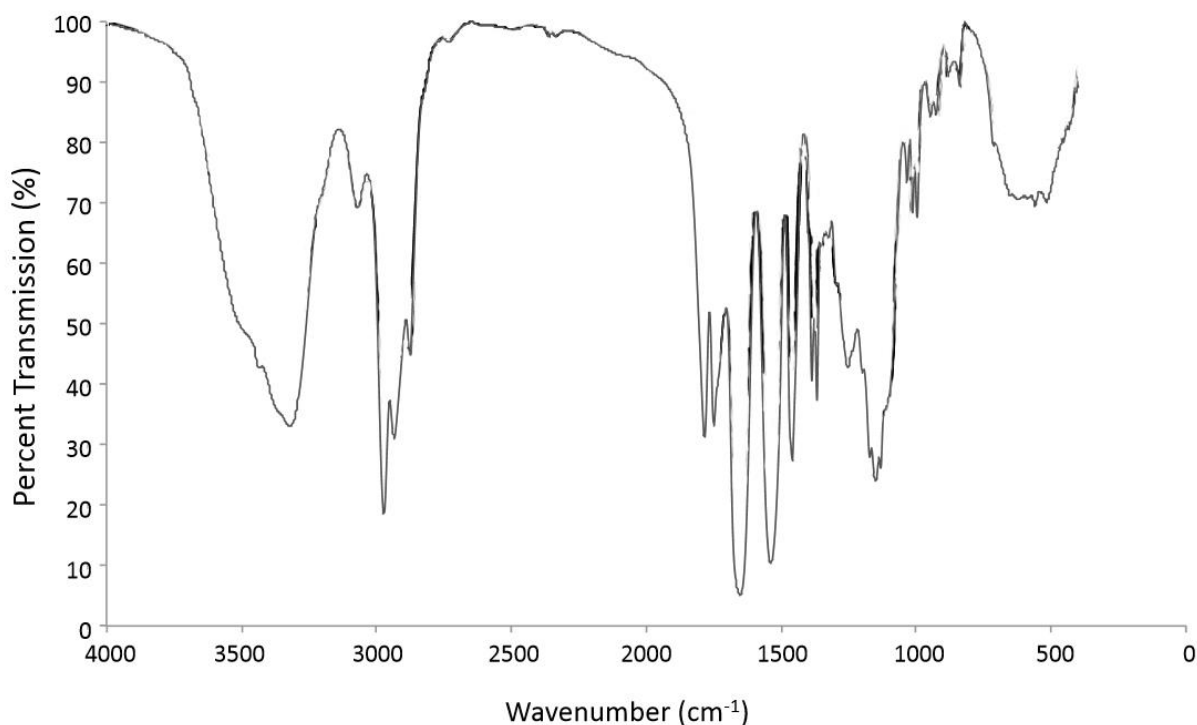


Figure 3 – FT-IR spectra of PNNPD copolymer

As seen in Figure 3, the FT-IR spectra shows appropriate C=O and N-H NIPAAm peaks at 1600cm⁻¹ and 1540cm⁻¹ respectively. There is an N-H stretching vibration at 3310cm⁻¹, and

isopropyl peaks at 1360cm^{-1} , 1380cm^{-1} and 1460cm^{-1} . The CH_2O from the PEG is evident at around 1100cm^{-1} . The carbonyl peak part of the DBA ring structure can be seen at 1780cm^{-1} .

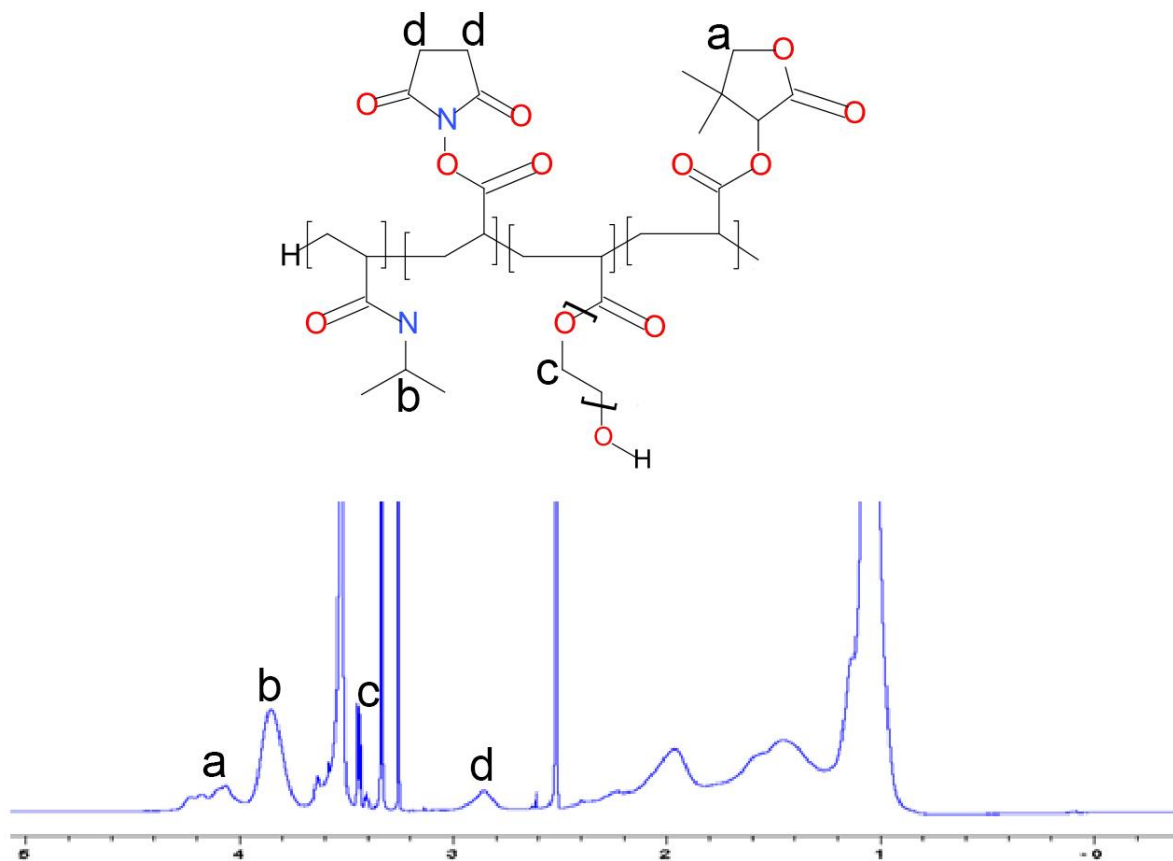


Figure 4 – $^1\text{H-NMR}$ confirming structure of PNNPD

$^1\text{H-NMR}$ was used to quantify copolymer molar content and verify structure as depicted in figure 4. PNNPD shows a NIPAAm CH peak from the isopropyl group between 3.7 – 4.0 (b), a NAS CH_2 ring peak between 2.8 – 3.0 (d), a PEG CH_2 peak at 3.4 ppm (c), and a DBA ring CH_2 peak between 4.0 – 4.4 ppm (a).

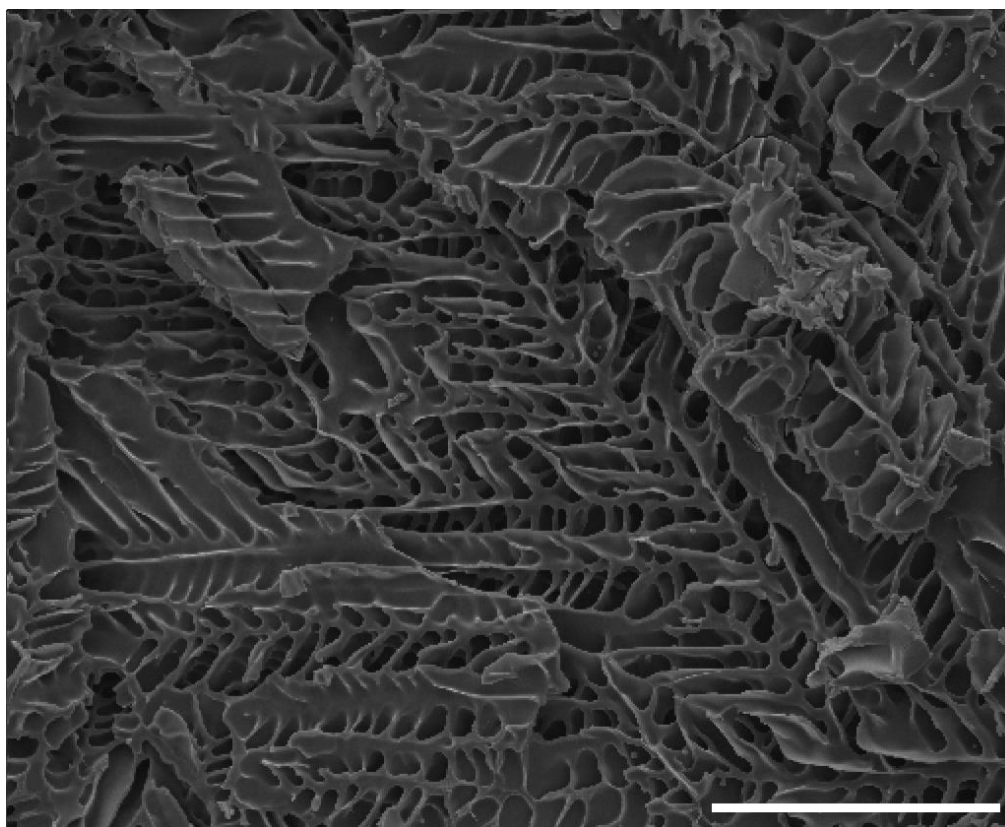


Figure 5 – SEM micrograph showing the microstructure of gels. Scale bar = 100 μ m.

Figure 5 is a scanning electron micrograph showing the ordered microstructure of PNNPD defined by its hydrophobic/hydrophilic domains. Gels were formed by heating polymer solutions (25% w/v in PBS) to 37°C for 48 hours and then rapidly immersing them in liquid nitrogen to preserve their gelled morphology. The samples were then lyophilized and coated in 15nm of gold to allow visualization of the microstructure.

Table 1 – List of potential cell scaffold materials

Polymer	Composition	LCST	Gel Appearance at 37°C
pNNP ₅ D ₄	75.8: 4.9: 14.1: 5.2	35.2	Soft, translucent
pNNP ₅ D ₈	76.1: 4.8: 9.3: 9.8	27.7	Stiff, opaque
pNNP ₅ D ₁₂	75.7: 4.5: 6.7: 13.1	18.7	Stiff, opaque
pNAP ₅ D ₄	75.2: 4.9: 15.2: 4.7	36.9	Soft, translucent
pNAP ₅ D ₈	76.1: 5.9: 8.8: 9.2	28.3	Stiff, Opaque
pNAP ₅ D ₁₂	75.3: 5.2: 6.2: 13.3	20.8	Stiff, Opaque
pNNP ₄ D ₄	75.4: 4.7: 15.4: 4.5	39.1	No gel
pNNP ₄ D ₈	75.9: 4.6: 10.2: 9.3	30.9	Stiff, Opaque
pNNP ₄ D ₁₂	75.3: 4.4: 7.3: 13.0	20.9	Stiff, Opaque
pNAP ₄ D ₄	76.0: 4.8: 13.1: 6.1	41.8	No gel
pNAP ₄ D ₈	76.2: 5.0: 9.2: 9.6	32.3	Stiff, Opaque
pNAP ₄ D ₁₂	75.9: 5.7: 5.9: 12.5	22.1	Stiff, Opaque
pNNP ₁₁ D ₄	76.2: 4.7: 13.1: 6.0	-	No gel
pNNP ₁₁ D ₈	76.0: 5.0: 8.3: 10.7	-	No gel
pNNP ₁₁ D ₁₂	76.0: 5.3: 5.7: 13.0	23.6	Stiff, transparent
pNAP ₁₁ D ₄	75.7: 5.1: 13.9: 5.3	-	No gel
pNAP ₁₁ D ₈	75.7: 4.8: 10.3: 9.2	-	No gel
pNAP ₁₁ D ₁₂	75.8: 4.8: 6.6: 12.8	26.8	Stiff, transparent

As seen in Table 1, arriving at PNNPD, which is, more specifically, PNNP₁₁D₁₂ was an iterative and very delicate process. The PEG used to ensure scaffolds are non-shrinking, and the NIPAAm necessary for gelation are fundamentally opposed in function. The NIPAAm gels through intramolecular hydrophobic interaction, while the PEG binds water and makes this process less

energetically favorable. Therefore, of the dozens of material combinations tried, of which Table 1 is only an excerpt, only a single formulation produced a material of sufficient stiffness to be considered a gel, and which had all of the characteristics required.

3.3 Organotypic *in vitro* model

Organotypic culture describes the *ex vivo* maintenance of a tissue which replicates its *in vivo* architectural microenvironment. Organotypic culture methods therefore allow researchers to characterize and manipulate complex tissues in a highly controlled *in vitro* setting. This approach can therefore fill the gap between dissociated cell culture systems, which allow a high degree of experimental reproducibility, control, and efficiency, and *in vivo* animal models that, with varying degrees of success, can reproduce the complexities of disease processes. The retina is an extremely intricate and interconnected tissue with an established precedent in organotypic modeling.[31] In order to harness this modeling paradigm to validate PNNPD as a cell delivery scaffold, novel organotypic *ex vivo* testing platform was created loosely based on the work of the Martin lab at Cambridge University.[32]

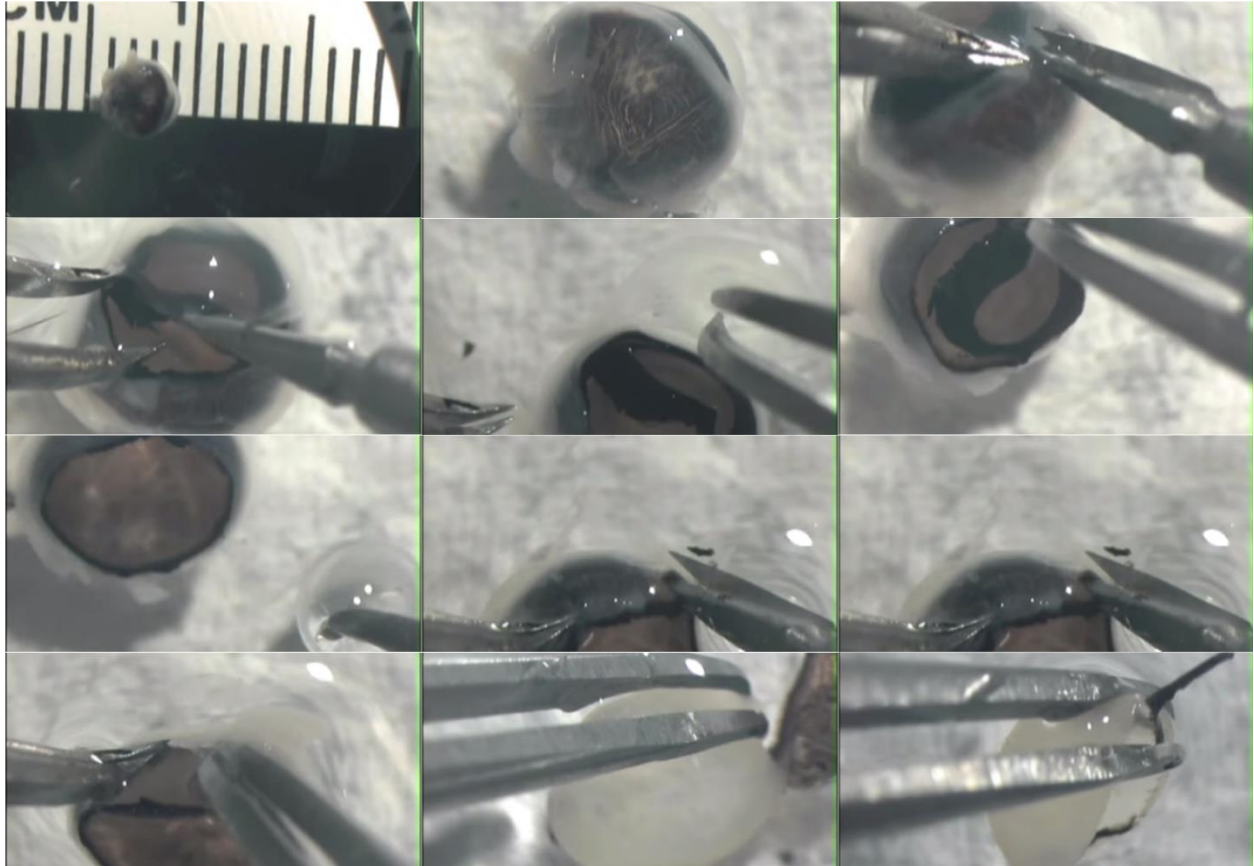


Figure 6 – Dissection of a rodent eye to create an organotypic culture model. An incision is made 1mm posterior to the corneal-scleral limbus. This incision is expanded until the anterior segment has been resected. The ciliary body and trabecular meshwork is pulled away with forceps. The lens is removed. Once the posterior cup has been isolated, the RPE layer, bound to Bruch’s membrane with associated choroid is dissected away, leaving a hemisphere of neural retina. The neural retina is dissected into 4 quadrants of roughly equal size for use in organotypic modelling.

This protocol utilizes neural retinal tissue from adult Sprague Dawley rats. Most organotypic retinal models utilize tissue from embryonic or neonatal animals which can remain viable *in vitro*

for several weeks. However, adult rats greater than 1 year old are used for this study – obviously an important consideration when modeling age-related neurodegenerative disorders.[33]

Depending on application, organotypic retinal culture methods can vary with regard to preparation and orientation of the tissue in culture. This protocol allows tissue to breach the media/air interface, where the outer nuclear layer is supported by a membrane. Nutrients diffuse into retinal tissue from below, and media forms a thin film over the explant. This configuration allows gas exchange from the air as well as minimizes tissue handling when maintaining cultures. Most importantly, the entire neural retina is in a configuration that closely approximates that found *in vivo*, unlike many organotypic equivalents which maintain floating, submerged, or adherent cultures.[34, 35]

The neural retina is dissected away from an enucleated rat eye globe under sterile conditions, as seen in Figure 6. During tissue isolation the optic nerve is transected to separate the retina from the posterior eye-cup. The intact neural retina is sectioned into four quadrants, which are placed on top of an adherent PET cell culture insert. In some cases, RPE tissue dissected from the neural retina was placed on top of the cell culture insert to act as a control. These cultures are able to reassociate and form an intact retina. A second well insert is placed on top of the explant, creating a ‘sandwich’ with an adherent PET membrane on the bottom and a non-adherent PTFE membrane on top to ensure flatness and stability. Non-control experiments did not have a layer of RPE to support photoreceptor outer segments, which will quickly lead to neurodegeneration similar to geographic atrophy seen in AMD. These cultures received an injection through a 32 gauge syringe of 150,000 RPE-J (ATCC CRL-2240) cells. This injection was handled in one of

two ways: either cells were injected in media, or within the PNNPD scaffolding. Explants were kept in culture for 7 days before being cryosectioned and examined immunohistochemically. The difference in retinal health resulting from the method of delivery was useful not only for validating the concepts buttressing PNNPD, but also as a convenient test bed for optimization for future iterations. This method generates 8 roughly equally sized, triangular-shaped retinal explants from a single rat. Explants cultured under these conditions were observed to maintain healthy retinal morphology and viability for at least 17 days.

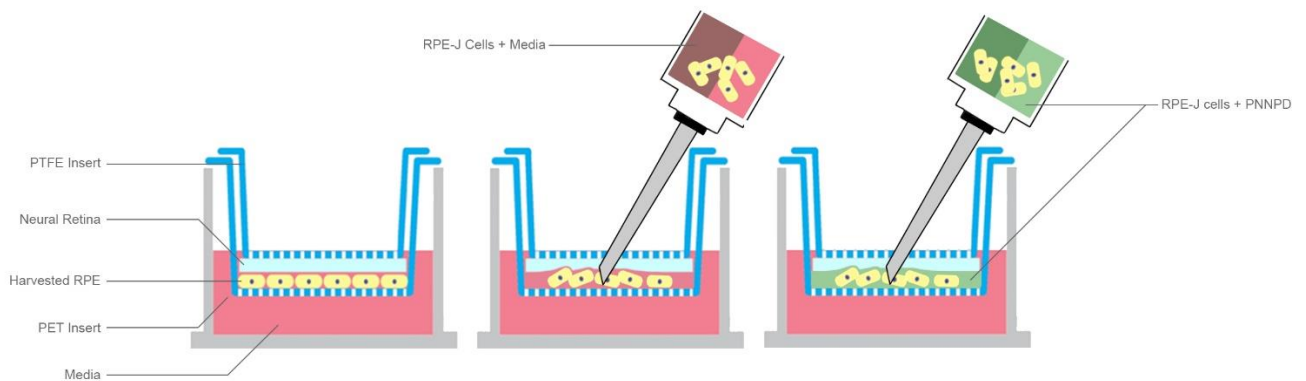


Figure 7 – Cartoon of organotypic culture. Control explants were grown with an intact RPE layer and Bruch’s membrane harvested at the same time as the neural retina (left). RPE-J cells were introduced into this model with the aim of sustaining the neural retina. In some cases, cells were injected suspended in media (middle). Otherwise, they were injected within PNNPD scaffolding. The two approaches were compared.

By far the most difficult part of this model was delamination of the ‘sandwich’ during some part of tissue processing for histology. With this admission, and an acknowledgment that methodological improvement is crucial to any future success, some data was able to be gathered. Seen in Figure 8 – a representative example from each of the relevant experimental categories was successfully embedded in paraffin wax, sectioned, and stained with H&E. As can be seen, RPE-J cells delivered into this culture model within PNNPD scaffolding were readily apparent as a pigmented mass in the correct tissue microenvironment. While there does seem to be some atrophy in the outer nuclear layer when compared with controls, this maybe have been caused at least partially by the delamination of this structure discussed earlier. The bottom of this construct certainly seems to have been truncated prematurely. Further, RPE-J cells, while relatively similar to natural RPE, are nevertheless an immortalized cell line which may not be able to properly support photoreceptors in this context. Otherwise, the inner nuclear layer and ganglion cells appear normal and healthy. Without PNNPD as a scaffolding biomaterial, there was no obvious sign of RPE cells at all, and tissues appear much more disrupted and irregular.

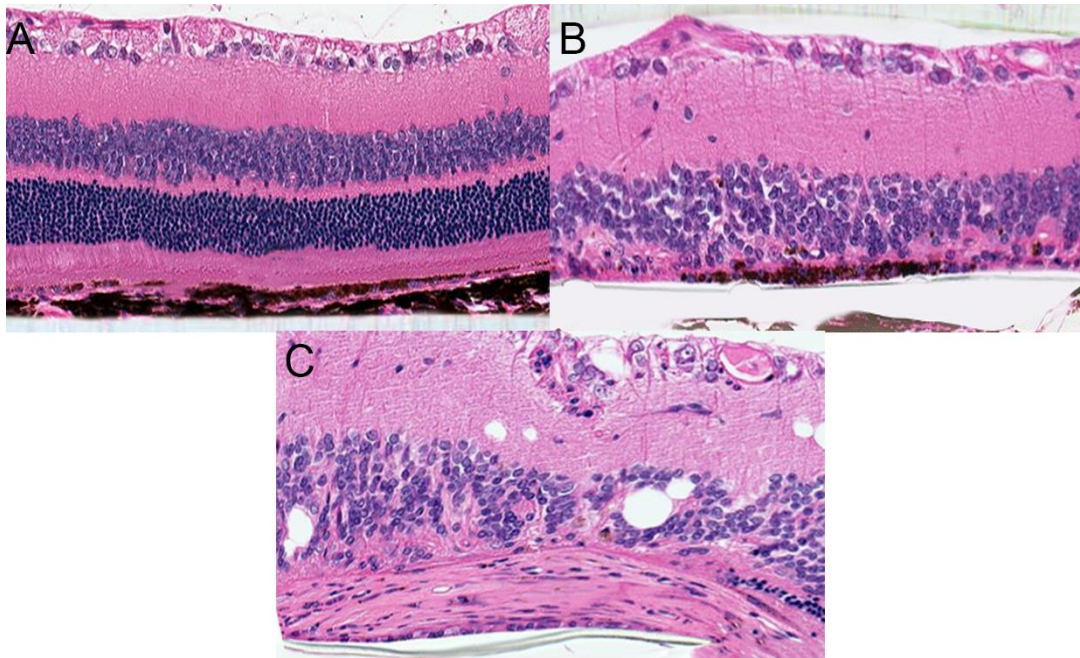


Figure 8 – Histology of organotypic ‘sandwich’ after excision from well inserts with a razor blade. (A) represents a control culture, where neural retina was grown on top of harvested RPE/choroid. (B) is the result after RPE-J cells were delivered using PNNPD scaffolding. RPE is clearly visible. Without scaffolding, there do not appear to be any surviving RPE-J cells (C).

In some cases, RPE-J cells were labeled with Qtracker cell labeling kit for contrast on a fluorescent microscope. As seen in Figure 9, cells delivered with PNNPD can be clearly identified growing within the organotypic model. Cells delivered without scaffolding have almost no Qtracker signal, indicating either cell death, where membranes have degraded enough for Qtracker to diffuse away, or cells were never able to find anchorage under the neural retina and diffused away from the site of injection. In this model setting, therefore, PNNPD has demonstrated a clear ability to enhance cell survival after injection.

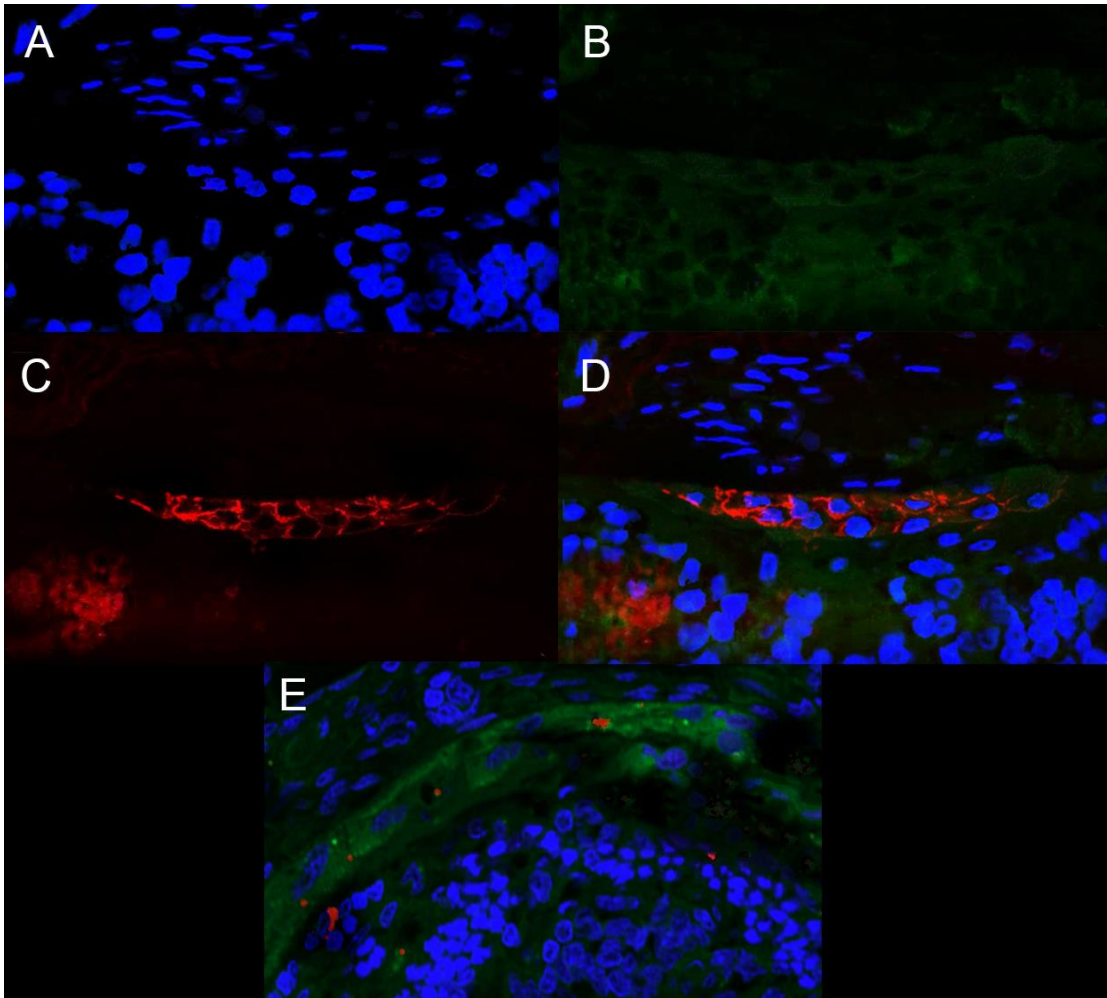


Figure 9 – fluorescent composite image of organotypic culture model. After excision, tissue samples were cryopreserved in a bath of isopentane, itself immersed in liquid nitrogen. After sectioning, samples were stained with DAPI. Where PNNPD was used to deliver cells, a composite image of DAPI (A), the autofluorescence of the retina (B), and Qtracker (C), verifies the presence of successfully transplanted RPE-J cells (D). Conversely, a similar composite image of a culture where PNNPD was not used shows almost no Qtracker labelled cells are present.

3.4 In vivo modelling

Ultimately, PNNPD is expected to be a useful clinical tool used to enhance cell based therapies to the retina. Subretinal injections of PNNPD were therefore performed in rats to test it in a relevant tissue microenvironment. Subretinal injections are rarely used in a clinical setting, although with an increase in exotic treatment possibilities of which PNNPD hopes to be a small part, perhaps these injections will become more common. Presently, however, there are several methods of reaching the subretinal space with no common standard. The method used in this section, as shown in figure 10, is transscleral. It should be noted that since this work was done, the transvitreal route has become my default, for reasons which will be discussed later.

Briefly, Lewis rats are used for these experiments, and are handled in accordance with the animal research ethics board (AREB) as well as McMaster University guidelines for animal work. Rats are anaesthetized with isoflurane gas by being induced at 5% with a 1L/min and maintained at 2% with a 200mL/min flow rate. Eyes are swabbed with iodine to minimize the risk of infection. Lids are retracted, and eyes are proptosed for access. A small tattoo of Nile blue stain is applied to the nasal side of the sclera to allow orientation after enucleation. The temporal side of the bulbar conjunctiva and temporal rectus muscle are resected to allow the eye greater range of movement within its orbit. The eye is rotated towards the nasal side to expose the posterior segment. The sclera is given a lancing incision with a 30-gauge beveled needle, and a 33 gauge blunt tipped syringe is inserted at as shallow an angle as possible. The injection is performed once the needle is forced into the subretinal space, implanting 2 μ l of copolymer. The use of

albino animals in this case allows visual confirmation of the injection as there is no pigmented RPE to obstruct vision, which can clearly be seen in the bottom panel of figure 10.

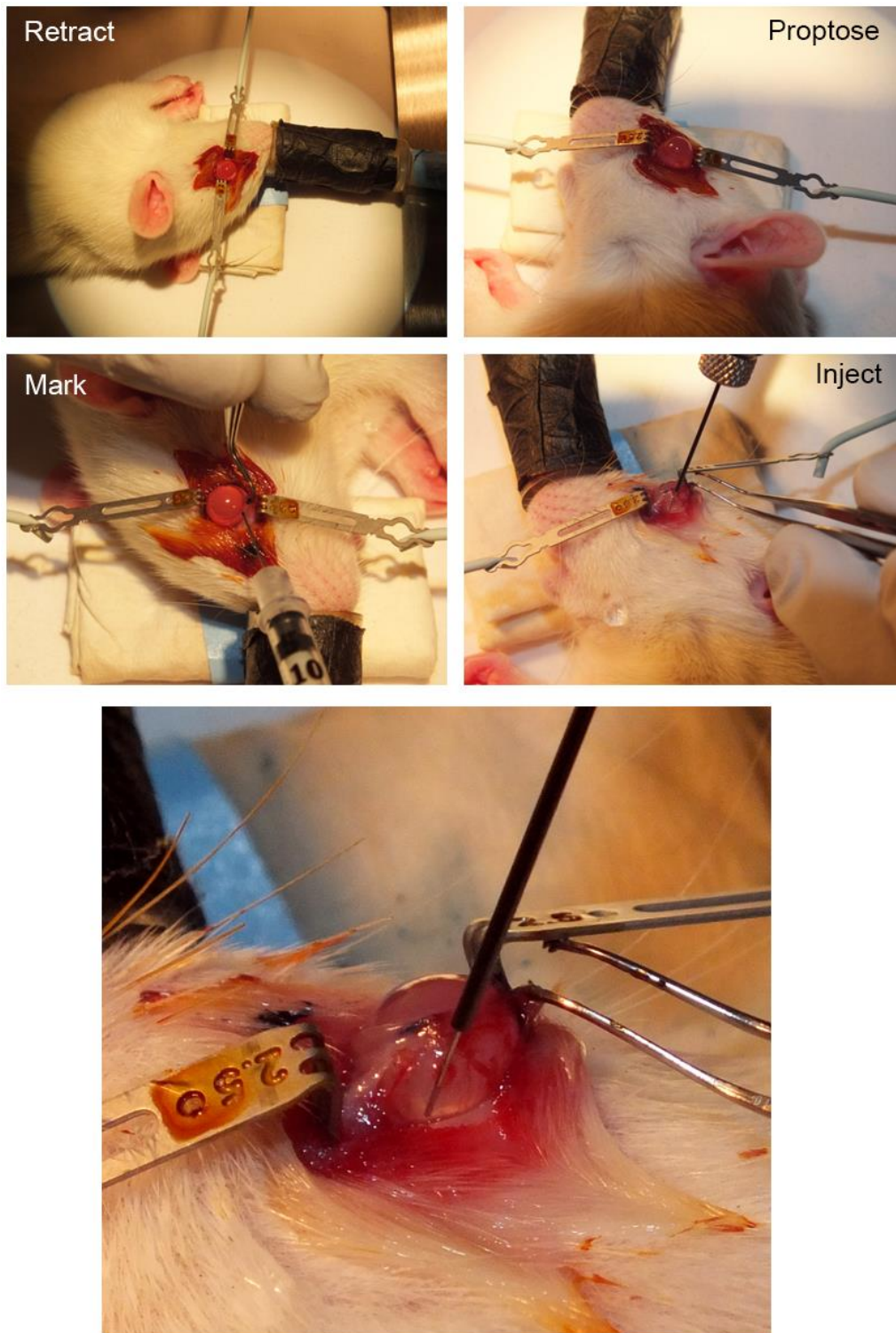


Figure 10 – Transscleral subretinal injection.

To track the progress of this subretinal injection, fundus ophthalmoscopy and optical coherence tomography (OCT) were utilized. By looking at the fundus in Figure 11, the successful subretinal implant can clearly be seen, particularly through contrast with a control eye. By taking an OCT scan along the implant, there is an empty void. PNNPD essentially has the refractive index of water; it is therefore unsurprising there is no optical scattering to produce an image. The bleeding evident after implantation is potentially troubling. The eye is generally considered as an immunologically privileged site. Both allogeneic and xenogeneic intraocular grafts can potentially enjoy a prolonged survival when compared with similar grafts implanted into other body sites.[36] By passing through the sclera and choroid, it is almost inevitable that transscleral injections will produce bleeding and compromise the tight junction barriers that typically exist between ocular tissues and systemic circulation. The leukocytes which migrate into the eye as a result may produce potentially catastrophic inflammation. Further, the transscleral injection method simply does not translate to the clinic; it is far too invasive. For these reasons, the transscleral approach was abandoned after this study, in favour of a transvitreal implantation route which will not be discussed further here.

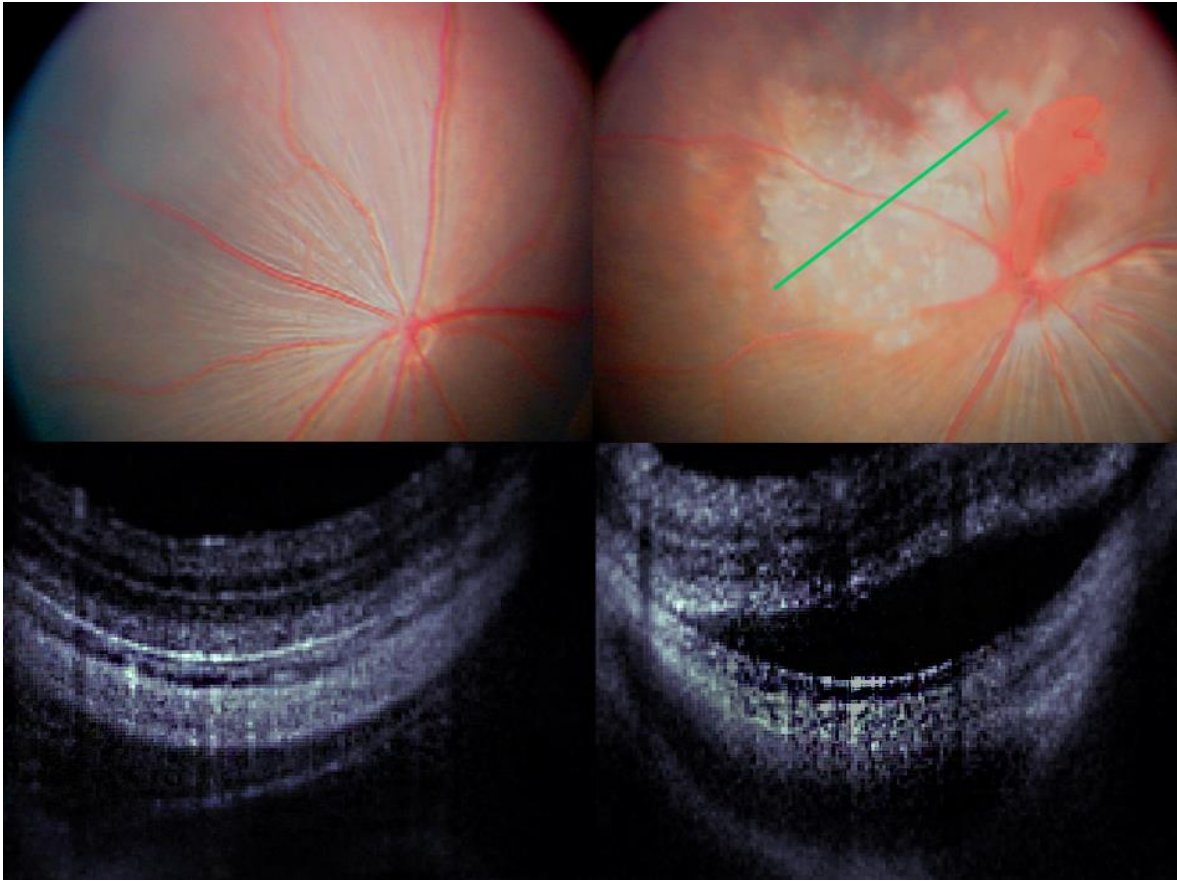


Figure 11 – Fundus ophthalmoscopy and OCT retinal images. A control eye (left column) shows a healthy retina without any disruption to its subretinal space. Following a transscleral subretinal injection of PNNPD, a retinal bleb can clearly be seen (top right), which is confirmed using OCT (bottom right).

Unfortunately, as described in Chapter 2, PNNPD does not survive the fixation process necessary for immunohistochemistry. Figure 12 shows a retinal section stained with DAPI taken from an animal sacrificed 24 hours after receiving the implant. While there is no evidence of any acute immune reaction, there is very clearly blood – mostly erythrocytes – pooling in the subretinal space, which can be seen in more detail in the zoomed image.

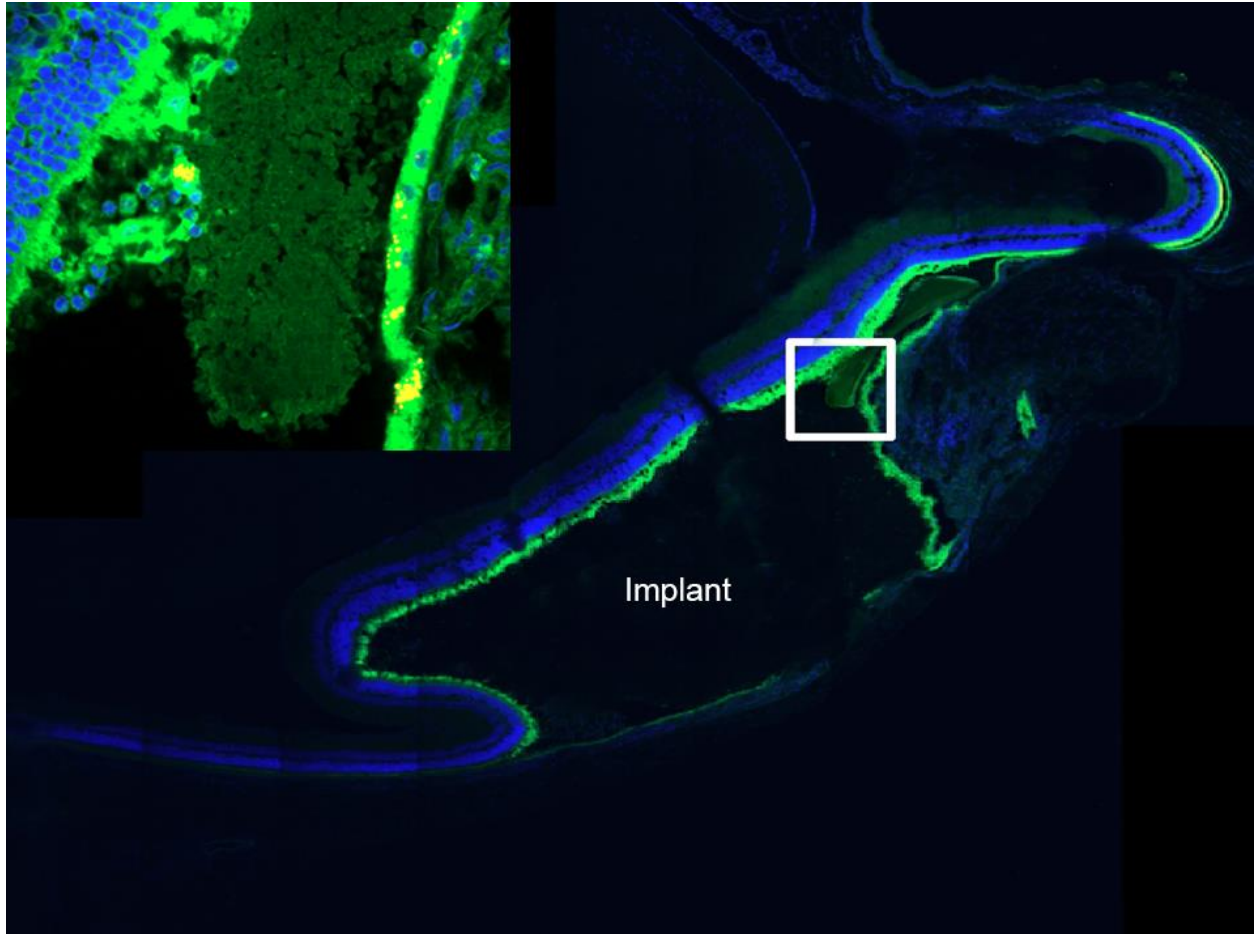


Figure 12 – DAPI and retinal autofluorescence image of the retina. Blood (top left) can be seen in the subretinal space.

3.5 Conclusion and future work

Cell delivery to the back of the eye is in need of a transformative approach to enhance cell survival and functional integration. By departing from the standard repertoire of accepted scaffolding materials, with poly(lactide-co-glycolide) PLGA,[37] polycaprolactone,[38] and poly(methyl methacrylate) (PMMA)[39] as popular choices, an enormous amount of *in vitro* and *in vivo* work is required to validate and optimize this novel approach. To address this unmet need, PNNPD was synthesized, characterized, and put through a comprehensive series of tests to prove its biocompatibility and suitability for this application. An organotypic testing platform was created using primary retinal tissue to refine PNNPD in a more controlled setting. 2 μ l of copolymer was successfully injected into the subretinal space with a 33-gauge syringe, utilizing body temperature to drive the *in situ* formation of a solid scaffold directly within this delicate microenvironment. While no deleterious changes were observed in retinal tissues after implantation, further testing is required to elucidate the long term fate of implanted materials, particularly as they degrade.

It was always my intention to test real cells in a disease model using PNNPD as a delivery scaffold. Sodium iodate (NaIO_3) can be used to produce a very convincing model of dry atrophic AMD and SMD by selectively depopulating the RPE, thereby inducing retinal degeneration.[40] New RPE can then be implanted to rescue this disease state, restoring vision. We are, however, not a stem cell lab, and an entire PhD can be spent optimizing precursor or progenitor cells for this purpose. As PNNPD is not a thin sheet like many RPE scaffolds, cells for implantation would need to be terminally fated to the RPE phenotype, while maintaining the flexibility to

migrate to a site of injury and integrate into existing tissues. This was found to be a daunting task for which there was not enough time. Advanced Cell Technologies, the world leader in human embryonic stem cell derived RPE for transplant, had agreed to a material transfer agreement (MTA) for their cells (MA09 cell line). They were acquired by another company before any could be sent, and the MTA was not honored. Recently, another collaboration has been established with the CCRM, a federal incorporated organization specializing in stem cell biology and regenerative medicine. As part of a postdoctoral fellowship, I hope to complete this project by implanting RPE precursor cells into the subretinal space of a NaIO₃ induced model of AMD. In addition to what has been presented in this chapter, tracking functional recovery with electroretinography would be essential. While I have injected cells into the subretinal space, these results added nothing substantive to this narrative and so were not included.

3.6 References

1. Genead, M.A., et al., *The natural history of stargardt disease with specific sequence mutation in the ABCA4 gene*. Invest Ophthalmol Vis Sci, 2009. **50**(12): p. 5867-71.
2. Oluleye, T.S., *Diabetic retinopathy: current developments in pathogenesis and management*. Afr J Med Med Sci, 2010. **39**(3): p. 199-206.
3. Mathew, C., A. Yunirakasiwi, and S. Sanjay, *Updates in the management of diabetic macular edema*. J Diabetes Res, 2015. **2015**: p. 794036.
4. Cheung, N., P. Mitchell, and T.Y. Wong, *Diabetic retinopathy*. Lancet, 2010. **376**(9735): p. 124-36.
5. Wu, L., et al., *Classification of diabetic retinopathy and diabetic macular edema*. World J Diabetes, 2013. **4**(6): p. 290-4.
6. Kozak, I. and J.K. Luttrull, *Modern retinal laser therapy*. Saudi J Ophthalmol, 2015. **29**(2): p. 137-46.
7. Curcio, C.A., et al., *The oil spill in ageing Bruch membrane*. Br J Ophthalmol, 2011. **95**(12): p. 1638-45.
8. Burton, D.S., M. Ali, and M. McKibbin, *Retinal phenotypes in patients homozygous for the G1961E mutation in the ABCA4 gene*. Invest Ophthalmol Vis Sci, 2013. **54**(1): p. 520.
9. Zhang, R., et al., *Associations of the G1961E and D2177N variants in ABCA4 and the risk of age-related macular degeneration*. Gene, 2015. **567**(1): p. 51-7.
10. Erasmus, M. and W.C. Lam, *Retina Canada 2009*. Can J Ophthalmol, 2009. **44**(5): p. 505-6.

11. Eckert, K.A., et al., *A Simple Method for Estimating the Economic Cost of Productivity Loss Due to Blindness and Moderate to Severe Visual Impairment*. *Ophthalmic Epidemiol*, 2015. **22**(5): p. 349-55.
12. Neubauer, A.S., et al., *[Cost-utility analysis of ranibizumab (Lucentis) in neovascular macular degeneration]*. *Klin Monbl Augenheilkd*, 2007. **224**(9): p. 727-32.
13. Zhang, N., et al., *Protein misfolding and the pathogenesis of ABCA4-associated retinal degenerations*. *Hum Mol Genet*, 2015. **24**(11): p. 3220-37.
14. Rivera, A., et al., *A comprehensive survey of sequence variation in the ABCA4 (ABCR) gene in Stargardt disease and age-related macular degeneration*. *Am J Hum Genet*, 2000. **67**(4): p. 800-13.
15. Bongso, A. and M. Richards, *History and perspective of stem cell research*. *Best Pract Res Clin Obstet Gynaecol*, 2004. **18**(6): p. 827-42.
16. Ameri, H., *Retinal prosthesis, potential future approaches*. *Clin Experiment Ophthalmol*, 2014. **42**(7): p. 599-600.
17. Bull, N.D. and K.R. Martin, *Concise review: toward stem cell-based therapies for retinal neurodegenerative diseases*. *Stem Cells*, 2011. **29**(8): p. 1170-5.
18. Mazzoni, F., H. Safa, and S.C. Finnemann, *Understanding photoreceptor outer segment phagocytosis: use and utility of RPE cells in culture*. *Exp Eye Res*, 2014. **126**: p. 51-60.
19. Jeon, S. and I.H. Oh, *Regeneration of the retina: toward stem cell therapy for degenerative retinal diseases*. *BMB Rep*, 2015. **48**(4): p. 193-9.
20. Grob, S.R., et al., *Clinical Trials in Retinal Dystrophies*. *Middle East Afr J Ophthalmol*, 2016. **23**(1): p. 49-59.

21. Kemp, K., A. Wilkins, and N. Scolding, *Cell fusion in the brain: two cells forward, one cell back*. Acta Neuropathol, 2014. **128**(5): p. 629-38.
22. Pearson, R.A., et al., *Donor and host photoreceptors engage in material transfer following transplantation of post-mitotic photoreceptor precursors*. Nat Commun, 2016. **7**: p. 13029.
23. Blenkinsop, T.A., et al., *Human Adult Retinal Pigment Epithelial Stem Cell-Derived RPE Monolayers Exhibit Key Physiological Characteristics of Native Tissue*. Invest Ophthalmol Vis Sci, 2015. **56**(12): p. 7085-99.
24. Kamao, H., et al., *Objective evaluation of the degree of pigmentation in human induced pluripotent stem cell-derived RPE*. Invest Ophthalmol Vis Sci, 2014. **55**(12): p. 8309-18.
25. Polinati, P.P., et al., *Patient-Specific Induced Pluripotent Stem Cell-Derived RPE Cells: Understanding the Pathogenesis of Retinopathy in Long-Chain 3-Hydroxyacyl-CoA Dehydrogenase Deficiency*. Invest Ophthalmol Vis Sci, 2015. **56**(5): p. 3371-82.
26. Schwartz, S.D., et al., *Human embryonic stem cell-derived retinal pigment epithelium in patients with age-related macular degeneration and Stargardt's macular dystrophy: follow-up of two open-label phase 1/2 studies*. Lancet, 2015. **385**(9967): p. 509-16.
27. Cramer, A.O. and R.E. MacLaren, *Translating induced pluripotent stem cells from bench to bedside: application to retinal diseases*. Curr Gene Ther, 2013. **13**(2): p. 139-51.
28. Tong, Z., et al., *Application of biomaterials to advance induced pluripotent stem cell research and therapy*. EMBO J, 2015. **34**(8): p. 987-1008.
29. Wert, K.J., et al., *Subretinal injection of gene therapy vectors and stem cells in the perinatal mouse eye*. J Vis Exp, 2012(69).

30. Oh, S.H., S.G. Kang, and J.H. Lee, *Degradation behavior of hydrophilized PLGA scaffolds prepared by melt-molding particulate-leaching method: comparison with control hydrophobic one*. J Mater Sci Mater Med, 2006. **17**(2): p. 131-7.
31. Feigenspan, A., J. Bormann, and H. Wassle, *Organotypic slice culture of the mammalian retina*. Vis Neurosci, 1993. **10**(2): p. 203-17.
32. Johnson, T.V. and K.R. Martin, *Development and characterization of an adult retinal explant organotypic tissue culture system as an in vitro intraocular stem cell transplantation model*. Invest Ophthalmol Vis Sci, 2008. **49**(8): p. 3503-12.
33. Moritoh, S., et al., *Organotypic tissue culture of adult rodent retina followed by particle-mediated acute gene transfer in vitro*. PLoS One, 2010. **5**(9): p. e12917.
34. Schnichels, S., et al., *Ex-vivo-examination of ultrastructural changes in organotypic retina culture using near-infrared imaging and optical coherence tomography*. Exp Eye Res, 2016. **147**: p. 31-6.
35. Gancharova, O.S., et al., *Organotypic culture of neural retina as a research model of neurodegeneration of ganglion cells*. Biochemistry (Mosc), 2013. **78**(11): p. 1280-6.
36. Taylor, A.W., *Ocular Immune Privilege and Transplantation*. Front Immunol, 2016. **7**: p. 37.
37. Redenti, S., et al., *Engineering retinal progenitor cell and scrollable poly(glycerol-sebacate) composites for expansion and subretinal transplantation*. Biomaterials, 2009. **30**(20): p. 3405-14.
38. Yao, J., et al., *Enhanced differentiation and delivery of mouse retinal progenitor cells using a micropatterned biodegradable thin-film polycaprolactone scaffold*. Tissue Eng Part A, 2015. **21**(7-8): p. 1247-60.

39. Tao, S., et al., *Survival, migration and differentiation of retinal progenitor cells transplanted on micro-machined poly(methyl methacrylate) scaffolds to the subretinal space*. Lab Chip, 2007. 7(6): p. 695-701.
40. Kannan, R. and D.R. Hinton, *Sodium iodate induced retinal degeneration: new insights from an old model*. Neural Regen Res, 2014. 9(23): p. 2044-5.

Chapter 4: Mucoadhesive phenylboronic acid based micelles for controlled, sustained anterior segment drug delivery

Scientific Contributions

- Develop and characterize a mucoadhesive copolymer that self assembles into micelles. Much of the chemical development was performed by a MASc student in the Sheardown lab.
- Show mucoadhesivity and drug release *in vitro* and *in vivo*
- Demonstrate biocompatibility *in vitro* and *in vivo*
- Adapt a scopolamine-induced rodent dry eye model with which to measure the effectiveness of these particles at rescue from this disease model

Publications from this work

- Proserpi-Porta G, Muirhead B, Sheardown H. (2016) Phenylboronic-Acid-Based Polymeric Micelles for Mucoadhesive Anterior Segment Ocular Drug Delivery. *Biomacromolecules*.
- Ben Muirhead, Kathleen Ingram, Heather Sheardown (2017) Mucoadhesive Drug Delivery Micelles for Dry Eye Disease (manuscript in preparation for IOVS)

Abstract

Despite their ubiquity, eye drops simply do not work very well. Barriers to bioavailability, including rapid turnover of tears and impermeable tight junctions, bring about a requirement for frequent dosing for drugs to achieve any clinical efficacy, resulting in systemic exposure, waste, and poor performance. Mucoadhesive drug delivery vectors can anchor drug to the ocular surface, greatly increasing bioavailability. To that end, poly(L-lactide)-b-poly(methacrylic acid-co-3-acrylamidophenylboronic acid) block copolymer micelles were synthesized and characterized to provide controlled, sustained release of therapeutics directly onto the ocular surface. These micelles were shown to be biocompatible and mucoadhesive *in vivo*. A scopolamine induced dry eye model was created and characterized, which could be rescued using this technology.

4.1 Background

The challenges with topical treatments for ocular diseases were discussed in some detail in Chapter 3; those points will not be belaboured here. Briefly, while they are the de facto standard for the treatment of tear film and ocular surface diseases, eye drops simply do not work very well. The cornea contains tight junctions in both its epithelial and endothelial layers, ensuring that anything applied to the surface has an extremely difficult time diffusing to a site of action. Medication applied via drop is furthermore quickly flushed away from the ocular surface through blinking and epiphora, resulting in systemic exposure, wasted drug, and compounding the extremely low bioavailability in target tissues. In effect, less than 5% of a drug applied via drop will be available to the anterior structures of the eye and less than 1% penetrates to posterior structures.[1]

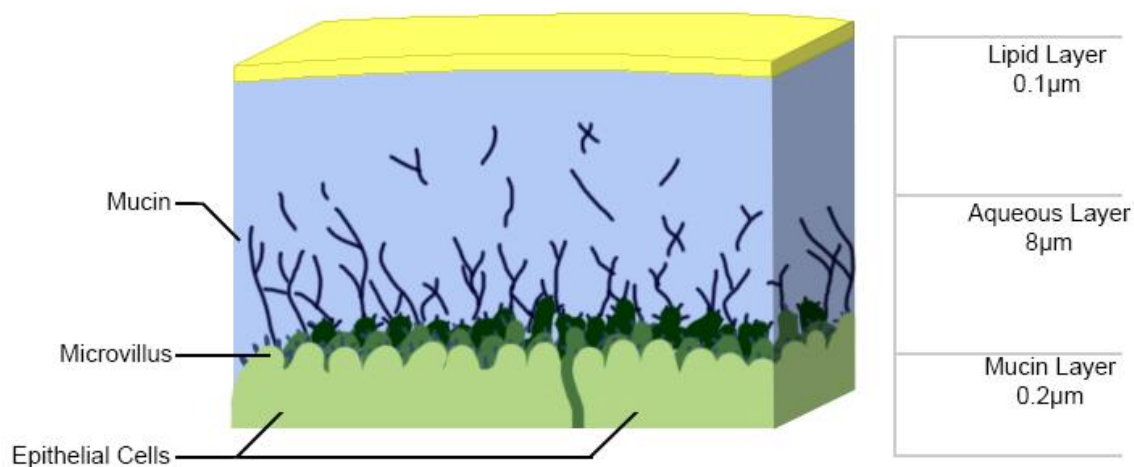


Figure 1 – Cartoon of tear film.

The tear film, depicted in Figure 1, is composed of an outer lipid layer, a middle aqueous layer, and an inner mucin layer immobilized on the glycocalyx covering the corneal and conjunctival epithelium.[2] A potential strategy to increase the bioavailability of a drug to ocular issues involves targeting these immobile mucins anchored to the ocular surface. There are many established materials capable of binding mucins, popular examples of which include polymers such as chitosans,[3] cellulose derivatives,[4] thiomers,[5] and many others, not least of which are hyaluronans used in the production of HASD discussed in Chapter 3[6]. However, these cationic polymers typically rely on electrostatic interactions with negatively charged mucins to facilitate binding. As discussed briefly in Chapter 3, one of the most consistent symptoms of DED is hyperosmolar tear film as aqueous volume decreases. The ionic density can interfere with electrostatic binding, making these cationic polymers ineffective – at least in the context of DED.[7] Phenylboronic acid (PBA) is also mucoadhesive,[8] but forms a complex with 1,2-cis-diol groups of sugar residues, such as sialic acids, common in mucins.[9] This affinity between PBA and diols has precedent throughout the mucin-membranes of the body. Based on this, a mucoadhesive copolymer micelle was developed to bind to the ocular surface and release cargo over a prolonged period of time. While ultimately this platform might be useful anywhere mucus exists, the current focus is on application for the treatment of ocular conditions. Ideally, any pharmaceutical normally dosed via drop could be packaged within these mucoadhesive micelles and provide prolonged controlled release while maintaining low costs, non-invasiveness and simple self-administration, as seen in Figure 2.

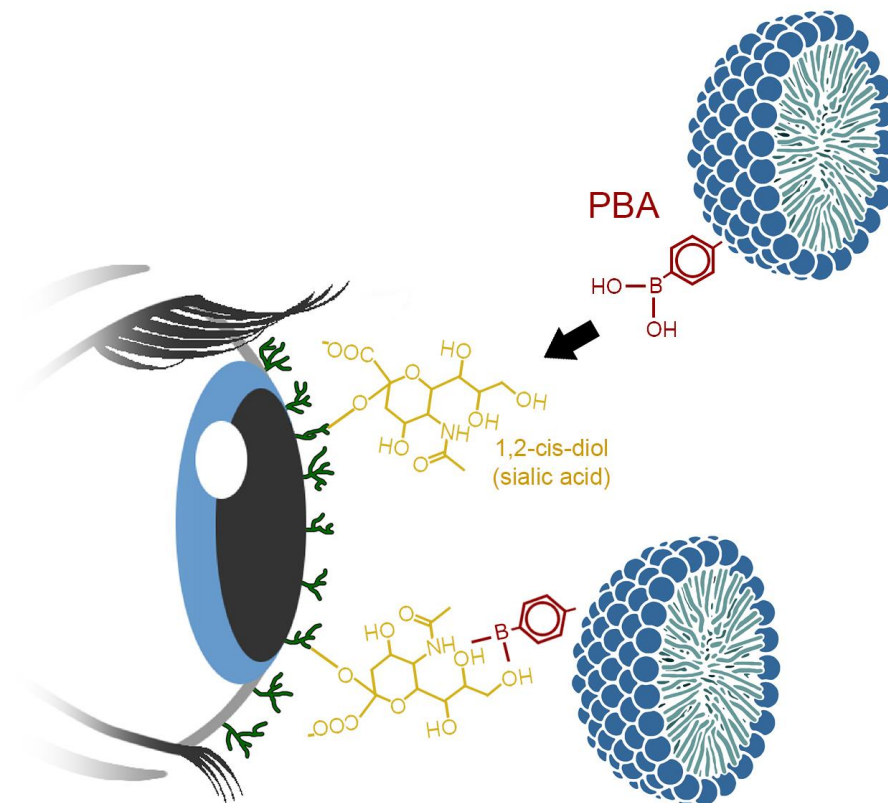


Figure 2 – PBA modified micelle binding to mucin on the ocular surface.

Due to the expertise and infrastructure developed to model and assess DED discussed in chapter 3, this indication was used to validate this approach. While these particles are designed as a platform, capable of entrapping and releasing a wide variety of cargo, and targeting mucosal membranes throughout the body, this approach needs to be validated in a specific area to establish feasibility. As this laboratory specializes in ophthalmics, targeting the eye makes obvious sense. Of all the ocular conditions which require a topically applied treatment (including glaucoma, uveitis, ocular infections, etc), DED is by far the easiest to model, requires the least sophisticated equipment to assess, and requires the least amount of time to measure

improvement. Cyclosporine A (CycA) is the active ingredient in Restasis, one of only two currently approved drugs prescribed to treat DED. Encapsulating CycA will therefore provide direct comparison with the current DED state of the art. By binding to the ocular surface and providing controlled release, a greatly reduced dosing schedule is theoretically possible, thereby reducing systemic exposure and improving patient compliance. Escaping the pulsatile delivery paradigm inherent to eyedrops, controlled release of a pharmaceutical within its therapeutic window may greatly improve clinical efficacy as well. CycA in particular is a notoriously poor performer, with the need for frequent dosing and an extended period of drop administration necessary prior to clinical efficacy being observed.

4.2 Micelle synthesis and characterization

pLA-b-p(MAA-PBA) (LMP) copolymers were synthesized by RAFT polymerization. The precursor monomers were selected to allow for degradation. All monomers selected have a history of use in the eye. In a typical reaction procedure (80:20:1.4:0.2 molar feed ratio of AA/PBA/pLA/AIBN), methacrylic acid (MAA; 192.9 mg, 2.24 mmol), PBA (107.1 mg, 0.56 mmol), poly(D,L-lactide) 4-cyano-4-[(dodecylsulfanylthiocarbonyl)sulfanyl]pentoate (pLA-CDP; 200.0 mg, 0.04 mmol), and AIBN (1.10 mg, 0.01 mmol) were dissolved in 5 mL of 90:10 1,4-dioxane/water to form a 10% (w/v) solution. The solution was degassed by performing three freeze-pump-thaw cycles, followed by replacement of the atmosphere with dry nitrogen. The flask was then heated to 70°C for 24 h under constant stirring. This copolymer is 20 wt % PBA in the poly(MAA-co-PBA) block, and was isolated by precipitation into 10 times excess of cold anhydrous diethyl ether and further purified by repeated precipitation into diethyl ether from

tetrahydrofuran two additional times. The copolymer was then dried in a vacuum oven at 50 °C for 24 h before further use.

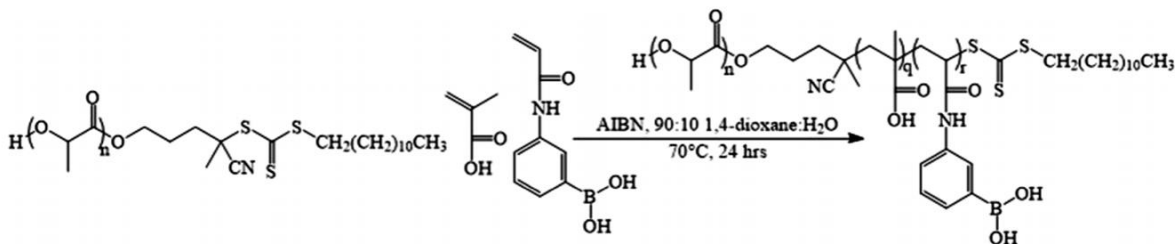


Figure 3 – Reaction schema for RAFT synthesized PBA modified micelles.

Micelles were formed by precipitation into purified water from acetone. In brief, 20 mg of LMP copolymer was dissolved in 2 mL of acetone and then added dropwise to 6 mL of purified water under constant stirring through a 30 G needle at a rate of 0.5 mL min⁻¹ using a syringe pump. The acetone/water solutions were then allowed to stir uncovered at room temperature for 48 h to evaporate the acetone before subsequent use. The micelle concentration was adjusted by dilution with purified water or further evaporation prior to characterization.

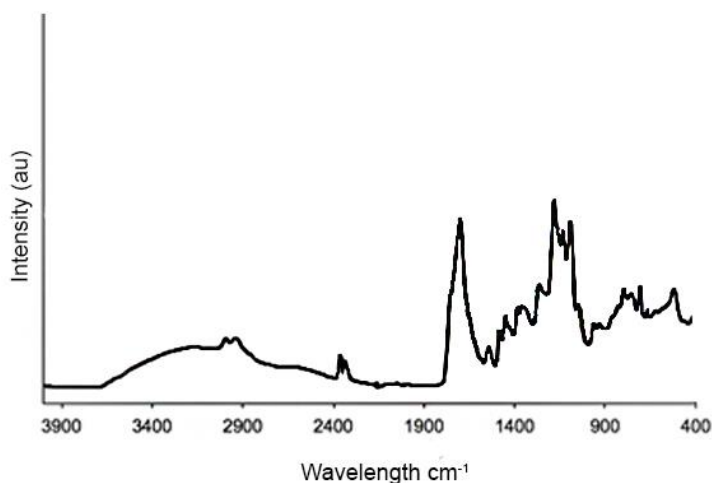


Figure 4 – FT-IR spectra of PBA modified micelles.

As seen in Figure 4, the broad stretch between 3520 and 3200 cm^{-1} represents the alcohol of the phenol group. The peak at 3030 cm^{-1} is indicative of the aromaticity of the PBA.

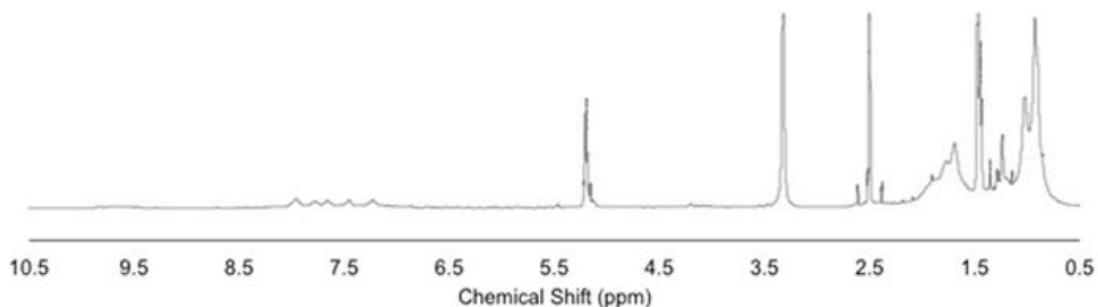


Figure 5 – $^1\text{H-NMR}$ spectra of PBA modified micelles.

As seen in Figure 5, the micelle spectrum shows peaks at 6.5-7.5 ppm belonging to the CH ring protons of the phenylboronic acid, peaks at 5.3 ppm from the methyl group on the polylactide, and CH(MAA)/CH₂(PBA)/CH₃(MAA) polymer backbone peaks from 1-2 ppm.

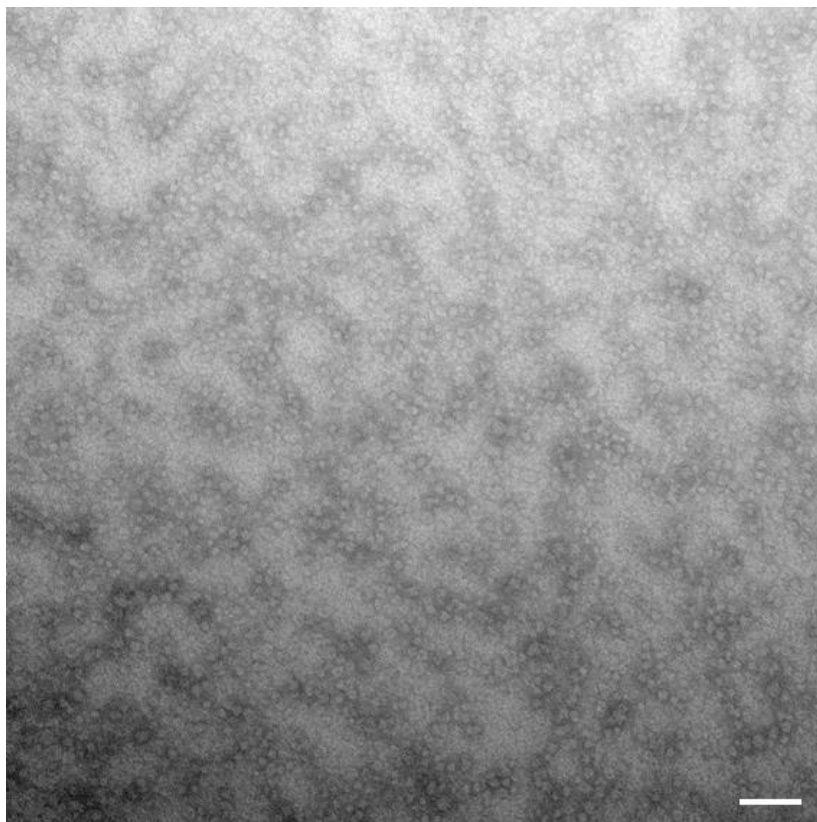


Figure 6 – TEM of micelle morphology. Scale bar = 100 μ m

Dynamic light scattering (DLS) was used to determine the z-average diameter and dispersity of these micelles. Micelles loaded with CycA showed a significant ($p > 0.01$) decrease in their average z-diameter, as shown in Table 1. Its possible CycA was able to interact with the hydrophobic PBA, creating intramolecular interaction responsible for the smaller size. TEM was performed to confirm the approximate size and low dispersity described by DLS (Figure 6). This scan confirms regular, spherical morphologies of appropriate size.

Table 1 – DLS of micelle diameter

unloaded micelles		CycA-loaded micelles	
diameter \pm SD (nm)	dispersity	diameter \pm SD (nm)	dispersity
59 \pm 2.9	0.29	44 \pm 3.8	0.34

Mucoadhesion was determined using Surface Plasmon Resonance. Briefly, SPR102-AU gold sensors were incubated in 100 μ L of 100 μ g mL⁻¹ bovine submaxillary gland mucin for 24 hours at 20°C and then rinsed with purified water to remove unbound mucin. SPR measurements were conducted by flowing simulated tear fluid for 10 minutes to achieve a stable baseline. The solution was then changed to a 1 mg mL⁻¹ solution of micelles for 50 minutes. At this point, the solution was changed back to simulated tear fluid to assess mucoadhesion stability. All measurements were conducted at a flowrate of 50 μ L min⁻¹, a temperature of 22°C, and a fixed angle scan of 65.4°. As seen in Figure 7, micelles containing PBA adsorbed to the sensor much more readily, and were much more resistant to removal during rinsing.

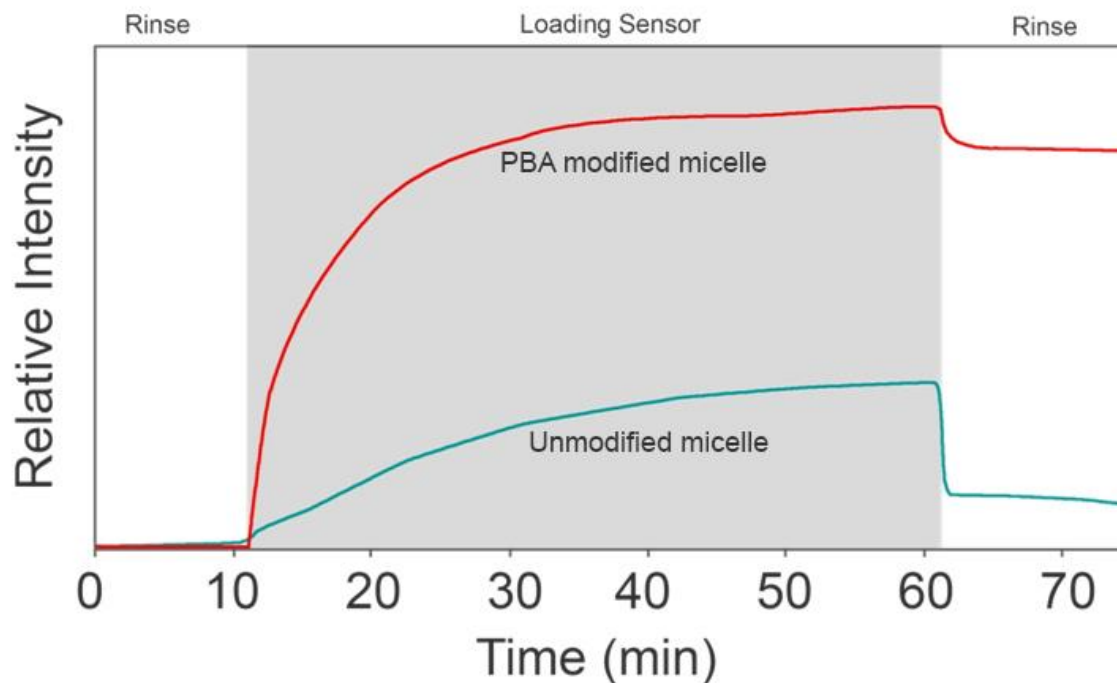


Figure 7 – SPR using a mucin-coated sensor. Intensity is proportionate to bound micelles.

CycA release from micelles was determined using high performance liquid chromatography (HPLC). Briefly, a 20 mg of the LMP copolymer was dissolved in 2 mL of acetone containing 1.5 mg/mL CycA. This solution was added drop-wise to 6 mL of purified water. The solution was left under stirring for 24 hours to evaporate the acetone. 0.5 mL was removed and filtered with Nanosep 10K Omega centrifugal to separate micelles from free CycA. The filtrate was collected to determine entrapment efficiency (EE). 5 mL of non-centrifuged sample was then added to 50 kDa MWCO dialysis tubes and placed in 15 mL of STF. At specified time points, 2.5 mL samples were removed and replaced with fresh pre-warmed simulated tear fluid (STF). These samples were analyzed using HPLC with a 0.7 mL min^{-1} isocratic flow rate of 80:20 acetonitrile:0.1% trifluoroacetic acid in purified water as the mobile phase, a 60°C column temperature, a $20 \mu\text{L}$ sample injection volume, and a 210nm detection wavelength. Sample

concentrations were determined based on a standard calibration curve of CycA in the mobile phase (not shown).

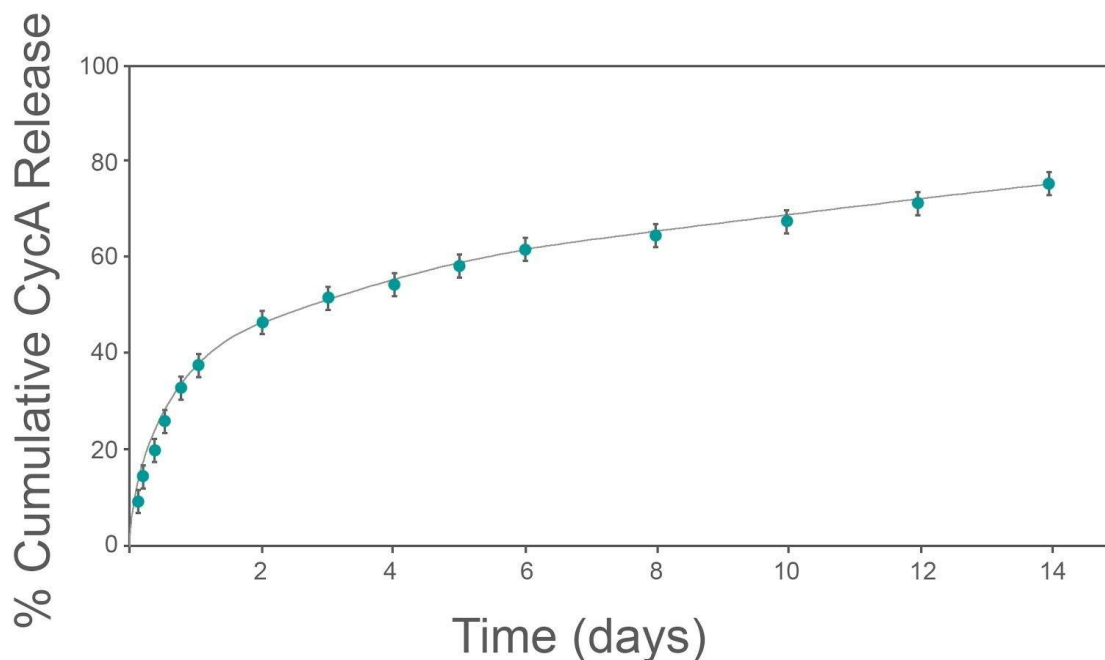


Figure 8 – Release curve for CycA from PBA modified micelles.

The release curve is characterized by a two-phase release, with an initial burst lasting ~24 hours releasing ~40% of entrapped CycA, followed by a non-linear release of ~80% of entrapped CycA over the next 13 days (Figure 8). While it is a contentious issue, the literature seems to agree that mucins bound to the ocular surface will be shed and replaced within a week at most.[10] If these micelles are to be bound to mucin, for this application at least there seems little reason to prolong release beyond the curve seen here.

4.3 In vitro testing

Cell viability data has typically been omitted from previous chapters due to its banality. In general, and particularly with respect to PNNPD materials, cells were completely unaffected. When grown with a human corneal epithelial cell line, the micelles showed a significant decrease in viability as well as an increase in morbidity that was both concentration and time dependent.

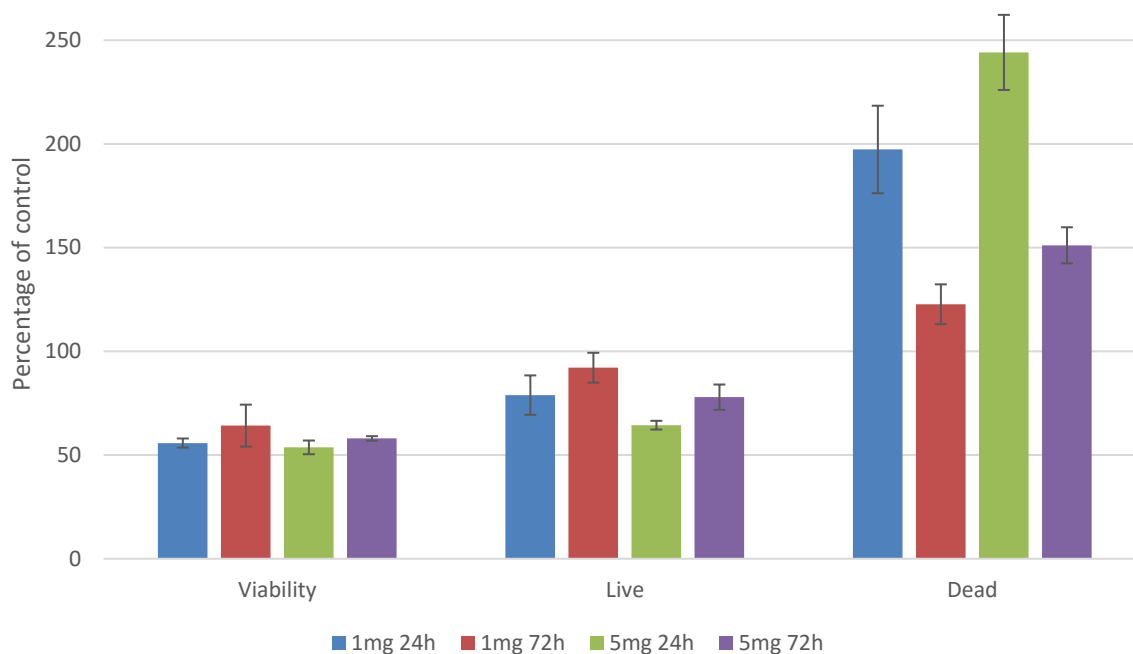


Figure 9 – MTT viability assay and calcein AM/ethidium homodimer-1 live/dead assay results.

The difference between all live and dead values is significant, $p < 0.05$, $n = 12$, error bars = standard deviation.

In this case, as seen in Figure 9, significant decreases in viability and cell death, along with a significant decrease in living cells was observed. As a class, it has often been observed that nanomaterials interfere with various cellular functions and can induce both apoptotic and necrotic cell death at relatively low concentrations.[11] While that is a plausible explanation in

this case, it is also important to note that the percentage of cells actually dying remains quite low. Interestingly, the data seems to describe a trend of recovery. In all cases, cells were affected the most after 24 hours, but then seemed to recover after 72 hours. The 1 mg dose of micelles moreover had a lesser effect than the 5mg dose, indicating a dose dependent toxic response. To put these findings into context, a visual comparison between the worst cast live/dead result (5mg, 24 hours) and a control is given in Figure 810. As can be seen, despite the several-fold increase in dead cells, the numbers are still relatively insignificant. Coupled with the fact that even the 1mg dose is much larger than would be seen in a clinical setting, these micelles were deemed safe for further experimentation and eventual human use.

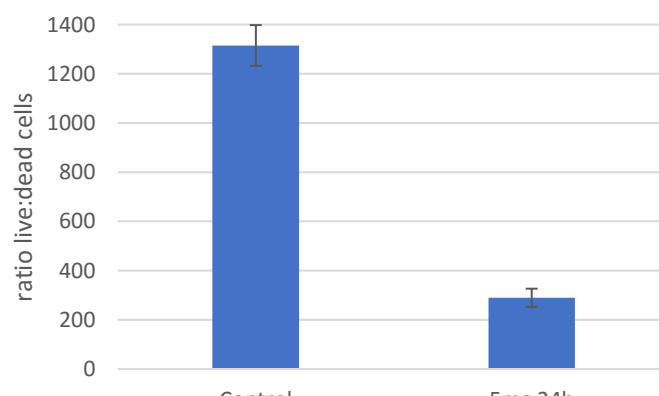
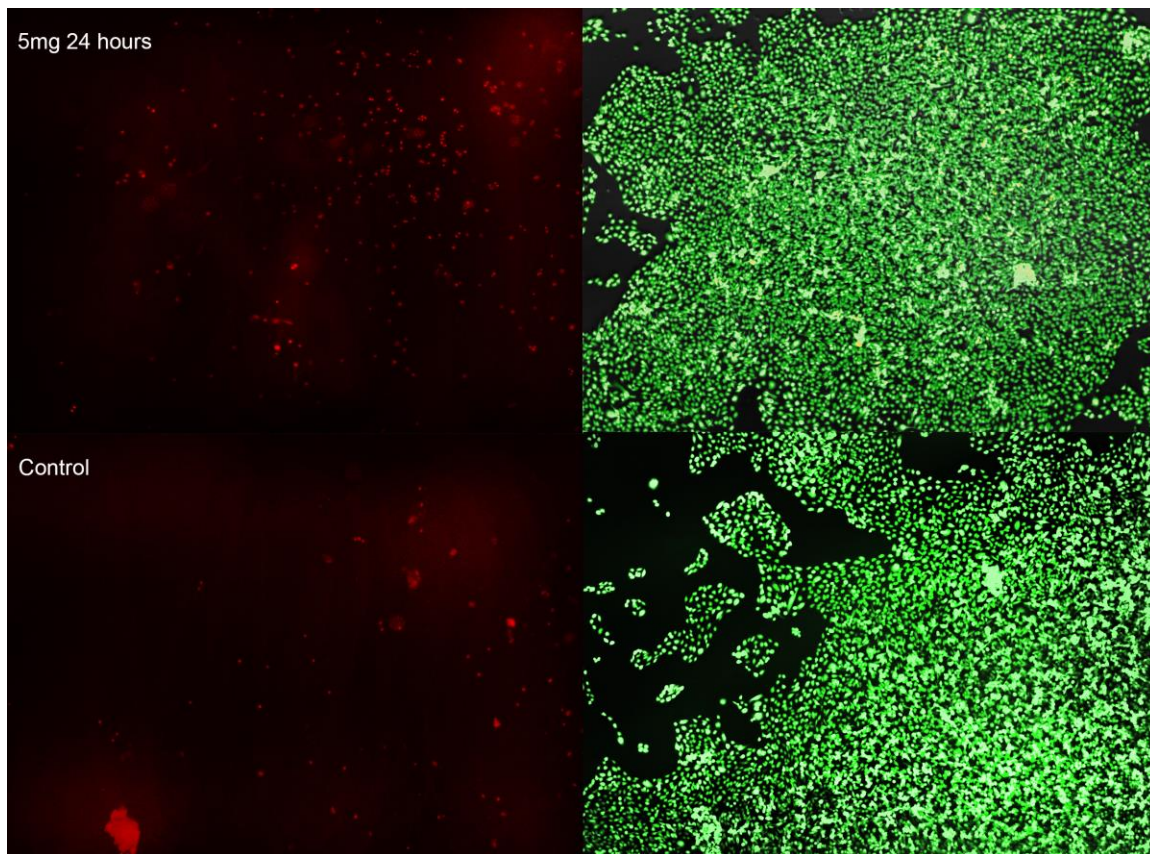


Figure 10 – An ethidium homodimer-1 stain (left) and a calcein AM stain (right) showing the dead and living HCECs within the worst performing testing category (Figure 9) and a control. Despite significantly more cell death, in both cases dead cells are a negligibly small minority of the overall culture. n = 12, error = standard deviation, p<0.05

4.4 In vivo testing

To verify the mucoadhesion by SPR described in Figure 46, an *in vivo* assay was developed. Initially, micelles were to be loaded with something easily detectable – probably some form of fluorescein – and applied to the ocular surface in the same fashion as if they contained a therapeutic. However, this approach would not measure how long the micelles were bound, but rather how long their fluorescent cargo was releasing. Therefore, to measure micelle binding directly, the particles themselves were modified with 5-aminofluorescein (Figure 11). Briefly, micelle copolymers were modified with 5-aminofluorescein using carbodiimide mediated coupling. In a typical reaction procedure, 53.5 mg of copolymer was dissolved in 5 mL of dry dimethyl sulfoxide in a sealed 25 mL round bottom flask containing a stir bar and covered in aluminum foil to avoid exposure to light. To this solution, 5-aminofluorescein (FA; 31.3 mg, 0.16 mmol), N,N'-Dicyclohexylcarbodiimide (DCC; 66.7 mg, 0.60 mmol), and 4-Dimethylaminopyridine (DMAP; 6.2 mg, 0.05 mmol) were added to achieve molar ratios of 100:30:110:10 for MAA:FA:DCC:DMAP respectively. The solution was sealed and left to stir

for 24 hours, after which the solution was placed in a 3.5 kDa dialysis tube and dialyzed in DMSO for 8 solution changes. At this point, the dialysis tube was transferred to acetone to remove DMSO for 2 acetone changes. Next, FA-modified copolymer in acetone was diluted to achieve a 20mg mL⁻¹ solution, which was added dropwise into stirring purified water at a volume ratio of 1 mL acetone:6 mL purified water. The copolymer/acetone/water solution was allowed to stir uncovered, but protected from light for 24 hours to allow the majority of the acetone to evaporate and the micelles to form. Next, the micelle solution was transferred to 3.5 kDa MWCO dialysis tubes for a final purification in water to remove any acetone or other water soluble by-products for 3 cycles.



Figure 11 - Carbodiimide-mediated coupling of 5-fluoresceinamine to micelle copolymer

Rat eyes were given a single instillation of 50 μ l FA modified micelles. While some micelles were modified with PBA, and therefore mucoadhesive, some were not. As seen in Figure 12, 4 hours post instillation, fluorescent PBA containing micelles continued to fluoresce strongly, while fluorescent micelles without PBA had no detectable fluorescence. This finding verifies not only that these micelles are mucoadhesive as designed, in a living, blinking eye, but that it is the PBA which is responsible for this property. After 4 hours, this fluorescent signal could no longer be observed. As a platform, this technology is designed to greatly reduce the dosing frequency

necessary to achieve clinical efficacy. The DED treatment Restasis, mentioned earlier, required twice daily instillations to be effective. Ideally, a dosing schedule of once per week could be achieved with this technology, as described elsewhere in the literature.[12] This conjecture seems ambitious given the apparent disappearance of these mucoadhesive micelles after only 4 hours. However, it is likely micelles remain on the surface of the eye, and this assay is simply not sensitive enough to detect them. Most of the mucins present in the tear film are soluble in its aqueous phase, as seen in Figure 1. Along with intramembrane mucins, glycocalyx are long chain molecules that immobilize some mucin to the corneal surface. Formed by corneal cells, glycocalyx migrate out from the surface of the corneal microvilli to form a hydrophilic network that holds mucin on the ocular surface.[13] While some portion of instilled micelles will bind to aqueous mucins which are quickly flushed away, some other portion will find and adhere to these more permanent mucins and remain for much longer. Despite losing the fluorescence signal, it remains entirely likely there are sufficient micelles remaining to deliver therapeutic levels of drug. A future experiment using radioisotope carbon-14 would have the sensitivity to determine how many, if any, of these micelles remain for longer periods of time.

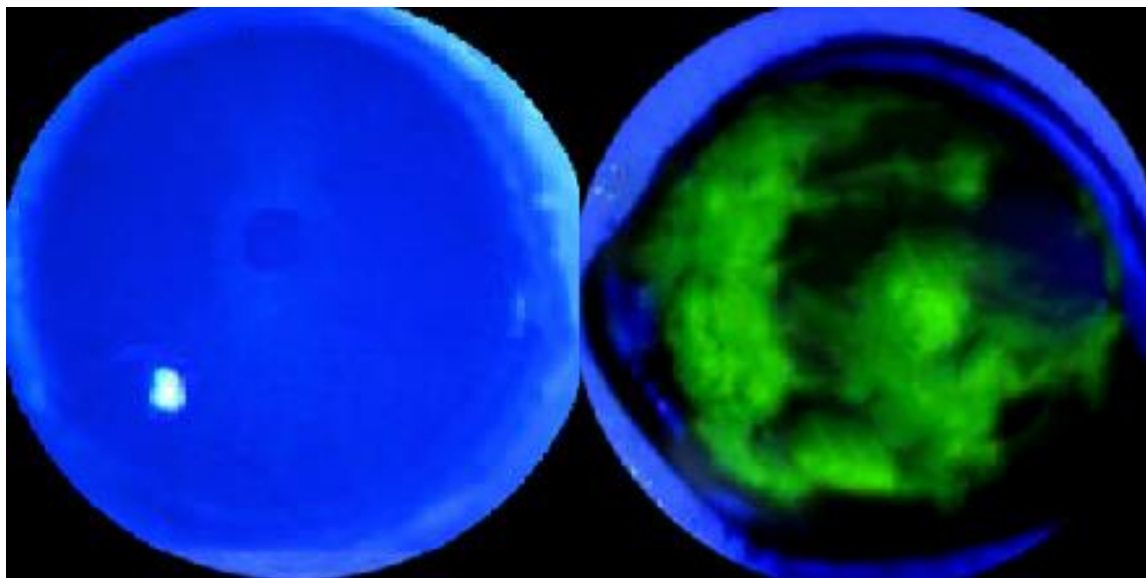


Figure 12 – 50 μ L of fluorescently labelled micelles instilled onto a rat eye. Some eyes (left) were instilled with micelles which did not contain PBA, while others (right) did contain PBA. After 4 hours, unmodified micelles were no longer fluorescing, indicating they had been washed away.

Only the PBA modified micelles continue to fluoresce on the ocular surface.

Given the somewhat ambiguous cell toxicity data, these micelles were assessed with a full battery of toxicity testing. A short, 24 h initially, assessment was performed which did not show any acute toxicity (data now shown). For a more thorough assessment, eyes were dropped twice daily for a period of two weeks. The micelle dosage given was significantly higher than what would be expected in a clinical setting to ensure that at whatever concentration, the data shown are transferable and conservative. This clinical dosage was roughly calculated based on the recommended dosage of Restasis, which comes as an emulsion containing 0.5mg mL⁻¹ CycA. Based on the paper published about these particles, they were shown to have an entrapment efficiency of >99%. [14] Therefore, a solution of 5mg mL⁻¹ was chosen so as to provide 10 times the amount of CycA that Restasis prescribes. Furthermore, as we anticipate a reduction in dosing

from twice per day to once or twice per week, the dosing regimen undertaken during this study represents a 7 to 14-fold overdose. There are also likely intangible benefits to consistent, controlled release which would probably further reduce dosage requirements, but even ignoring that possibility, this toxicology study has conservatively applied 70 to 140 times more micellular particle to the ocular surface than would be necessary were it being used to carry drug. If these particles do not cause any irritation or damage at this concentration range, they could be assumed safe for their intended purpose.

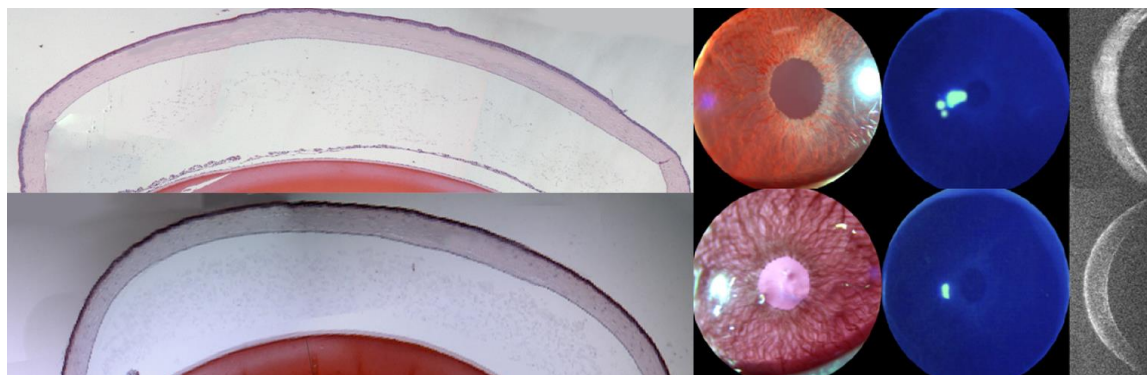


Figure 13 – Ocular toxicity of 20% PBA micelles on the ocular surface of Sprague-Dawley rats. H&E histology (left), slit lamp examination (middle-left), fluorescence imaging (middle-right), and OCT (right) were performed on the cornea. Test eyes (top row) show no significant difference from control eyes dosed with PBS (bottom row).

As seen in Figure 13, eyes treated with twice daily instillations of 5mg mL^{-1} (top row) show no significant difference from control eyes treated with PBS on the same dosing schedule (bottom row). In these representative images, corneal histology, slit lamp ophthalmoscopy, corneal

staining, and corneal OCT show no obvious signs of inflammation or other damage, suggesting excellent biocompatibility on the ocular surface.

Once it was established that these micelles are benign, they could be tested in a DED model, similar to HASD in chapter 3. Unlike the hypothesized MMP-9 inhibition capabilities of HASD, which could be a counter for the inflammation found in all subtypes of DED, the CycA encapsulated by these micelles targets a much more specific etiology. Cyclosporines belong to the group of compounds known as calcineurin inhibitors, which also includes tacrolimus and voclosporin. The drug binds to various cyclophilin isoforms found in lymphocytes, and this complex inhibits calcineurin, ultimately preventing it from activating the transcription product of interleukin-2. Because IL-2 is necessary for T-cell replication, cyclosporine is a potent inhibitor of T-cell proliferation and thus drastically downregulates T-cell-mediated immune responses.[15] When applied topically, CycA can reverse the suppression of tear production associated with DED derived inflammation. Consequently, CycA is only effective in the subset of DED sufferers who are aqueous deficient. Our previous model used the cationic surfactant benzalkonium chloride which, due to its nature, is able to dissolve or emulsify the lipid layer of the tear film. As a result, an animal model induced as described in Chapter 3 would could not be rescued with CycA, regardless of how it was packaged.

Scopolamine is an anticholinergic agent that blocks the activity of the muscarinic acetylcholine receptor.[16] The effect of this pharmacological blockade on the lacrimal gland is a significant decrease in tear production. Along with being a very good model of generalized aqueous deficient DED, scopolamine is a near perfect proxy for Sjögren's syndrome, in which

autoimmune mediated inflammation specifically disrupts lacrimal gland production.[17] To create this model, scopolamine was administered to female Sprague Dawley rats via an implanted osmotic pump (0.1 mg/day, Alzet model 1002). After shaving the animal, an incision was made in the scapular region of the back. A hemostat was used to create a space for the pump, which was then inserted under the skin (Figure 14). This treatment was combined with a desiccating environment, including a reduction in humidity to <30% and multidirectional airflow from fans. While not necessary to induce DED symptoms, a desiccating environment produces a much more accurate model than simply reducing tear production. Animals are kept in this state for up to 28 days until predetermined endpoints are met.



Figure 14 – Insertion of an Alzet model 1002 osmotic pump under the scapula of a Sprague Dawley rat.

To measure the impact of this model, along with recovery, slightly different metrics were used than described in chapter 3. A modified Schirmer's test was employed to measure tear volume. Normal test strips were cut lengthwise into thirds, as rats do not produce enough tear volume to

resolve a measurement on conventional Schirmer strips. As described in Figure 15, there was a significant decrease in tear volume 2 days after model induction which remained for 4 weeks compared with control. While tear volume itself decreases very rapidly, this does not necessarily indicate the DED model has reached an endpoint. It takes time for this lack of moisture to produce inflammation, and the subsequent cascade of pathological changes which resembles clinical DED. If tear film alone is used to characterize recovery, as it often is in industrial settings which do not want to complicate their drug trials with the esoterica of a more realistic DED, then animals would be ready to use perhaps 5 days post induction. In this case, a more mature DED model will be allowed to develop to improve clinical congruency as much as possible.

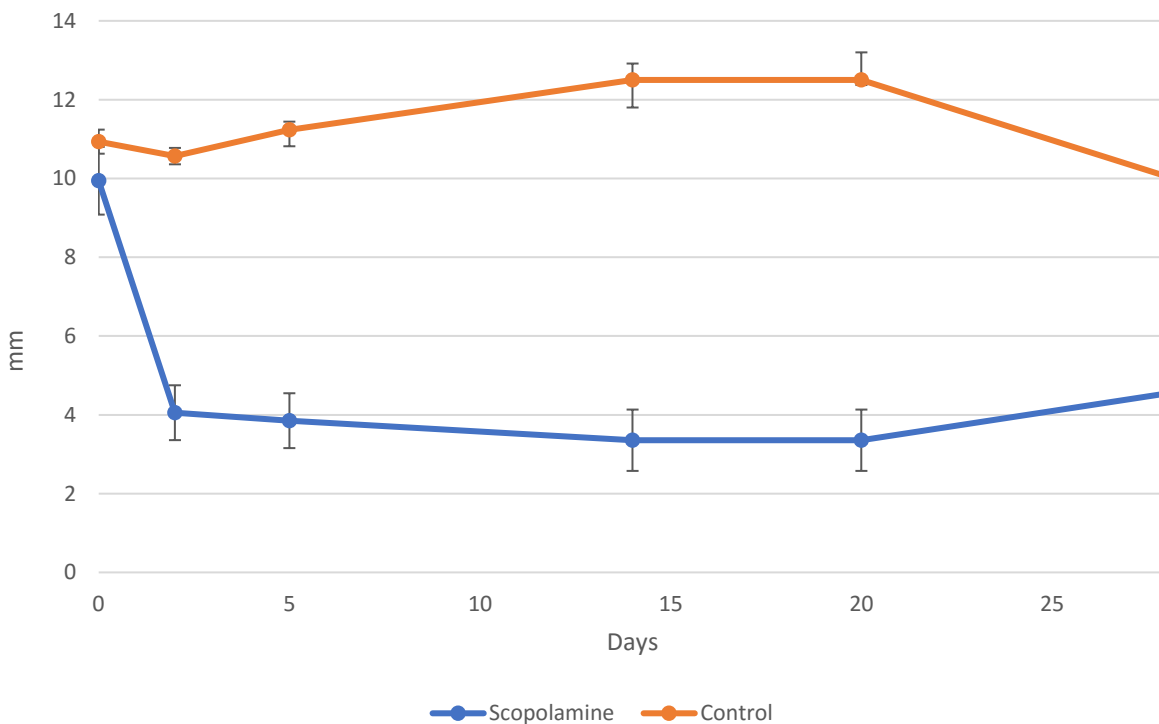


Figure 15 – Scopolamine treated rats (blue, n=9) had significantly less tear production than control rats (orange, n=3). Error bars = standard deviation, all time points after day 0 are significantly different, $p < 0.05$.

Tear film osmolarity is a new addition to this testing suite since Chapter 3. One of the most persistent problems with DED is its inconsistent presentation at clinics. Some patients complain of a gritty feeling while others complain of a stinging pain. Some people have a reduced tear film breakup time, and others have corneal thickening and ocular inflammation. Perhaps the most confounding symptoms is excessive watering, which, of course, has a somewhat oxymoronic relationship with ‘dry eye’ disease. One of the few characteristics essentially every case of DED has in common is hyperosmolar tears. In fact, tear hyperosmolarity is now one of the de facto definitions of DED according to the Definition and Classification Subcommittee of the International Dry Eye Workshop (DEWS).[18] Tear film osmolarity (TFO) provides a quantitative, objective, repeatable measure of DED presence and severity, and is considered the ‘gold standard’ of DED diagnosis in the clinic.[19] Until recently, measuring TFO was a cumbersome process which was essentially impossible in rodents due to their relatively low tear volume. The TearLab corporation has developed a ‘lab on a chip’ which measure TFO in seconds with a single use testing chamber. Because this device only requires 10 nL of tear fluid, it has worked well in this rat model. As seen in Figure 16, TFO quickly climbs from a trail average of $291.2 \text{ mOsmol L}^{-1}$ to a peak of $327 \text{ mOsmol L}^{-1}$ after 5 days. Perhaps equally relevant, the variance in the scopolamine treated cohort is significantly greater than in the control cohort. The average standard deviation of each data point, excluding day 0, for the scopolamine cohort was 6.96; the average for the control group was 2.44. It seems that in addition to

increasing the TFO, this scopolamine model also increase flattens its distribution, which is reported in the literature as a phenomena in human DED.[20]

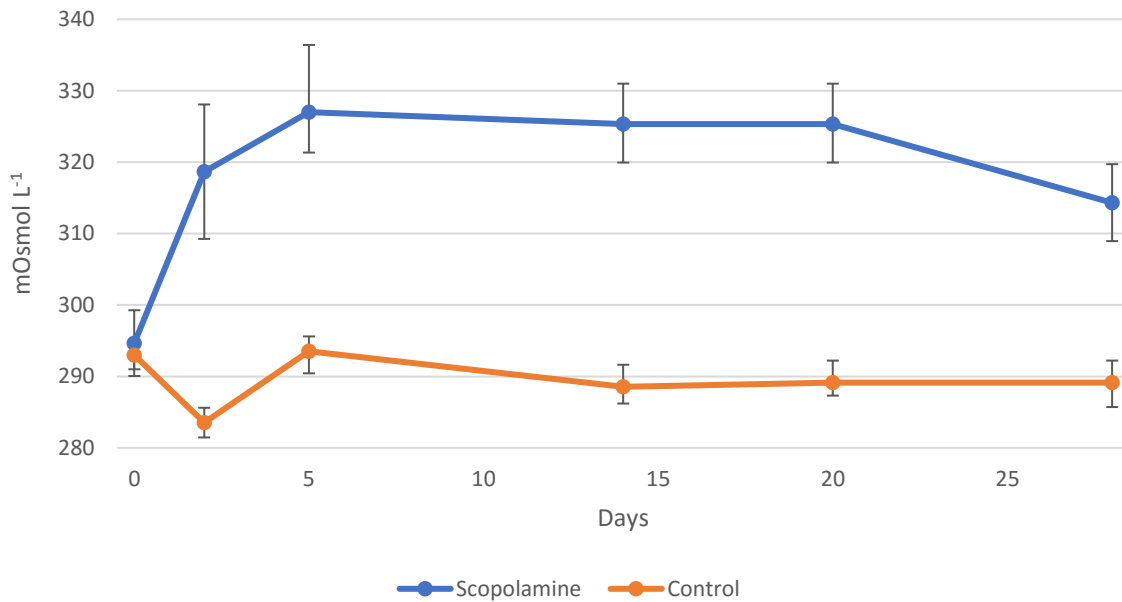


Figure 16 – TFO after DED induction with scopolamine. Error bars = standard deviation, all time points after day 0 are significantly different, $p < 0.05$

Corneal redness and irritation were evaluated using a rodent-customized slit lamp. Corneal staining was measured using ophthalmic fluorescein strips and an anterior segment lens for a Micron Phoenix ophthalmoscope. These results are presented in Figures 17 and 18 respectively using a modified Draize and Oxford Scheme. In both cases, scores increase after induction with scopolamine, although not as dramatically as with Schirmer’s test or TFO.

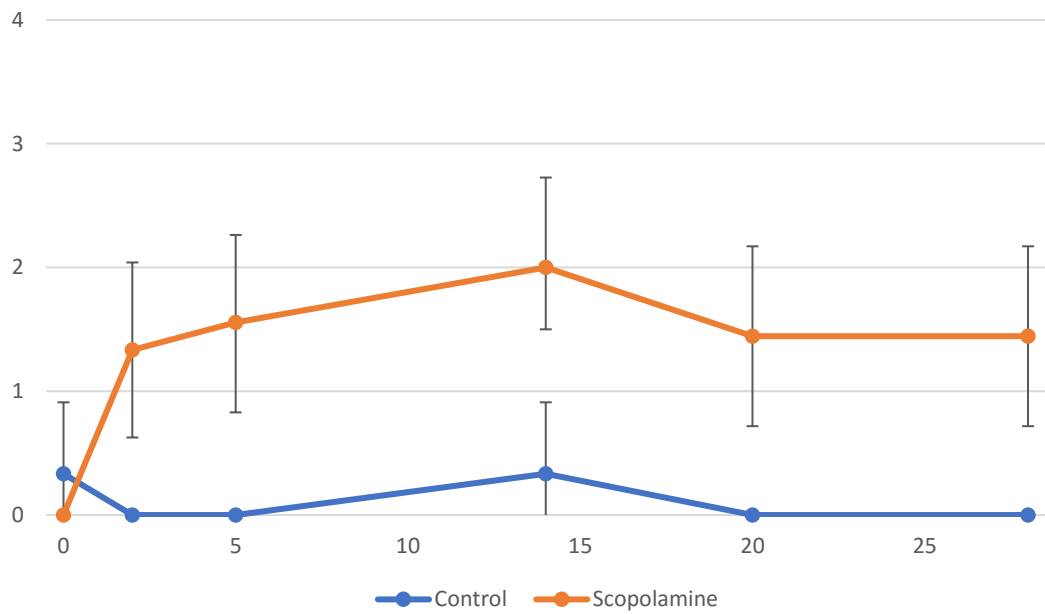


Figure 17 – Modified Draize assessment of corneal irritation. Control n=3, Scopolamine n=9.

Error bars = standard deviation all time points after day 0 are significantly different, $p < 0.05$.

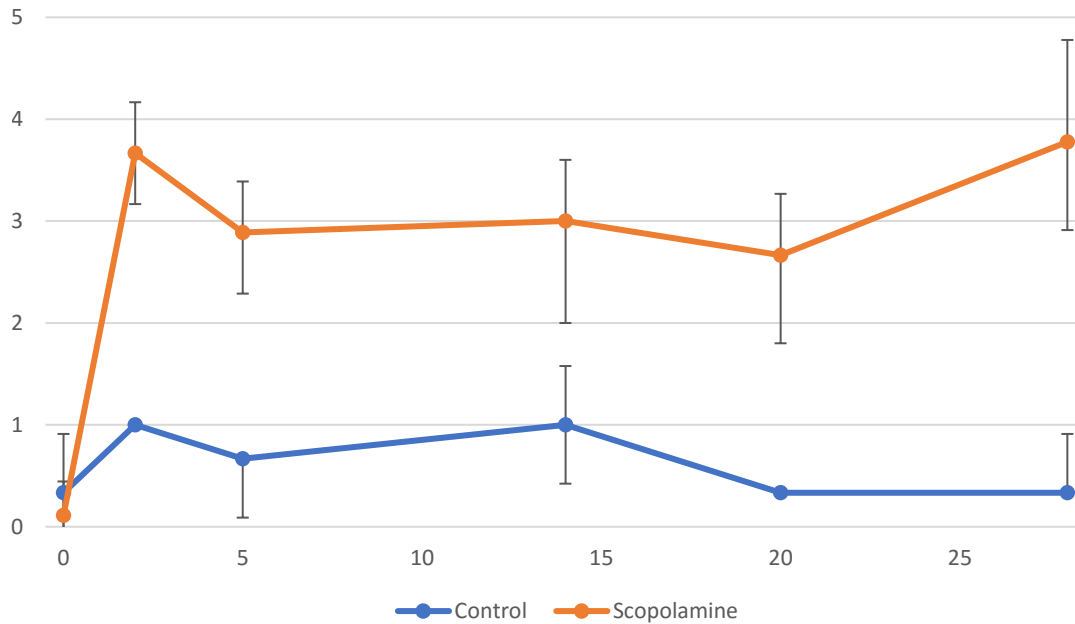


Figure 18 – Oxford Scheme assessment of corneal staining. Control n=3, Scopolamine n=9. Error bars = standard deviation all time points after day 0 are significantly different, $p < 0.05$.

Corneal histology and conjunctival impression cytology samples were taken, but have not yet been processed for publication. Taken together, a scopolamine based model of DED in rats has been developed and characterized to compare the ability of CycA containing micelles against Restasis to treat this condition. Before these treatment approaches were compared, it was decided to measure what effect, if any, these micelles have on this model.

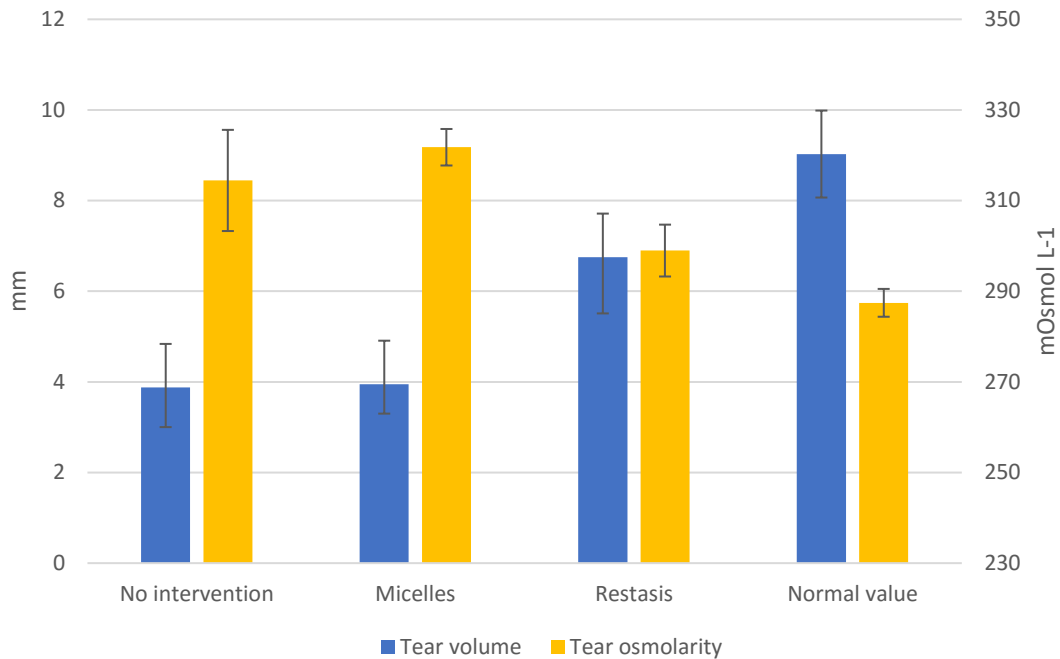


Figure 19 – Combined tear volume (left axis) and TFO (right axis). Micelles did not improve tear volume or tear osmolarity over doing nothing, whereas Restasis brought values back to normal. n = 3, error bars = standard deviation. No intervention and Micelles categories were significantly different from their normal values, $p < 0.05$.

Combined on Figure 19 are tear volume and TFO measurements under various conditions. The DED model was induced, after which animals were left to recover after removing the micro-osmotic pump and desiccating conditions for 7 days. In some cases, nothing was given to the animals to speed their recovery (no intervention column). In other cases, micelles without any loaded CycA, or Restasis, a known treatment for DED was given to speed recovery (micelles and Restasis columns). This recovery was compared with normative values from animals which had not been induced with DED (normal value). With both tear volume and TFO, micelles had no effect on this DED model. While Restasis did show significant improvement in both TFO and tear volume, instilling micelles was equivalent to doing nothing at all. This result is completely

expected, as without being loaded with CycA, micelles should not have any therapeutic effect.

This is further corroboration of the data presented in Figure 13, which demonstrates how benign these particles are.

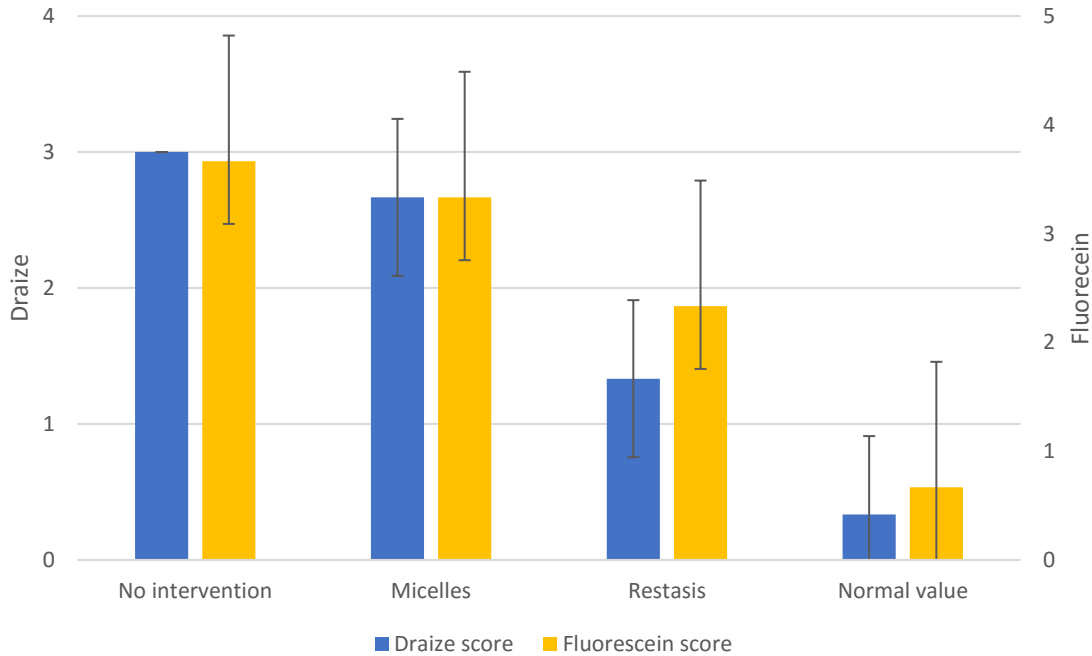


Figure 20 – Combined modified Draize scheme (left axis) and Oxford corneal staining scheme (right axis). Restasis partially rescued the DED model, significantly reducing staining and irritancy close to normal levels. Micelles were not significantly better than doing nothing.

Restasis and normal values cate $n = 3$, error bars = standard deviation, $p < 0.05$.

Similarly, with slip lamp and fluorescent examination, micelles offer no benefit, but also no disadvantage to doing nothing at all, as seen in Figure 20.

4.5 Conclusions and future work

Mucoadhesive micelles could offer a revolutionary increase the bioavailability of topically applied ophthalmic drugs. By packaging drug within these particles, dosing can be greatly reduced, thereby reducing off-target systemic exposure so common with traditional drops. Furthermore, by providing prolonged, controlled release, pharmaceuticals can be kept within their therapeutic window, escaping chronic over- and under-dosing so emblematic of pulsatile drug delivery. 20% PBA poly(L-lactide)-b-poly(methacrylic acid-co-phenylboronic acid) copolymer micelles were synthesized by reversible addition-fragmentation chain-transfer polymerization. These micelles have shown excellent mucoadhesion and the ability to encapsulate and deliver cyclosporine A. While cell viability did show some change to cell viability and morbidity, there was insufficient cytotoxicity to suggest any real danger. Animal studies have further confirmed the benign immunological characteristics of these particles.

The decision to create these particles using RAFT polymerization was, in hindsight, a bad one. Any scaling to industrial levels of production would be quickly stymied by this multi-pot, cumbersome approach. It is therefore a priority to transition this technology to free radical polymerization, while keeping properties sufficiently consistent for eventual regulatory approval. The proverbial elephant in this chapter also needs to be addressed: how do these particles compare with current options – particularly Restasis – at treating DED. In other words, do they work? Unfortunately, due to production issues outside of my control, we have only recently been

able to produce a sufficient quantity of CycA loaded micelles for animal testing. A DED study is currently underway, and results are expected by the end of the second quarter 2017.

4.6 References

1. Gaudana, R., et al., *Recent perspectives in ocular drug delivery*. Pharm Res, 2009. **26**(5): p. 1197-216.
2. Jacob, J.T. and B. Ham, *Compositional profiling and biomarker identification of the tear film*. Ocul Surf, 2008. **6**(4): p. 175-85.
3. de Oliveira Fulgencio, G., et al., *Mucoadhesive chitosan films as a potential ocular delivery system for ofloxacin: preliminary in vitro studies*. Vet Ophthalmol, 2014. **17**(2): p. 150-5.
4. Hansen, K., et al., *Feasibility Investigation of Cellulose Polymers for Mucoadhesive Nasal Drug Delivery Applications*. Mol Pharm, 2015. **12**(8): p. 2732-41.
5. Bhatia, M., M. Ahuja, and H. Mehta, *Thiol derivatization of Xanthan gum and its evaluation as a mucoadhesive polymer*. Carbohydr Polym, 2015. **131**: p. 119-24.
6. Shinkar, D.M., A.S. Dhake, and C.M. Setty, *Drug delivery from the oral cavity: a focus on mucoadhesive buccal drug delivery systems*. PDA J Pharm Sci Technol, 2012. **66**(5): p. 466-500.
7. Khutoryanskiy, V.V., *Advances in mucoadhesion and mucoadhesive polymers*. Macromol Biosci, 2011. **11**(6): p. 748-64.
8. Liu, S., L. Jones, and F.X. Gu, *Development of mucoadhesive drug delivery system using phenylboronic acid functionalized poly(D,L-lactide)-b-dextran nanoparticles*. Macromol Biosci, 2012. **12**(12): p. 1622-6.

9. Ivanov, A.E., et al., *Boronate-containing polymer brushes: characterization, interaction with saccharides and mammalian cancer cells*. J Biomed Mater Res A, 2009. **88**(1): p. 213-25.
10. Linden, S.K., et al., *Mucins in the mucosal barrier to infection*. Mucosal Immunol, 2008. **1**(3): p. 183-97.
11. Shvedova, A.A., V.E. Kagan, and B. Fadeel, *Close encounters of the small kind: adverse effects of man-made materials interfacing with the nano-cosmos of biological systems*. Annu Rev Pharmacol Toxicol, 2010. **50**: p. 63-88.
12. liu S, G.F., *Phenylboronic acid modified mucoadhesive nanoparticle drug carriers facilitate weekly treatment of experimentally-induced dry eye syndrome*. Nano Research, 2014. **10**: p. 1007.
13. McCulley, J.P. and W.E. Shine, *Meibomian gland and tear film lipids: structure, function and control*. Adv Exp Med Biol, 2002. **506**(Pt A): p. 373-8.
14. Prosperi-Porta, G., et al., *Phenylboronic-Acid-Based Polymeric Micelles for Mucoadhesive Anterior Segment Ocular Drug Delivery*. Biomacromolecules, 2016. **17**(4): p. 1449-57.
15. Schultz, C., *Safety and efficacy of cyclosporine in the treatment of chronic dry eye*. Ophthalmol Eye Dis, 2014. **6**: p. 37-42.
16. Ru, Y., et al., *alpha-Melanocyte-stimulating hormone ameliorates ocular surface dysfunctions and lesions in a scopolamine-induced dry eye model via PKA-CREB and MEK-Erk pathways*. Sci Rep, 2015. **5**: p. 18619.

17. Yoon, K.C., et al., *Tear production and ocular surface changes in experimental dry eye after elimination of desiccating stress*. Invest Ophthalmol Vis Sci, 2011. **52**(10): p. 7267-73.
18. Herrero-Vanrell, R. and A. Peral, [*International Dry Eye Workshop (DEWS). Update of the disease*]. Arch Soc Esp Oftalmol, 2007. **82**(12): p. 733-4.
19. Potvin, R., S. Makari, and C.J. Rapuano, *Tear film osmolarity and dry eye disease: a review of the literature*. Clin Ophthalmol, 2015. **9**: p. 2039-47.
20. Tomlinson, A., et al., *Tear film osmolarity: determination of a referent for dry eye diagnosis*. Invest Ophthalmol Vis Sci, 2006. **47**(10): p. 4309-15.

Chapter 6: Conclusions and future work

Either through collaboration or the pursuit of my own ideas, numerous ophthalmic biomaterials were created and tested. PNIPAAm based thermosensitive hydrogel materials were perhaps the most consistent thread in this thesis. Two PNIPAAm derivatives, one modified with collagen, the other with PEG, NAS, and DBA were used as case studies to highlight the development of a biocompatibility testing platform now in use in the Sheardown lab. Not just the materials themselves, but also degradation products and extratables were tested with cell types relevant to ocular tissue microenvironment. An assay to measure cell ejection driven by intramolecular hydrophobic *in situ* gelation was developed. An *in vitro* immunoassay using the THP-1 cell line was created to provide meaningful insight into the interaction between materials and monocytes. While this assay may not have been definitive, it may still serve as a simple check before materials transition into animal models. Extensive histology was performed using a variety of staining techniques to better understand the foreign body response to soft materials. Ultimately, PNNPD materials were injected into the vitreous to assess their feasibility as a drug releasing scaffold.

Building on this *in vivo* expertise, a novel dry eye disease therapeutic, HASD, was synthesized and validated in a BAC induced rabbit dry eye model. By combining the mucoadhesivity and CD44 activation of hyaluronic acid the matrix metalloproteinase inhibitory capacity of sulfadiazine, it was hypothesized a synergistic and highly effective treatment for dry eye disease might result. By looking at tear volume, corneal staining, and conjunctival impression cytology, HASD was significantly more effective at rescuing disease models than simple rinsing, and at least as effective the most effective artificial tear solution currently available. By complexing a

different MMPi, it might be possible to achieve even greater clinical efficacy with less potential for deleterious side effects.

Along with its potential as a drug releasing device, PNNPD materials hold enormous potential as a cell delivery scaffold. Despite several retinal cell therapies in clinical trials, the potential of cell replacement cannot be realized without appropriate scaffolding to provide guidance and improve cell survival and functional integration. PNNPD was chosen after dozens of iterations as an ideal ophthalmic cell delivery scaffold due to its transparency, degradability, tunability, and static gelation volume. A novel organotypic *ex vivo* retinal model was created to refine and accelerate the scaffold material design process. A suite of ophthalmic techniques, including optical coherence tomography and fundus imaging, were employed to assess the surgical viability of PNNPD as a subretinal cell carrier.

Due to their simplicity, eye drops serve as a ubiquitous front-line intervention for many ocular diseases. Unfortunately, eye drops simply do not work very well. Most medication applied via drop is flushed away from the ocular surface after the first blink, resulting in systemic exposure, wasted drug, and low bioavailability in target tissues. A mucoadhesive micelle was created using RAFT polymerisation with a lactic acid core and a methacrylic acid corona, and functionalized with phenylboronic acid to facilitate mucoadhesion. This drug delivery platform has been spun off into a company with which we hope to commercialize this technology for a variety of indications. As a proof of concept, a scopolamine-induced dry eye model was created with which these micelles could be compared against Restasis, the current market leader in the dry eye space.

Future work will focus on completing what has been begun. A new PNNPD iteration has been created which is loosely crosslinked before gelation using azide/alkyne ‘click’ chemistry. Upon gelation, this scaffold is much stiffer and less porous than conventional PNNPD. This new version is designed to more effectively encapsulate and slowly release protein based anti-VEGF drug which are ubiquitously used to control neovascularative retinal pathologies. PNNPD materials will also be used to deliver stem cells to the subretinal space. In collaboration with CCRM, a retinal pigment epithelial precursor line will be generated and used to treat a sodium iodate induced model of dry age related macular degeneration. OptimEyes was created to commercialize the mucoadhesive micelles, and so work on them will be ongoing outside the scope of this thesis. Dry eye animal studies are expected to be complete by May of 2017, with first in human trials beginning soon after. As these micelles are a platform, capable of providing controlled release and increased bioavailability wherever mucosal membranes exist, other indications will also be assessed in the future